DNA Driven Assembly at Solid and Liquid Interfaces

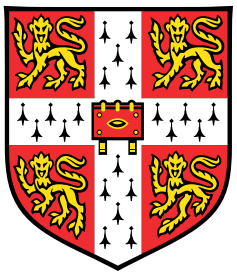

Darshana Joshi

Cavendish Laboratory - Department of Physics
University of Cambridge

This dissertation is submitted for the degree of
Doctor of Philosophy

Hughes Hall

October 2017

This thesis is dedicated to

Udayan Care,

&

My parents

. . .

Declaration

- This dissertation is the result of my own work and includes nothing which is the outcome of work done in collaboration except as declared in the preamble and specified in the text.
- It is not substantially the same as any that I have submitted, or, is being concurrently submitted for a degree or diploma or other qualification at the University of Cambridge or any other University or similar institution except as declared in the Preface and specified in the text. I further state that no substantial part of my dissertation has already been submitted, or, is being concurrently submitted for any such degree, diploma or other qualification at the University of Cambridge or any other University or similar institution except as declared in the Preface and specified in the text
- It does not exceed the prescribed word limit of 60,000 words in length

Darshana Joshi

October 2017

Acknowledgements

First of all, I would like to start by expressing immense gratitude to my supervisor and guide for the last three and half years, Dr. Erika Eiser. From the beginning when I joined her group (after moving from another group) until now at the end of my Ph.D., the immense support I have received from her cannot be expressed in mere words. Her support and pearls of wisdom made me sail through the various ups and downs in my life seamlessly. Her support is completely holistic: Spurring me on when my experiments did not work, suggesting problem solving strategies when research hits a roadblock, encouraging me when experiments worked as expected, sharing the excitement when they worked more than expected, she walked alongside me in this great journey step by step. Along with being an academic advisor, she also assisted me when my scholarship was ceded for a year, sympathized when I was going through tumultuous personal times and encouraged me when I was part of various extra curricular activities. Dinner times at her place with Daan were some of the best times I have had here. I am very fortunate to have worked under her guidance, as it is not possible to have asked for anything more from a supervisor.

I would also like to extend my heartfelt gratitude and thanks to my college tutor Dr. Jean Lambert. She has been a constant pillar of support in my time here, like a wonderful local guardian. She held me up at various points in my PhD. She managed to assist me with a bursary when my scholarship was ceded for a year and also pro-actively looked out for practically saving my PhD at Cambridge. Her emotional support during my despondent times at Cambridge were instrumental in bringing me peace and calm, as a result of which I was able to bounce back and complete a successful thesis. Her unconditional support extended right from the time when I wanted to shift groups and has been consistently high right up until now. Her insight into making the right calls and sometimes tough ones at extra-ordinary times has definitely made me more mature and insightful. I would not be here without her support and will forever be grateful for her contribution in my Ph.D. and life at Cambridge.

I would also like to thank my College - Hughes Hall, for providing me with such a comfortable and welcoming atmosphere in Cambridge. It is a college I am very proud to be associated with and will keep the association strong for long times to come. A special thanks to our senior tutor Dr. Philip Johnston who made me feel very welcomed to the college upon my arrival and has been always around to help, ever since. My heartfelt regards to the Hughes Hall administration staff in assisting me with everything, from providing accommodation and taking care of my scholarship invoices and many more. I would like to thank the Library

Staff, Academic Office Staff, Bursary Office and the Tutorial Office staff for the various support they provided over the years that made my time at Cambridge very productive.

Next I would like to thank another major influence in my academic and interpersonal journey - Dr Kiran Modi and Udyan Care. Reflecting at my past 13 years of association with Udayan Care and how my academic and personal journey shaped - I couldn't have made it without their support. They redefined my life! Dr. Modi is in particular the role model I aspire to be on a day today basis. Her enthusiasm, energy and commitment to make a difference to the lives of thousands of Children across India is truly inspiring. She is like an all watching God-Mother and who watches and protects her innumerable children. I hope one day I can be as self-less and make an impact on so many young girls as she has inspired me to do so. My induction into the Udyan Care family as a teenager provided me with the amazing mentor support that primarily shaped me into what I am today. I am very fortunate to have been nurtured under their care. My gratitude towards Udayan Care cannot be expressed in words, thoughts or emotions but go beyond. Dedicating this thesis to them is a very small token of love and gratitude. Further, I would also like to thank Faheem bhaiya and whole Udayan Shalini fellowship and Udayan Care family for all the love and faith they have bestowed upon me.

Now, I would like to extend my thanks to my funding bodies without whom this PhD wouldn't have happened. First of all my sincere thanks to Udayan Care, Vcare trust of Vatika Real Estate group, Mr. Anil Bhalla and Mrs. Divya Bhalla for providing funds and making this whole journey even imaginable. Their generous support laid the foundation of my PhD at Cambridge and I would forever be grateful to them for posing their faith in me. Their story of supporting young minds of the country to pursue excellence in academics is very inspiring and is the need for the day in a country like India. It is heart-warming to be associated with them. I would also like to express my unwavering gratitude to the Nehru Trust and Dr. Anil Seal for providing me consistent financial support and mentoring right from the start. The trust's contribution in making this dream like journey possible for a large number of aspiring students is a great achievement. I am privileged to be an awardee of this trust. A special thanks to also Dr. Anil Seal who has supported me personally through the Nehru Trust. His 'Save Darshana's PhD' campaign due to the cessation of my one year of scholarship ensured the continuation of this special journey. Finally, I would like to specially thank the Schlumberger Foundation's FFTF grant and the associated staff (Ms. Eve Millon, Ms Regina Hand and Mr.Axel Zeppenfeld) for providing me a large source of funding to successfully complete my PhD here and attend several conferences in the due course. It is again a privilege and an honour to be a Schlumberger Fellow and part of such an international community of wonderful and inspiring women academicians. I hope to contribute something back to my country as has always been my desire. I would also like to thank the Santander-Hughes Hall Bursary for providing me with crucial funds at an important time and for their travel support to attend the annual MRS fall meeting, Boston.

This exciting academic journey would not be possible if it were not for the mentors in my life who have been the guiding light in my life over the last decade. Mr. Sajan Mathew and Prof. Vikram Dutt have been the backbone of my development and have shaped my personality into who I am today. Sajan bhaiya helped me break that shell of a shy teenager

and his mentoring coupled with the super-powers of Vikram sir guided my transformation into a liberal, self-confident and a proud woman who is now ready to dream for changing the world. A sincere thanks to both of them for being the amazing guide, parent and friends over the years and helping me to become more loving and caring. Vikram sir, my super-mentor - watching his commitment and his ability to perform at the highest level not only is inspiring but is also highly contagious; so as to spur me to reach for the highest endeavours in life. He is not only a mentor but also a great friend and a soulmate.

Thinking of people who shaped me into what I am today, I am grateful to all my teachers for their commitment to making a difference to their student's lives - from school to college and beyond. In particular, I would like to extend my heartfelt gratitude to Dr. Rita Chandra and Mrs. Sudarshan Khare - my wonderful teachers and 'now' mentor mothers and their families for their constant shower of love and support over the years. Their faith in me when I lost mine - kept my head held high even in the toughest of hours. I would also like to thank my other teachers and mentors over the years - Prof. Shobana Narsimhan, Prof. Umesh Waghmare and Prof. Hari Das for their unconditional support and guidance in my endeavors. Shobana has always been one of my inspirations for promoting younger women in science and I will always be grateful for the enthusiasm she showed in mentoring us in my most founding years . With Prof. Hari Das and Prof Wghamre, I learnt the virtue of clarity of thought and the importance of dedication. Hari Das sir has always been a call away, always ready to help and support me with all his might whenever I needed his support or words of wisdom. In due course over the years there were many teachers who augmented my personal passion of science with their own passion. Their guidance, advice and mere words of encouragements went a long way in bolstering my self-confidence to pursue my dreams. Dr. Pratibha Jolly, Dr Monika Tomar who first introduced me to active research, our school science teacher Sadaf Madam, Physics teacher Mahesh Chander, School principal Mano Rana Ma'am and many more who have made my journey until Cambridge very beautiful and cherishable. Also would like to thank Dr. S.M. Shivaprasad for introducing me into the world of solid state and experimental research. I would also like to thank Dr. Eileen Nugent from BSS for being a great friend and a mentor. Also a special call out to Dr Nalin Patel for so many instances of support, from outreach works to personal mentoring; his door is always open for gaining insightful advises and ideas.

Next, goes without saying is a big shout-out to my lab-Mates : Both Present and Past members of the Eiser group. Thanks to my colleagues Simon and Rob, who introduced me to this field of Soft-Matter and trained me in the basics of DNA coated colloids. I would like to thank my wonderful colleagues Myk, Zhongyang, and Alessio with whom collaborating is a joy on a day to day basis. Also, thanks to Zach, Jerome, Paycheng , Tom and Iliya for being the cool lab-mates that they are and for their support in taking my work forwards. My regards to all members of the BSS and OE who created a hospitable and a joyful atmosphere to work at in the lab, office and recreational spaces of the institutes. I would like to thank my academic collaborators, Dr. Jasna Brujic, Dylan Bargteil, Diogo and Dr. Nuno A.M. Araujo for their simulation studies. I look forward to more fruitful collaborations in future. I also need to mention the immense contribution of the various technical and administration staff at Cambridge. Their support helped me shed my administrative loads and gave me ample

time and a hassle free ind to concentrate on research and science. I would like to than the Administrative Admin for both OE and BSS heavily for this. I would also like to thank the Trumpington Medical services whom I visited regularly, unfortunately! Support and care from them has been heartening. They took care of my health and still continue to do so, and for this I am highly grateful.

A special mention of thanks to Rob, Myk and Zhongyang for being such wonderful friends and being there for me in the hours of despair - which are unfortunately inevitable in a PhD!! Your friendship and love is really precious to me and has certainly brightened my days in Cambridge. I would like to thank Robin Lamboll, Zhongyang and Myk for reading the thesis and suggesting corrections at a super-fast rate and a laser-cut precision. Thanks to their critical suggestions the thesis has taken a great shape.

Swati Bhabhi and Mukesh Bhaiya are like my family and their home has been my second home at Cambridge. Playing with Pihu, dropping at their place uninvited for free meals, lodging and an awesome time with Pihu will stay with me for ever. I would like to thank Abhishek Bhaiya and Soni Bhabi for providing the comfort of home away from home in London. Weekend stays at their house and Aarauu were like vacations with family. Finally Kumar Uncle and Aunty require a special mention here : beautiful people, beautiful house, beautiful children, beautiful food and a family that makes you want more. With always open doors, Uncle and Aunty are very loving and and never felt I missed my parents for the few days of the year I am with them. I am lucky to have met them and have them as part of my life. Thank you uncle and aunty for welcoming me into your home and hearts from my very first step in this unknown land!!

Finally I would like to thank my flatmates Aditya, Shahab and Uzma who have made living life a great pleasure on a day to day basis and never made me miss my home half the globe away. Guys, you are The pillars that kept me sane during my PhD. Thanks for all the wisdom, support and this friendship of a lifetime. I can never thank you all enough. I would like to thank Sagar, Nimisha and Sumita Di for being such loving friends. Thanks to Hari for keeping me sane and better informed throughout! Raju for being a great friend and a co-traveler and for helping in whatever is required. Nikhil for being a classmate type figure in PhD and a great house mate too; working late hours for CPGS and PhD thesis will soon be nostalgic I can imagine. There are so many more friends who made this journey special that I need to mention, Megha Di, Rohit, Emily, Nishit, Abhishek, Abhay, James, Jayeta, Ravi, Satya, Kanwar and Maryam di.

I would also like to specially mention team VIGYANshaala which is one of the most beautiful chapters of my graduate life!From securing the huge MRS grant to execution - everything is very special: Thanks to Shruti for being so dedicated adorable and loving., Aditya for being so professional, inspiring and a great executor, Vijay for all the back-end support, love and the calming charm, Himadri bhaiya for all his support and the practical 'gyaan', Shivani for being the most fun-filled and intelligent mentee.

I would like to specially mention Dhanya and Sharmila my two favourite people from my MS days. The best of friends and such lovely ladies who also do science, their presence has been calming, loving, peaceful and joyful for which I adore them unconditionally. Would like to take a special leaf out for my school friends Amit and Nitish who have been my

fellow journeymen in Science and my first inspiration!! Their enthusiasm and inquisitiveness is contagious - who actually me introduced me to the world of science; surely this long association will continue for a lifetime.

Srishti and Renu deserve a special mention of thanks – along with whom I make the famous trio. Apart from being best of besties we also journeyed and ventured together in the world of science, relationships and much more. I could ever imagine a world without you two. Science, travel, family and beyond - there is so much we have shared in last 10+ years. Thanks for being the constant fuels and pushing me to excel in life. This thesis couldn't have been a reality without your support :) A special thanks to Dweepan - our non scientist friend for all her love and commitment to the three of us.

Would also like to thank my friends Shipradi, Shilpi, Archana, Ankit, Anuj, who have made my life so joyful. A great contribution in this journey also made by MS batch-mates Prashant, Annie, Dibyajyoti, and Ajmala. I would like to thank Ram Uncle and Family whom I consider as my second parents.; so loving and welcoming I can but express my words for my love and reverence for them,.

I would like to thank for my family for their unparalleled support and confidence in me and for giving me an opportunity to chase my dreams. First of all I would like to thank my younger brother Bhuwan - the friend, the partner in crime with whom I have shared so much of the ups and downs in life. Our understanding of each other and mutual love and friendship has always been cherished. Thanks Bhuwan for surviving all my scientific crap all these years!! My elder sister Hema deserves a special mention here for she has always taken care of me and never gone anything less than a million steps out of her way for me. I am fortunate for having such a loving and protective didi. I am also very thankful to my Jijaji for being always being there for me and for all his love and confidence . Thank you both for bringing my bundles of joys - Riddhi and Manana into my life!! Would like to thank my cousins for making my childhood no less than awesome to grow up with, my lil brother Umesh for all the love and my Maternal and Paternal grand-parents for their blessings and support.

The best part about my PhD has been meeting my partner - Dr Vijay venugopalan, for all the love and joy he has brought into my life ! The foundation of this PhD was laid by him, by his perseverance in pushing me to excel in life. Over past 6 years, he has been the constant support taking equal interest in my research, helping me grow personally and professionally and been the most wonderful friend. The commitment and enthusiasm he has shown for every aspect of into my personality and interest areas makes living more fun!! I am sure together we will cross many more milestones and grow together. Its joy to be a part of your life and family. Thank you very much for everything Vijay. Thanks to my wonderful father-in-law for being the constant source of inspiration and pushing both of us towards excellence in life.

Last but not the least I would like to convey my heartfelt thanks to my Mother and my Father. Their perseverance and persistence to walk that extra mile for their children is commendable. Despite having limited resources, they never limited our horizon. Both of them have sacrificed many of their comforts and struggled immensely to see their children excel in their lives. My father's innate love for me and his selfless commitment has guided me over the years. My mother has been a constant source of inspiration for strength, values system, unconditional commitment and inner beauty. It I because of her I stand today as

a strong independent woman at the cusp of finishing her PhD. This thesis and my whole academic journey is a testimony of her innumerable sacrifices and the pain she went through. This thesis is for your courage and dedication Ma. Thank you very much for everything.

Abstract

This thesis presents work on the DNA directed assembly of colloids at liquid and solid interfaces under specifically sculpted attractive interactions via depletion forces and/or a magnetic fields. The highly specific and thermally reversible nature of binding between two complementary single strands of DNA allows us to encode binding rules among various (solid or liquid) components of the system. The thesis begins by presenting a new approach for introducing mobile DNA linkers on oil droplets, enabling a reversible adsorption of colloids at the oil/water interface. In comparison to previous cumbersome approaches involving expensive biotinylated lipids, this simple method provides a relatively higher grafting density of DNA anchors at the interface. Further, it is possible to kinetically control the surface coverage of oil droplets with colloidal particles while preserving fully ergodic colloidal dynamics on the droplets. The equilibrium nature of the absorbed colloids is illustrated by exploring the quasi-two-dimensional (2d) phase behaviour under the influence of depletion interactions. Colloids bound to the oil water interface are found to be significantly less diffusive compared to their bulk counterparts. Simulation studies from a collaboration reaffirm the experimentally observed phase behaviour and the nature of compositional arrest. Further, some preliminary results on the phase behaviour of binary colloidal mixtures at the oil/water interface are also presented. The last section of this thesis demonstrates an approach for creating novel superstructures of DNA coated colloids (DNAcc) directed via an externally applied magnetic field. Raspberry-like and long coaxial skeletons of smaller colloids around larger superparamagnetic colloidal cores in a two component system are shown. The rigidity

of these mesoscopic superstructures is enhanced by adding a suitably functionalized third component. Finally, the thesis concludes by presenting various dimensions that have emerged out of this work and are being currently pursued.

Table of contents

List of figures

List of tables

Chapter 1

Introduction

1.1 Preamble

As children, our imagination is set on fire while looking at interfaces forming soap bubbles or foams. These omnipresent interfaces, whether between different phases of liquids, gases or solids have also captured the fascination and scientific curiosity of researchers across various disciplines for their importance in day-to-day life and industrial processes. For instance, in biology, cell walls present a complex interface between the outside and inside of the cell, the fundamental unit of all living organisms. Many industrial and technological products such as cosmetics, paints, agrochemicals, medicines, petrochemicals, food, and energy harvesting and storage devices derive their function from interfaces [1–3]. 'Predictive capability' for governing the self-assembling behaviour of macromolecules and mesoscopic particles into ordered structures and their controlled release at the aforementioned interfaces could pave the way for the development of newer and better industrial formulations with end-user functionalities such as personalised medicines and smart drug delivery systems [2, 4, 5].

However, one of the key challenges that remains in appropriating complex self-assembly is the creation of controlled and ordered patterns, such as quasi-2d patterns or small 3d

scaffolds of many distinct colloids or nano-particles which could then be utilized as primitive for building more complicated structures. For the creation of such 2d patterns and/or 3d scaffolds, it is important to incorporate reversible - 'polygamous' interactions between various colloidal species in the system. Further, it is also important to ensure that the thermodynamic pathways to these desired equilibrium structures are kinetically accessible [1, 2, 4–7].

1.2 Thesis outline

This thesis presents work on the DNA directed assembly of mesoscopic particles at liquid and solid interfaces under specifically sculpted attractive interaction via depletion forces and/or magnetic fields. While DNA is mainly regarded for its biological function as the carrier of genetic information, its unique structural properties make it an excellent tool for engineering self assembling systems. Single-stranded DNA (ssDNA) having complementary arrangement of base pairs hybridize to form a double-stranded DNA (dsDNA). The hybridization between complementary base pairs can be reversed by increasing the temperature of the system. This highly specific and thermally reversible binding between two complementary ssDNA makes them an 'intelligent molecular glue' for holding mesoscopic particles together. With the ease of chemically synthesizing and end functionalizing arbitrary bits of DNA, it has emerged as one of the most promising monodisperse polymers and has opened a plethora of applications for the non-biological materials engineering [6–8].

Throughout this thesis, DNA is employed as an 'intelligent glue' to reversibly bind colloids and/or oil droplets coated with complementary (ssDNA) sequences. Streptavidin-biotin chemistry is used to surface functionalize colloids and oil droplets with ssDNA linkers. Using the right combination of DNA, it is possible to encode sequential binding rules among various (solid or liquid) components of the system and control their release [6–8]. A precise control over the assembly and release of particles at these liquid/solid interfaces could lead

to the development of materials with tunable properties for optoelectronic applications and programmable drug delivery systems. This thesis is organized in the following manner.

Chapter 2 presents necessary background information comprising the important colloidal interactions and a detailed literature survey highlighting the utility of DNA as a tool for assembling colloidal particles. Chapter 3, demonstrates a novel approach for functionalising oil droplets with DNA that enables a reversible adsorption of colloids at the oil/water interface. In comparison to previous cumbersome approaches involving expensive biotinylated lipids [9, 10], this method provides a relatively higher ($\sim> 100$ times) grafting density of DNA anchors at the interface for binding colloidal particles. These colloids can then be desorbed from the surface of the oil droplets by increasing the temperature of the system and reattached upon cooling.

Further, chapter 4 demonstrates that it is possible to control the surface coverage of oil droplets by colloidal particles, by exploiting the fact that during slow adsorption, compositional arrest takes place well before the structural arrest occurs. As a consequence, we could prepare colloid-coated oil droplets with a 'frozen' degree of loading, but with fully ergodic colloidal dynamics on the droplets. However, their diffusivities were found to reduce by at least a fifth compared to their free counterparts in solution. Depending on the solvent conditions, our seemingly simple system exhibits an unexpectedly rich quasi-2d phase diagram of colloid aggregation. The equilibrium nature of the adsorbed colloidal phase is illustrated by exploring their quasi-2d phase behaviour under the influence of depletion interactions. As the concentration of free surfactant in solution is increased, the colloids bound to oil droplets undergo a purely entropic transition from a fluid like phase to a compact crystalline packing of colloids at the interface forming colloidal 'islands'. This transition is attributed to the depletion interaction caused by the excess surfactant micelles in the system. The experimentally observed phase behaviour is reaffirmed by simulation studies done in a collaboration with Nuno A. M. Araújo's group at the Universidade de Lisboa. These

simulations of a simple model system illustrate the nature of the compositional arrest and the structural ergodicity observed in the experiments.

Chapter 5 summarizes some preliminary results on the dynamics and phase behaviour of binary colloidal mixtures at the oil/water interface. Various ratios of large (1.2 µm) and small (0.5 µm) polystyrene colloids are bound to oil droplets and their phase behaviour is studied above and below the critical micelle concentration (CMC)of Soduim Dodecyl Sulphate (SDS). Despite the mobile anchoring of colloids that can support rearrangement of the colloids at the interface and the size difference between the different kinds of surface bound colloids, we do not observe any phase segregation for various ratios of the large to small colloids. It is also observed that the presence of larger colloids forces the smaller colloids to aggregate at the interface at a concentration of SDS much lower than the CMC. These preliminary results present an exciting opportunity for designing recyclable bi-dispersed systems.

Further, chapter 6 presents an approach for directing the assembly of a multi-component system of DNA-coated colloids (DNAcc) via an externally applied magnetic field. Using the right combination of DNA it is possible to tune the sequential interactions for this multi-hierarchical system while ensuring thermoreversibility of the assembled superstructures. Colloidal superstructures with topological complexity such as 'raspberry' like and long coaxial skeletons of smaller colloids around larger superparamagnetic cores are demonstrated in a two component system. By adding a suitably functionalized third component, the rigidity of long coaxial scaffolds can be enhanced, leading to greater stability of these mesoscopic superstructures. Self-assembly of these long, straight, mesoscopic scaffolds of colloids can be utilised as a primitive for building more complicated structures. Possible applications for the work include their use as micro-fuse switch or template materials in efficient smart energy-storage devices.

Lastly, chapter 7 concludes the thesis and presents an outlook for the future work and the new dimensions that have emerged out of these experimental systems. The novel approach

for functionalizing oil droplets with DNA linkers and attaching colloids at the oil water interface detailed in chapter 3, presents a versatile model system for studying colloids in a quasi-2d setting. An added advantage of the system is its ability to gently tune the colloidal interaction potential. One of the most promising and exciting extensions of this work has been the utilization of optical tweezers for trapping colloids at the liquid-liquid interface and the observation of optical binding. It is demonstrated that the system can be successfully used as a model system for colloids in quasi-2d settings and could be used to study optically induced crystallization at the fluid-fluid interface. Among other things, attempts for building a micron sized electrical fuse by utilizing a conducting layer in between our coaxial scaffolds (chapter 6) are underway.

Parts of the findings presented in this thesis have been published or are awaiting submission as manuscripts are being prepared.

Publications

Experimental methodologies and data analysis techniques listed in chapter 3 and 4 have contributed to the work published in

- Z. Ruff, S. H. Nathan, R. R. Unwin, M. Zupkauskas, **D. Joshi**, G. P. C. Salmond, C. P. Grey and E. Eiser, Designing disordered materials using DNA-coated colloids of bacteriophage fd and gold, *Faraday Discussion*, $2016, 186, 473-488 DOI: 10.1039/C5FD00120J$

- M. Zupkauskas, Y. Lan, **D. Joshi**, Z. Ruff and E. Eiser, Optically Transparent Dense Colloidal Gels, (*Chemical Science*, 2017,8, 5559-5566, 10.1039/C7SC00901A)

The findings summarized in chapter 3 and 4 that form the core of this thesis are published in

- **D. Joshi**,, D. Bargteil, A. Caciagli, J. Burelbach, Z. Xing, A. S. Nunes, D. E. P. Pinto, N. A. M. Araújo, J. Brujic, E. Eiser, Kinetic control of the coverage of oil droplets by DNA

functionalized colloids, *Science Advances*, 05*Aug*2016 : *Vol*.2, *no*.8, *e*160088, *DOI* : 10.1126/*sciadv*.1600881

Manuscript under preparation from the work summarized in this thesis and other collaborative projects

- **D. Joshi***, M. Zupkauskas*, S.H. Nathan, J. Kotar, E. Eiser, Magnetic-Field Assisted Assembly of DNA-Coated Colloids (manuscript under preparation). * - *equal contribution*
- **D. Joshi**, A. Caciagli, M. Zupkauskas, E. Eiser, Phase behaviour of binary colloidal mixtures in a quasi-two-dimensional environment (manuscript under preparation)
- A. Caciagli, **D. Joshi**, J Kotar E. Eiser, Optical trapping of colloids at liquid-liquid interfaces
- P.Xu, Zhongyang Xing, **D. Joshi**, Y. Lan, Erika Eiser, Liquid-crystalline behaviour of self-assembled clay/polymer nano-composites, (manuscript under preparation).

Chapter 2

Background – Colloids and DNA Functionalization

Self-assembly is abundantly utilized by nature at all length scales to reliably produce complex yet symmetrical structures from smaller building blocks [1]. Ordered aggregates found in viral and bacterial assemblies, macromolecules, crystals, opals, micelles and vesicles are some examples of the naturally occuring self-assembling systems [1, 2]. Utilizing bottom up self-assembly techniques with mesocopic components as building blocks to engineer novel materials and industrial formulations is one of the prime focuses of contemporary research in condensed matter physics and materials science [2–5].

Engineered self-assembly mostly harvests non-covalent interactions to direct smaller building blocks into an ordered target state upon equilibration. This equilibrated or ground state of the system is determined by local interactions between its components and the thermodynamic pathways leading to equilibration. Since the self-assembling processes are primarily governed by thermal energy, 'ideal' building blocks for self-assembling systems have certain size restrictions. They should be 'small' enough to exhibit stochastic motion when dispersed in a medium but larger than atoms or small molecules so that we can handle and manipulate them in the lab.

Constant quest for finding suitable building blocks for designing materials with desired optical, mechanical or electric properties has led to the discovery of several nano and micron sized particles with well controlled morphologies and interactions. These comprise a class of materials called 'colloids', composed of small solid particles or immiscible liquid droplets, typically ranging from 1 nm to 1 µm in size, dispersed in a continuous liquid or gaseous medium. For the dispersed particles to remain suspended in the continuous medium, the thermal forces acting on them must be greater than or comparable in magnitude to the gravitational forces. The effective interparticle interactions in colloids, also known as *'the potential of mean force'* depends explicitly on the temperature and their interactions with the medium they are dispersed in [11, 12], while their dynamics is described by thermal motion. The phase behaviour of colloidal suspensions is determined by their coarse grained properties such as shape, flexibility and charge. Colloids represent one of the most diverse classes of soft materials and are particularly relevant to our everyday lives for their ubiquitous presence in food, paints, pharmaceutical, cosmetics and petrochemical industries [13, 14]. For instance milk - fat droplets and protein clusters suspended in a water-like medium, smoke - solid particles suspended in air, foams, ink, butter and mayonnaise are all examples of colloidal suspensions.

2.1 Dynamics of colloidal particles

In a dilute suspension colloidal particles resemble an atomic gas and their equilibrium dynamics is characterized by Brownian (thermal) motion. An isolated micrometer-sized particle dispersed in a liquid medium performs random motion due to its interaction with the liquid molecules. Because of thermal fluctuation ($\sim k_B T$) the fluid molecules are in a constant state of motion and they collide with the particle from random directions. These collisions result in a net instantaneous force on the particle and force it into a random walk through the medium i.e. Brownian motion. In 1905 Einstein described that the mean square

displacement of such a particle would be given by [15]

$$\langle \triangle x^2 \rangle = (2n)D \triangle t, \tag{2.1}$$

where, $\triangle x$ is the displacement in time period $\triangle t$ in n spatial dimension. The diffusion coefficient, D, is related to thermal energy by the Stokes-Einstein equation

$$D = \frac{k_B T}{6\pi\eta R} \tag{2.2}$$

where k_B is Boltzmann's constant, T is the temperature, η is the viscosity of the continuous phase, and R is the radius of the colloidal particle. Jean Perrin, later experimentally verified Einstein's predictions. These days, using microscopes equipped with a digital camera, image analysis and particle tracking algorithms, it is possible to measure the diffusivities of colloidal microspheres and gather information about the solvent environment. In this thesis single particle tracking experiments are utilized to estimate the diffusivities of 1.2 µm polystyrene colloids bound to the surface of oil droplets and those moving freely in solution.

In a concentrated colloidal suspension, in addition to their interactions with the solvent medium, colloids also interact with each other. Consequently, the phase behaviour of a colloidal system emulates that of an atomic system and they self-assemble into gas, liquid, solid, and glassy phases. A good control over their polydispersity and interaction potential has made colloids ideal candidates for emulating atomistic or molecular systems and probing their dynamics [14]. Behaviour of colloidal systems under given conditions can be largely dependent on only three phenomena and their associated length scales – namely Brownian motion due to the influence of thermal energy, the depth and range of the London-van der Waals forces, and electrostatic interactions between the highly charged colloids and charged electrolyte ions around them [11, 12]. Typical colloid-colloid interactions are elaborated in the following sections.

2.2 Interactions in colloidal suspensions

2.2.1 Hard sphere repulsion

Colloidal particles have definite geometries and are fairly solid and highly impenetrable. As a consequence of the Pauli's exclusion principle at very short inter-particle separations, the colloid-colloid interactions are harshly repulsive. This implies that as soon as the particles come in contact they interact through volume exclusion. For spherical colloids with a hard-sphere radius R and inter-colloidal separation r, the hard sphere potential is given by

$$V = \begin{cases} \infty & r \leq 2R \\ 0 & r > 2R \end{cases} \tag{2.3}$$

2.2.2 London-van der Waals forces

London-van der Waals forces are quantum mechanical in nature and arise between all molecules and particles irrespective of the medium (air, vacuum or liquid) they are in. When two atoms/particles are brought in close proximity, instantaneous fluctuations in particles' electric dipole distributions give rise to attractive van der Waals forces (also known as London dispersion forces). These forces are very short ranged and exceed the thermal energies for colloidal particles only in the proximity of contact. The net attractive interaction between these instantaneous dipoles scales as Ar^{-6}, where r is the separation between these instantaneous dipoles and A is the Hamaker constant that depends on the square of the difference in electric polarizabilities between the colloidal material and the solvent, $(\rho_c\alpha_c - \rho_s\alpha_s)^2$ [11, 12]. For larger inter-particle distances these dispersive forces become negligible compared to thermal energy k_BT. Note that the van der Waals interactions can be repulsive between dissimilar colloids in a dispersion medium when the value of the electric

polarizability of the solvent α_s lies between the polarizabilities of two colloids made of different material [11, 12, 16]. Various uncoated nanoparticles have very high van der Waals forces and tend to aggregate when dispersed in inert non-polar solvents.

The Lennard-Jones potential, given by Eq 2.4, is often used to model these short range interactions arising from the van der Waals attractive forces and the hard-sphere repulsion

$$V(r) = 4\varepsilon\left[\frac{R}{r^{12}} - \frac{R}{r^{6}}\right] \tag{2.4}$$

Here, r is the separation between the centers of hard spheres and ε is the potential at the energy minimum (defined as $r = 2^{1/6}R$). The total dispersion interactions are obtained by integrating pairwise over the volume of the interacting colloids and is given by

$$V_{disp}(r) = -\frac{A}{6}\left\{\frac{2R^2}{r^2-4R^2} + \frac{2R^2}{r^2} + ln\frac{r^2-4R^2}{r^2}\right\} \tag{2.5}$$

A potential of this form (Eq 2.5) is only accurate for inter-particle separations much larger than the radii of the particles. However in colloidal suspensions, the size (hard-sphere radii) of the colloidal particles is much larger than their distance of closest approach and also the effective interaction between two colloidal particles decays over a distance much smaller than their radii. In such a case, the Derjaguin approximation states that the total interaction energy can be obtained by integrating only over the interaction between the two facing surfaces. This further simplifies the form of net dispersion potential to

$$V(r) = -\pi^2 R\frac{\rho^2 C_{disp}}{12d} = -\frac{A}{12}\frac{R}{d} \tag{2.6}$$

where, A is the Hamaker constant: $A = \pi^2 R\rho^2 C_{disp}$, accounting for the dielectric properties of the colloids and the solvent.

Further, the dispersion forces acting between the colloids across a homogenous solvent depend on their difference in polarizability per unit volume [12, 11]. The polarizability density of the bulk phase is directly related to the refractive index, which is given by the Clausius-Mosotti equation as

$$\frac{n^2-1}{n^2+2} = \frac{4\pi\rho\alpha}{3} \tag{2.7}$$

where α is the polarizability, ρ is the density and n is the refractive index of the individual colloidal particles. Hence, effective dispersion forces could be reduced to zero by attaining refractive index matching between the solvent and the colloidal particles.

As a result of these strong attractive dispersion forces, colloidal suspensions aggregate by falling into the energy minimum corresponding to hard contact. Methods like 'steric' and 'electrostatic' stabilization have been employed to prevent aggregation due to dispersion forces in colloidal systems. Both methods try to replace the strong contact adhesive forces by a weak, non-covalent adhesive force that aids in manipulating the assembly of colloidal particles into desired structures. Steric stabilization is usually achieved by coating the nano/micron sized particles with polymers or surfactant monolayers, whereas electrostatic stabilization can be utilized in aqueous solvents where colloids can become charged and/or surrounded by a hydration layer and hence preventing aggregation [16]. These are discussed in the following section.

2.2.3 Electrostatic interactions: forces between charged colloids

Charged colloids of the same kind would exert an equal and opposite force on each other when dispersed in a non-polar solvent. These pairwise additive Coulombic interactions are

given by ,

$$V_c = \frac{Q^2}{4\pi\varepsilon r} \tag{2.8}$$

where, Q is the net charge on each colloidal particle, r is the distance between their centers, and ε is the dielectric constant of the medium. However, if the colloids were instead dispersed in an electrolyte solution, the oppositely charged ions (counter-ions) from the electrolyte would screen the direct Coulomb repulsion between the colloids. These counter ions will form a halo around the charged colloid, known as the electric double layer or the Stern layer and an exponentially decaying diffuse layer of ions in solution (Fig 2.1) [14]. This double layer screens the effective surface charge of the colloidal particles for a distance greater than its characteristic Debye screening length, κ^{-1} given by

$$\kappa^{-1} = \sqrt{\frac{4\pi}{\varepsilon k}\sum_i \rho_i q_i^2} \tag{2.9}$$

The ionic strength I of the electrolyte, defined by (Eq 2.10), plays a key role in tuning the electrostatic interactions between charged colloids and hence guiding their phase behaviour.

$$I = \sum_i \rho_i q_i^2 = \sum_i \rho_i e z_i^2 \tag{2.10}$$

Here, ρ_i are the densities of the added species (salt ions) i, e is the elemental charge and z_i the valence of the salt. Therefore, we can conclude that the Coulomb interaction is screened by counterions and coions in solutions and decays much faster than the bare interaction. An increase in the salt concentration effectively screens Coloumbic interactions and may lead to aggregation.

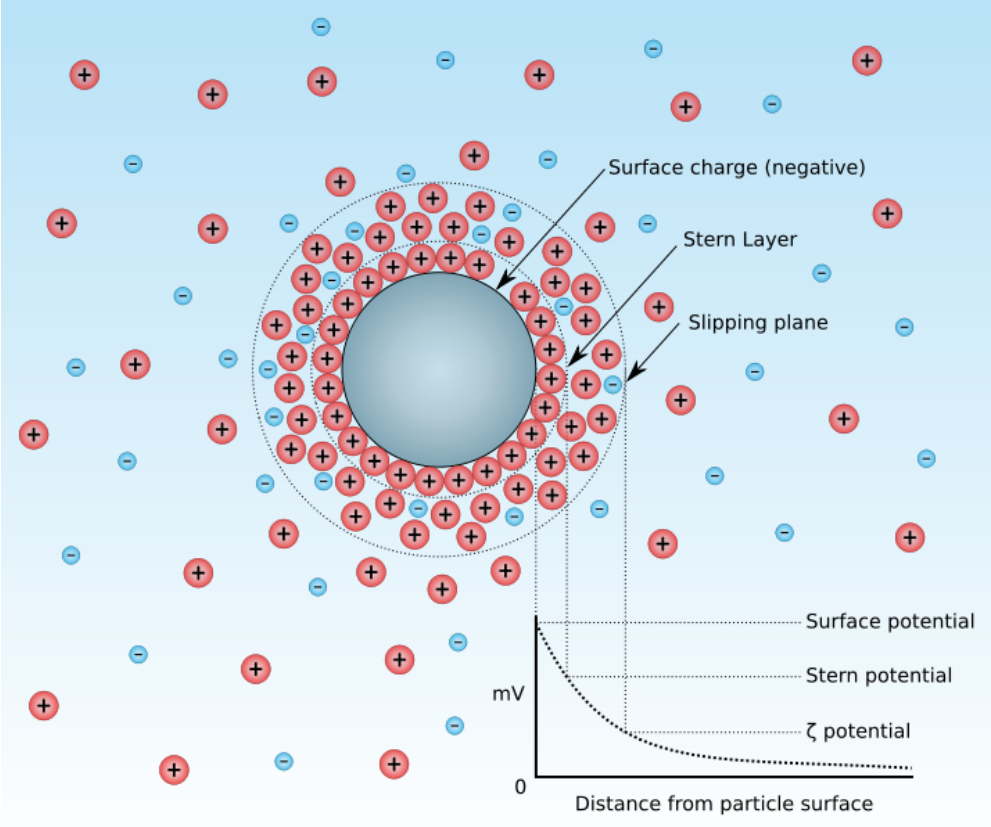

Fig. 2.1 Schematic representation of the Coulombic interactions present at the surface of a negatively charged colloidal particle. The ζ potential is defined as the electrostatic potential of the system at the shear plane, where counter-ions are no longer immobilized to the surface and hence don't experience a synchronised transport with moving particles. It is generally used as a good measure of the stability of a colloidal suspension. Figure taken from Wikipedia

Hence, the effective electrostatic interaction between two charged colloids dispersed in an electrolyte solution scales as $e^{-\kappa R}/r$, also known as the Yukawa potentia, is given by

$$V_{Coulomb} = \left(\frac{Qe^{\kappa R}}{1+\kappa R}\right)^2 \frac{e^{-\kappa R}}{4\pi\varepsilon r} \tag{2.11}$$

2.2.4 DLVO potential

A complete description of the inter-colloid interaction is given by combining the equations for electrostatic and dispersion forces. Derjaguin and Landau [17] simultaneously with

Verweij and Overbeek [18] independently proposed expressions for the effective inter-colloid interaction between two charged colloids dispersed in an electrolyte solution, now known as the DLVO theory. This theory describes the effective interactions between charged colloids as a sum of two interaction potentials, an attractive potential V_A due to the dispersion forces and a repulsive potential V_R due to the electric double layer

$$V = V_A + V_R \tag{2.12}$$

Combining equations 2.5 and 2.11 the overall interactions between two identical spherical colloids is then given by

$$V_{DLVO}(r) = \left(\frac{Qe^{\kappa R}}{1+\kappa R}\right)^2 \frac{e^{-\kappa R}}{4\pi\varepsilon r} - \frac{A}{6}\left\{\frac{2R^2}{r^2-4R^2} + \frac{2R^2}{r^2} + ln\frac{r^2-4R^2}{r^2}\right\} \tag{2.13}$$

It can be seen from equation 2.13 and Fig 2.2 that at short distances the DLVO potential has a deep minimum and hence the system is more likely to aggregate here due to the dominance of dispersion forces. However, for low salt concentrations the aggregation will be prevented by strong electrostatic interactions and we will have stable colloidal suspensions. As the salt concentration increases, the height of this electrostatic interaction decreases and a secondary minimum appears. This is known as the flocculation minimum. At higher salt concentrations these interactions are screened and the system favours aggregation [14, 12, 11]. If the Coulomb's barrier is $>> k_BT$, the system is said to be in a meta-stable equilibrium else otherwise it will have an irreversible aggregation.

To save the colloids from sedimenting under the effect of gravity, usually the solvent is density matched to that of the colloidal particles. This provides an effect similar to microgravity and the colloids behave as if they have almost zero effective mass in the solvent.

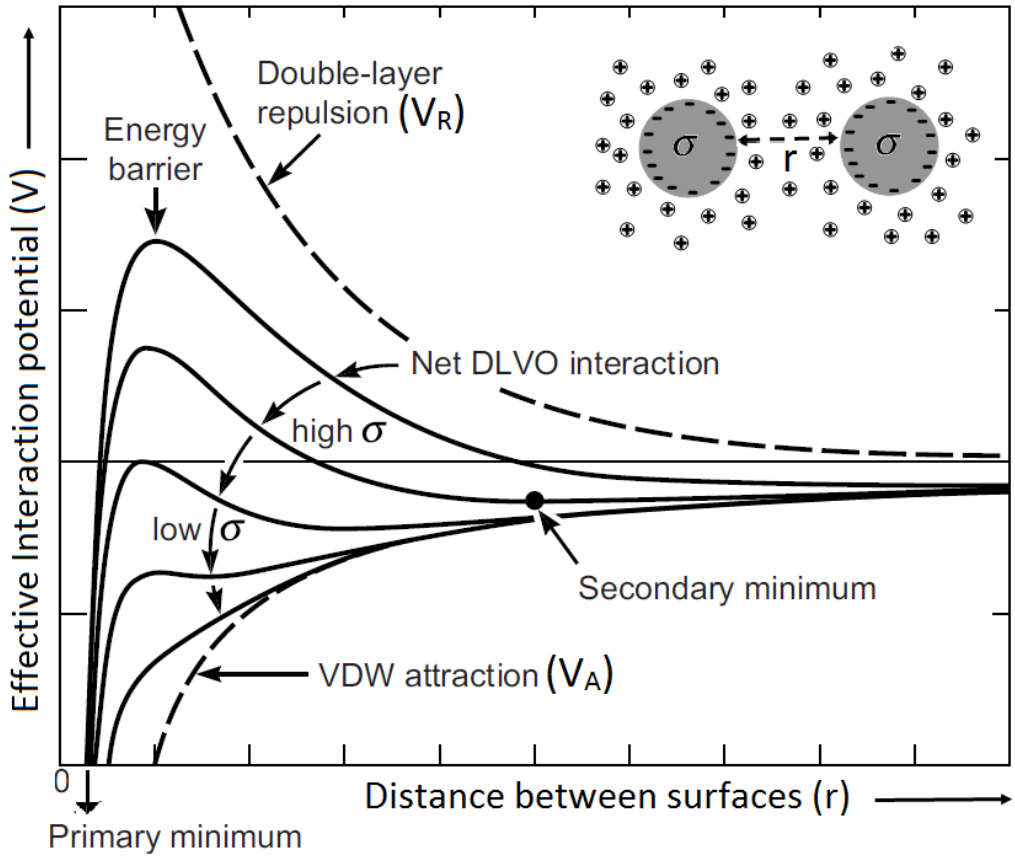

Fig. 2.2 Plot showing DLVO potential as a sum of van der Waals attraction potential (V_A) and electric double layer repulsion potential (V_R) as a function of distance (r) from the surface of a spherical particle. At a distance far from the surface of the colloid, both van der Waals attraction potential and electrostatic repulsion potential reduce to zero. Near the surface is a deep minimum in the potential energy due to the van der Waals attraction. The height of the repulsive barrier (close to the surface of colloidal particle), determines the stability of colloidal suspension. For colloids having low surface charge density (σ) or potential, the energy barrier will be lower [11].

2.2.5 Depletion interactions

In a colloidal suspension having purely hard sphere repulsions, aggregation can also be driven by addition of smaller particles (or polymers). This is a reversible attractive force having its origin purely attributed to entropy. These interactions were first described by S. Asakura and F. Oosawa [19], in the year 1958 where they derived an expression for an attractive force acting between non-interacting particles suspended in a solution of macromolecules. They concluded that the force was of the order of the osmotic pressure of the macromolecule and

its range proportional to their diameter. This polymer/macromolecules induced attraction between the colloids is an entropic effect, as the macromolecules have access to a larger volume and hence a larger no of conformations when the colloids are aggregated [11, 12].

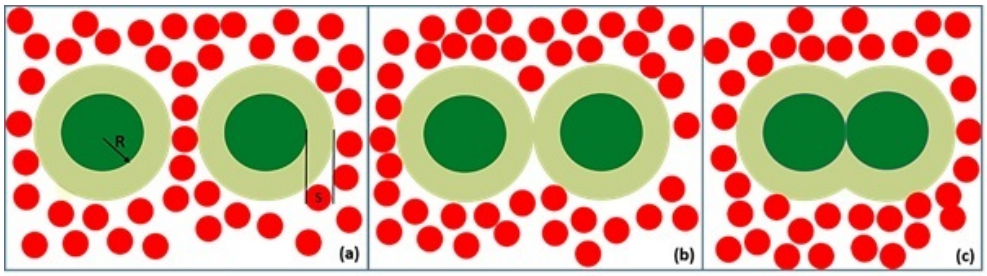

Fig. 2.3 Effect of depletion forces: (a) larger colloids are farther apart, feel an isotropic force on them and have an exclusion volume around them that is proportional to the radius S of the smaller particles (b) as they approach each other, reaching a separation less than 2S. (c) Once the exclusion volumes overlap an attractive force appears that causes aggregation.

In a system having two different kinds of colloids, larger ones with radius R and smaller ones with radius S, when the large colloids are far apart (Fig 2.3(a)), they move in a random walk and experience an isotropic force from smaller colloids. The larger colloids have a volume of exclusion around them wherein the smaller colloids are not permitted. As the larger colloids approach each other to a separation between them of about $2S$, smaller particles experience a reduced entropy in this confinement and tend to escape from that gap. This results in a local imbalance of small particle density which is experienced as an anisotropic force acting on the larger colloids, which pushes them further together and hence favours aggregation. This sets up an osmotic potential that draws the solvent out from the overlap region and hence pulls the colloids together.

This depletion induced aggregation is reversible in nature [14]. The strength of depletion attraction is proportional to the concentration of the depletant and can reach several k_BT. Hence to tune the strength of these interactions, we can either dilute the solution or increase the temperature of the system. Similar effects could be produced by using polymers with radius of gyration R_g, which cannot unfold themselves beyond $R_g$while free in solution. One major advantage of using active polymers such as PNIPAM) [20] instead of hard particles

is that their radius of gyration is tuneable with temperature, which can allow us to tune the range of attraction with small changes in temperatures [14].

2.2.6 Steric stabilization

While free polymers in solution can cause an attractive interaction between colloidal particles, polymers bound to their surfaces can add to the repulsive interaction between them, thereby stabilizing colloidal suspensions. When high enough densities of ideal non-interacting (amongst themselves) polymer chains are grafted to the surface of the colloids, they can prevent the colloids from aggregating under the influence of van der Waals attractive forces. Under the approximation that the radius of gyration $R_g \ll R$ (radius of the colloids), steric repulsion between "hairy" colloids is described by the Alexander – de Gennes scaling theory [21, 22] which states that under good solvent conditions the pressure between two parallel plates separated by a distance, r, both bearing a brush layer of equilibrium length, L_0, and grafting density, σ, is described by

$$P(r) = \begin{cases} \sigma^{\frac{3}{2}} \left[\left\{ \frac{2R_g}{r} \right\}^{\frac{9}{4}} - \left\{ \frac{r}{2R_g} \right\}^{\frac{3}{4}} \right] & \text{for} \quad r \leq 2R_g \\ 0 & \text{for} \quad r > 2R_g \end{cases} \tag{2.14}$$

For $r \leq 2R_g$, The first term in Eq 2.14 correspond to an increase in the osmotic pressure (which is purely repulsive). As the polymer brushes start touching each other, this term favours the expansion of grafted polymer brushes and hence acts to increase r . While the second term comes from the elastic stretch energy of the polymer brushes, which favors contraction and so acts to decrease r. Additional repulsive forces arise from the finite size of the confined segments (excluded volume effect). Hence, an overall repulsive force is experienced by colloidal particles as the brushes start touching each other.

For uncharged colloids steric stabilization is the most popular way of stabilizing suspensions. Polymers like polyethylene glycol (PEG) is one of the most commonly used hydrophilic polymers for coating colloidal particles in aqueous solutions in order to make them resistant to the absorption of large molecules like proteins. Steric stabilization also finds applications in designing self-cleaning and antifouling surfaces as well as in paints, in which the pigment particles are required to be stabilized in solution [14]. Colloidal particles can also be functionalized by attaching a number of biomolecules like enzymes, lipids, proteins, RNA and DNA molecules [4, 23, 24]. These functionalizing molecules govern how the colloids interact with the surrounding solvent or among themselves. Following sections establish the necessary background for utilizing DNA as a tool for appropriating the self assembly of colloidal microspheres.

2.3 DNA: A ‘smart’ polymer

Since the discovery of the double helical structure of Deoxyribonucleic acid (DNA) in 1953 [25], it has been widely acknowledged as the fundamental building block of all life forms. Apart from being the carrier of genetic information, DNA is also a handy tool for designing and engineering self assembling systems. The highly specific, temperature sensitive, reversible, complex yet predictable thermodynamic behaviour of DNA has paved the way for new programmable materials [3, 6, 26].

In principle, we can use DNA to code binding rules into mesocopic building blocks and direct their self assembling behaviour. However, full control over the programmability is yet to be established. With our quantitative understanding of DNA thermodynamics and the ability of grafted DNA to give rise to specific inter-particle attractions through hybridization of complementary single strands, it is possible to direct the system to reversibly assemble into equilibrium and non-equilibrium structures [3, 6, 8, 26].

Before dwelling more into the DNA assisted self-assembly of colloids, a primer on the structure and chemistry of the DNA is presented in the following section.

2.3.1 DNA: Structure and Chemistry

DNA is a naturally occurring polymer made up of repeating units called nucleotides. Each nucleotide contains a phosphate group, a sugar group and a nitrogen base. The hydrogen bonding between its constituent bases and their stacking interactions are responsible for its double helical structure. The double helical structure of DNA can be understood as having a ladder like geometry with two linear antiparallel sugar-phosphate polymer backbones. A combination of four different bases namely Adenine (A), Cytosine (C), Guanine (G) and Thymine (T) are attached to each backbone in a way to satisfy the specificity of hydrogen bonding between these bases. The base A on one strand can only bind to T on the other strand and similarly C with G by forming two and three hydrogen bonds respectively. The base pairing process occurs in an antiparallel fashion. 'Handedness' of the helical structure as well as the steric effects on the hydrogen bonding prohibit formation of structures with mismatched base pairing.

The interior of double-stranded DNA is very hydrophobic which is vital for stabilizing and protecting the hydrogen bonds between complementary bases. A schematic highlighting the key features of the double helical structure of DNA along with its chemical structure showing the hydrogen bonds between complementary bases is shown Fig 2.4.

Scientific inquisitiveness lead ways to the methods of chemically synthesizing arbitrary bits of DNA sequence in the mid 1980s [27] which then coupled with the polymerase chain reaction (PCR) [28, 29] revolutionized the outlook of the scientific community towards using DNA as a fundamental building block for programmable self-assemblies. Since then synthesized DNA strands have been exploited evolving the fields of DNA origami and genetic engineering [26, 30]. With these recent developments, DNA has emerged as one of the most

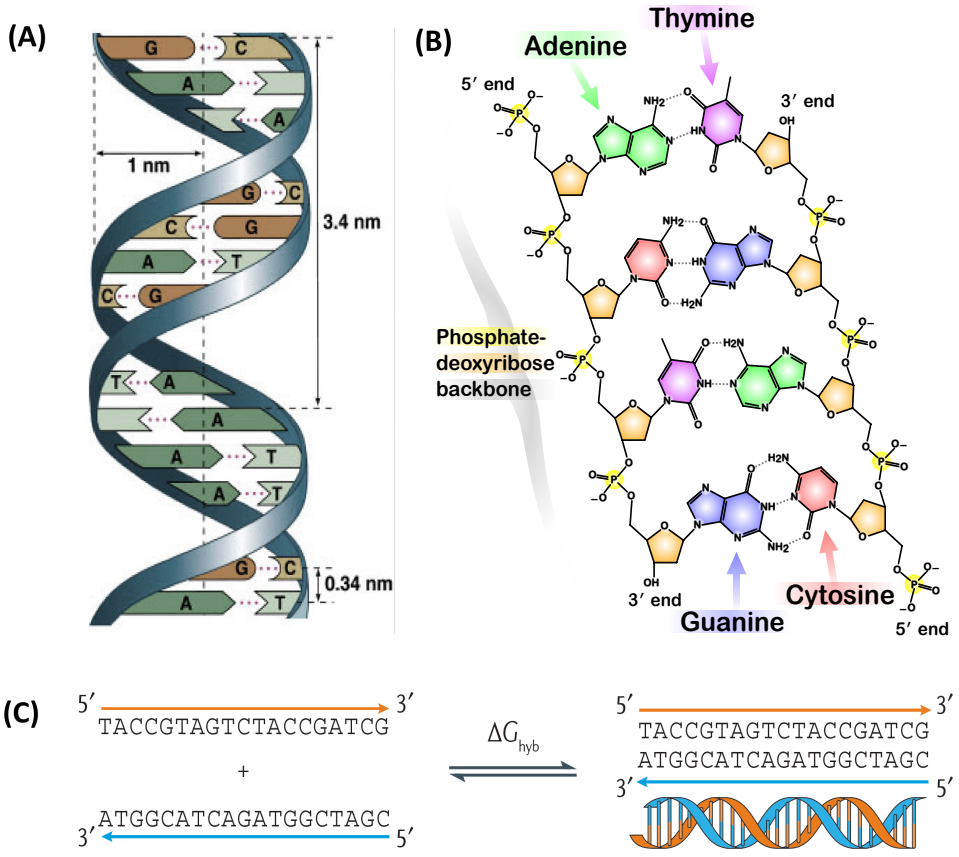

Fig. 2.4 (A) A schematic highlighting the key features of the double helical structure of DNA (image courtesy - Pearson Education, Inc.) (B) Chemical structure of DNA showing the hydrogen bonds between complementary bases as dotted lines. The hydrogen bonding between complementary base pairs gives rise to this secondary structure (image courtesy - Madeleine Price Ball, Wikipedia). (C) Hybridization of two single stranded DNA (ssDNA) consisting of linear sequence of nucleotides (5’ to 3’) with an associated change in free energy (ΔG_{hyb}) . A single sequence will bind to its ‘complementary’ pair only if it has the matching sequence in an antiparallel direction (image taken from [3]).

promising monodispersed polymers. Its highly charged stiff backbone with good electron transport ability along its axis [31], double helical structure, highly specific and thermally reversible binding of its base pairs makes it stand out among its other industrial counterparts.

2.3.2 DNA: An ‘intelligent glue’ for building complex materials

In order to utilize nano- or micron-sized building blocks for designing complex superstructures with novel properties, it is of utmost importance to be able to precisely control both, the

spacing between individual building blocks and the overall symmetry of the superstructure. DNA strands with desired length and tailored interactions can be used as intelligent glue to bind these building blocks. Although innumerable examples of highly specific binding between biomolecules like proteins and nucleic acids exist in nature, it was only in 1996 that two groups [32, 33] publishing in the same issue of Nature, proposed the potential of DNA as a "selective glue" to bind nano-colloids and guiding their assembly. While Mirkin *et al.* [33] showed that DNA oligonucleotides could be bound to gold nanoparticles and hence guide the formation of larger assemblies. On the other hand Alivisatos *et al.* [32] demonstrated that the large persistence length ($\sim$ 50 nm) of double stranded DNA (ds DNA) allows the freedom to tune the separation between colloids to form a guided assembly. These papers opened wider prospects for utilizing the potential role DNA linkers could play in a reversible guided assembly of three dimensional nanostructures (Fig 2.5).

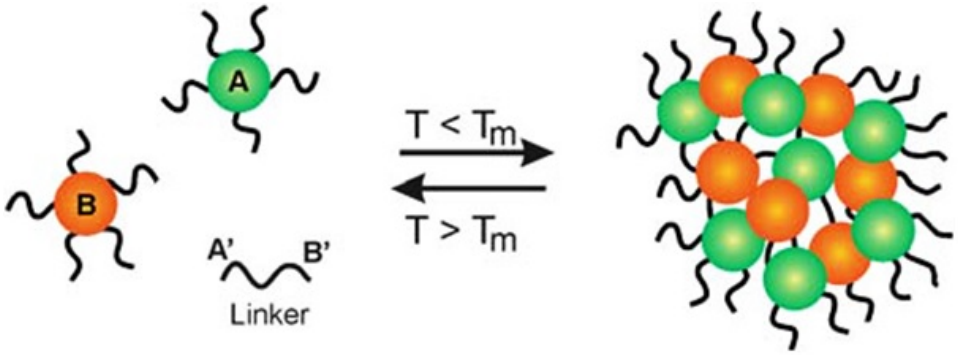

Fig. 2.5 Two kinds of colloids coated with non-complementary ssDNA (A and B) and a linker ssDNA having complementary sticky ends (A'and B') are mixed in a solution. Below the melt temperature T_m of the DNA the colloids assemble into clusters, which redisperse upon raising the temperature of the system (taken from ([6])

Owing to the knowledge of enzyme chemistry and their ability to bind to DNA strands with atomistic precision, a variety of super-selective DNA strands with functionalizable ends could be designed. For example, earlier experiments of DNAcc utilized thiol bonds to bind DNA to the colloid surface [33]. Later ssDNA labelled with amine groups were

linked covalently to the surface of polysteryne colloids modified with carboxyl group [34, 8]. Another approach to graft ssDNA to the colloidal particles is to end functionalize them with biotin, which can bind to the colloidal surface carrying either neutravidin or streptavidin. The biotin/streptavidin bond is one of the strongest known non-covalent bonds and is stable under most of the experimental conditions [34, 8]. All the experiments in this thesis have utilized the biotin/streptavidin chemistry for functionalizing colloids with DNA. Following section describes the thermodynamics and properties of DNA coated colloids.

2.3.3 Properties of DNA coated colloids

A number of factors play a deterministic role in defining the properties of DNA coated colloids (DNAcc). The length of the single-stranded 'sticky end' determines the hybridization strength per DNA duplex. The grafting density of DNA strands on the colloidal particles determines the total potential energy between colloids by virtue of DNA brush (U_{DNA}). The ionic strength of the solvent that shields the interaction between negatively charged ssDNA strands facilitates a better grafting density of the DNA. Finally, the length of double stranded (ds)DNA spacer affects the configurational entropy of hybridization as it directly dictates the freedom of the sticky ends to explore available configurations.

The melt temperature T_m of a dsDNA oligomer is defined as the temperature at which half of all possible hydrogen bonds are broken; hence the other half is bound. As detailed above, T_m depends on the specific sequence and length of the duplex as well as on the total DNA concentration and the ionic strength of the solution. One way to determine the melt temperature is to measure the adsorption of 260 nm UV-radiation as a function of temperature, as ssDNA adsorbs at this particular wavelength much stronger than the double-strand. It was found that the melt behaviour of DNA grafted to colloids is different compared to that of the same DNA free in solution (Fig 2.6(a)). The melt transition in case of DNA grafted to colloids is much sharper, with $\Delta T \sim 1^{\circ}\mathrm{C}$ between free and bound states, and is also shifted to higher

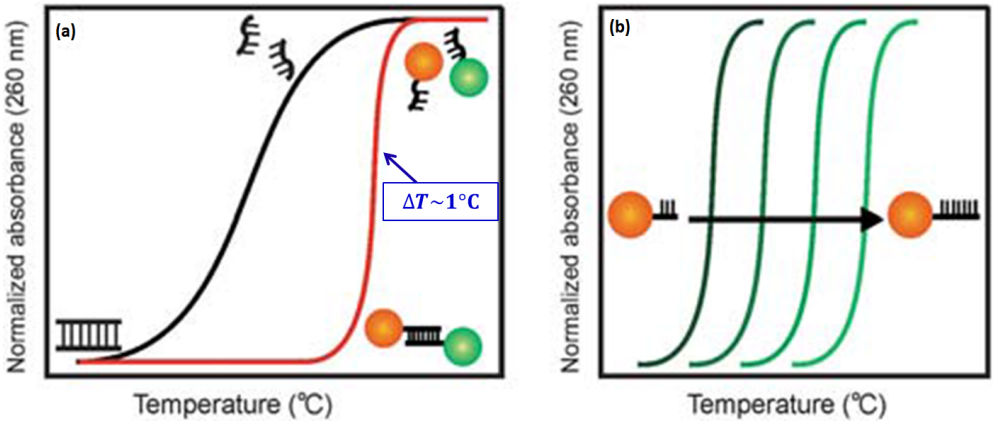

Fig. 2.6 Schematic representation of typical melt curves for DNAcc measured as UV-adsobtion of 260 nm. (a) Adsorption profiles measured as function of temperature show the different melt transitions for tethered DNA, which is much sharper and occurs at higher temperatures compared to the same DNA duplexes free in solution. (b) The melt temperature increases with an increase in the length of sticky end, corresponding to the total number of hydrogen bonds that can form in the contact region. (taken from ([6])

temperatures [6]. Geerts *et al.* have explained this by using simple probabilistic calculations to show that as the maximum no of intercolloidal bonds N increases, the probability of unbinding a pair of colloids decreases doubly exponentially and the temperature at which half of the pairs of colloids are in an unbound state increases logarithmically with N [6]. Also, Fig 2.6 (b) shows that the length of the sticky ends is a great deterministic factor for the melt temperature. The higher the number of bases in the sticky end, the higher will be its melt temperature [6]. Here, it should be noted that a G-C pair imparts greater stability than an A-T base pair due to higher no of hydrogen bonds. There are a number of ways to design the DNA coatings on the colloids depending on the desired binding rules. Various possible geometries of the DNA coatings are discussed at length in [8, 34].

2.3.4 DNA driven self-assembly and colloidal crystallization

DNA mediated self-assembly of colloids is driven by the weak, specific interactions between complementary DNA strands grafted to appropriate particles. From the melt-curves shown in Fig 2.6, we know that DNA-hybridization is thermally reversible and occurs in a narrow

temperature range. Hence, choosing the DNA strands with the right melt-temperatures is one of the most crucial parameters in designing any experiments with DNAcc [35].

The idea of DNA assisted assembly of colloidal particles was proposed in 1996 [32, 33], and it was expected that the attractive interactions caused by complementary DNA strands would drive these colloidal systems to aggregate in various crystalline phases observed in nature, but experiments proved otherwise. However, it was only recently that the observation of ordered crystalline phases via DNA assisted self-assembly was reported [36–38]. Most of these crystal structures have been realized for nanoparticles only. In most cases, however, the aggregation of DNAcc resulted in amorphous, fractal-like phases caused by the strength of the intercolloid attractive forces and the narrow temperature window around the melt temperature mentioned above [6, 37–40]. The narrowness of this melt temperature makes it difficult for the system to be ‘annealed’ into its equilibrium structure. However, the resulting ‘dynamically arrested states’ could be utilized to form new materials with well-defined porous structures for photonics and battery applications[8, 41].

A number of strategies including using mobile DNA linkers [10, 42, 43], grafting both DNA and an inert polyemer to the colloidal particles [34] and using nanoparticles instead of micron-sized colloids [36, 44] have been proposed to overcome these kinetic barriers. Because of their low DNA binding capacity and high diffusivity, DNA coated nanoparticle systems have been more successful for realizing a number of crystal structures [36, 44, 45]. Crystalline superstructures realized using DNAcc nanoparticles are extremely fragile as they consist roughly of 90% water, owing to the length of spacer used [6]. Recent work by Wang *et al.* [46] has demonstrated a number of different crystal phases in systems with high DNA to colloid grafting density. Their high DNA grafting density permits the bound colloids to roll over each other and hence allows the system to relax into thermodynamically favourable crystalline structures. However, the slow cooling of the system to allow for effective hybridization which is required for obtaining well equilibrated structures is very

time consuming [46]. When thermodynamic pathways for relaxation of the system are extremely slow and are hindered greatly by kinetic barriers, externally applied force fields such as gravity, compressive or shear stress, electric and/or magnetic fields can be used to direct the assembly of micron sized building blocks into well defined complex structures [47, 16]. Since, it is more difficult to thermally organize larger particles ($> 1.0\,\mu m$) into ordered assemblies, these methods can play a crucial role in engineering their self-assembly.

Chapter 3

Mobile DNA Linkers : A New Approach

This chapter presents a new approach for introducing mobile DNA linkers at the oil/water interface for studying the equilibrium self assembly of DNA coated colloids on a perfectly smooth substrate. This chapter also covers the general experimental protocols including designing DNA coatings, sample preparation, data acquisition and analysis techniques that are common to the remainder of the thesis. The work presented here was largely published in Joshi *et al.* [42].

3.1 Introduction

Ever since its discovery [25] DNA has received wide attention as a carrier of genetic information and the fundamental unit of life. After the seminal papers by Mirkin *et al.* [33] and Alivistos *et al.* [32], its utility as a tool for engineering the assembly of nano and micron sized building blocks became popular. Due to the highly specific and thermally reversible binding between two single stranded DNA, it can be used to as an 'intelligent-glue' for assembling complex superstructures [6–8]. Because of the ease of thermal annealing, it was intitally envisioned that it would be rather straightforward to assemble nano and micron sized building blocks into regular structures using DNA linkers [36–38, 48, 49, 44]. However,

the DNA attached to hard colloids is immobile and acts as a 'molecular velcro', hindering the system from annealing into equilibrium structures [6, 50]. The resulting 'dynamically arrested states' could be utilized to form new materials with well-defined porous structures for photonics and battery applications [8, 41].

To design DNA driven equilibrium self-assembly, various groups have explored functionalizing lipid layers on hard spheres [51], vesicles [43] and oil in water emulsion droplets [9, 10] with single-stranded (ss)DNA. The motivation for using such fluid substrates was to ensure that the grafted ssDNA could diffuse on the surface and enable annealing into equilibrium superstructures. The DNA can then accumulate into 'rafts' at the point of contact between two particles with complementary functionalization. Hence, enabling them to access otherwise kinetically hindered equilibrium pathways to self assembly using mobile anchors. Apart from being expensive and cumbursome, a major drawback of the above strategies is the limited amount of ssDNA that could be incorporated into the phospholipid mono/bilayers becasue the cholestrol anchors holding the DNA tend to phase seggregate and crystallize at higher concentrations [9, 10]. Here, we present a two-step approach that allows us to create oil droplets densely coated with mobile ssDNA that can reversibly bind DNA coated colloids at the interface.

The following section covers the general experimental methods, sample preparation protocols, data acquisition and analysis techniques utilised for all the experiments covered in this chapter and protocols that are common to the remainder of the thesis. Sample preparation typically comprises of the following steps – DNA hybridizaion to assemble double stranded (ds)DNA spacer, grafting desired DNA constructs to micron sized colloids or oil droplets, washing to remove excess supernatant, density matching the colloids (if needed) and finally mixing them and placing them in the sample chambers and sealing. These samples are then imaged under a Nikon Ti-E inverted epifluorescence microscope. Image processing and

further analysis of the video microscopy data is done using homebuilt ImageJ and Matlab scripts.

3.2 DNA functionalization

We buy custom designed DNA strands from Integrated DNA Technology having the structure 5'-Biotin-TTTTT-rigid DNA spacer-TTTT-sticky end-3'. Fig 3.1 shows the geometry of a typical DNA coating used in our experiments, with a biotin functionalisation on the 5' end, a double stranded (ds)DNA spacer, flexible joints (TTTTT) and a 'sticky overhang' at the 3' end. Table 3.1 lists various DNA constructs used throughout this thesis. The name of the DNA constructs refers here to the single stranded (ss)DNA sticky end with the numeral subscript indicating the number of base pairs it is comprised of in such way that A_6 only hybridizes to the complementary A_6' strand. The choice of sticky end gives freedom for coding numerous binding rules in our experiments whereas the hybridized S/S' pair acts as a rigid spacer. Since the length of this dsDNA spacer (usually 60 base pairs

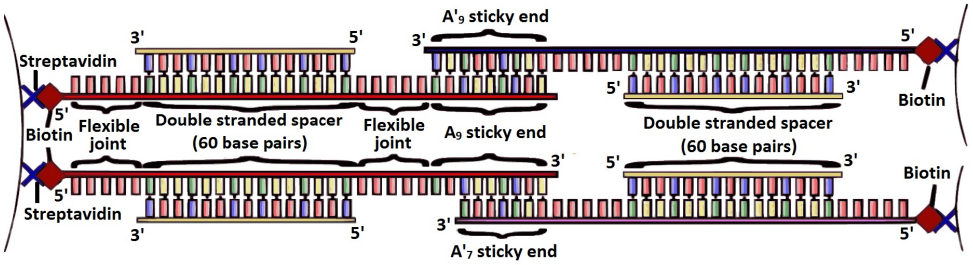

Fig. 3.1 Artistic depiction of a typical DNA coating. A biotin functionalisation on the 5' end, a double stranded (ds)DNA spacer, flexible joints (TTTTT) and hybridization between the 'sticky overhang' at the 3' end.

$\sim$20 nm) is less than the persistence length for dsDNA ($\sim$ 40 nm), they act as rigid rods forcing the sticky ends away from the surface of colloids. The 5-thyamine (T) bases attached on either sides of the dsDNA spacer act as flexible spacers to enhance the pivoting motion of the DNA constructs. The flexible joints and the dsDNA spacer aids the sticky end to

explore a larger volume around their grafting point (like an elbow joint) thereby reducing the entropic cost for hybridization between two complementary tethered strands. The range of DNA mediated attractions is of the order of a few nm, which is less than 50 % of the colloidal diameter. Under our experimental conditions (ionic strength, pH, temperature), electrostatic and dispersion interactions become negligible at intercolloidal distances < 2 nm, while steric repulsions have a much broader range. Hence, stabilizing the colloids against non-specific aggregation. Explained below is a general protocol followed for most of our sample preparations. System specific binding rules have been mentioned as and when needed.

Table 3.1 Various DNA constructs used in the experiments. A_n sticky ends are complementary to A'_n while the S/S' pair forms the double stranded (ds) DNA spacer.

B	5' — Biotin — TTTTT — S — TTTTT CG CAG CAC C — 3'
A_9	5' — Biotin — TTTTT — S — TTTTT ATC CCG GCC — 3'
A'_9	5' — Biotin — TTTTT — S — TTTTT GGC CGG GAT — 3'
A_7	5' — Biotin — TTTTT — S — TTTTT CCC GGC C — 3'
A'_7	5' — Biotin — TTTTT — S — TTTTT GGC CGG G — 3'
A_6	5' — Biotin — TTTTT — S — TTTTT CCG GCC — 3'
A'_6	5' — Biotin — TTTTT — S — TTTTT GGC CGG — 3'
S	5' — GAG GAG GAA AGA GAG AAA GAA GGA GAG GAG AAG GGA GAA AAG AGA GAG GGA AAG AGG GAA — 3'
S'	5' — TTC CCT CTT TCC CTC TCT CTT TTC TCC CTT CTC CTC TCC TTC TTT CTC TCT TTC CTC CTC — 3'

3.2.1 Hybridizing dsDNA spacer

The first step in preparing DNA coatings involves hybridizing the S/S' pair to form a rigid dsDNA spacer. This is achieved by mixing equal amounts of the desired single stranded DNA (ssDNA) say A_6 construct with an inert ssDNA - S', which is complementary to the spacer between the flexible T joints in the DNA construct, at 50 mM NaCl in the Tris-EDTA (TE) buffer. This solution is then incubated at 90 °C for an hour and then cooled to 4 °C at

the rate of 1 °C/min. The slow cooling rates ensure DNA equilibrium hybridization with maximum matching between the ssDNA pairs.

3.2.2 Preparing DNA coated colloids

A chosen volume (typically 5 µL) of a colloidal polystyrene (PS) suspension (from Microparticles GmbH) are diluted 100× by adding TE buffer and sonicated for 30 minutes to break non-specific aggregates. Two different sizes of PS colloids, $d_s = 0.527$ µm and $d_l = 1.2$ µm with either Green or Red fluorescence are used. These colloids are surface functionlised with streptavidin with an estimated DNA binding capacity per unit surface area of $bc_s \sim 2.5 \times 10^4/\mu m^2$ and $bc_l \sim 6.5 \times 10^4/\mu m^2$. After sonication, the colloids are then mixed with the solution of biotinylated DNA with a hybridized S/S' spacer and an overall NaCl concentration of 50 mM is established. DNA concentration is usually set to a ten times excess with respect to the overall binding capacity of the colloids. DNA attaches to the surface of the colloids via the biotin-streptavidin linkage. The concentration of NaCl was subsequently raised to 100 mM, 200 mM and 300 mM while incubating on the rollers for 4-6 hours after each increment. Constant motion prevents the colloids from aggregating under gravity. Adding excess salt helps increase the grafting density by reducing the Coulomb repulsion among closely packed negatively charged DNA brushes. In the presence of excess salt, colloidal aggregation due to charge screening competes with DNA grafting to the colloidal surface. The rationale behind doing an incremental salt addition is that, low salt concentration favours packing finite amount of DNA on the surface of the colloids. This DNA brush is needed to prevent the colloids from aggregating non-specifically at higher salt concentrations while facilitating a denser packing in the DNA brush. In certain experiments, we add a small fraction (usually 0.3× excess with respect to the overall binding capacity of colloids) of the biotin functionalised polyethylene-glycol (PEG-Bio – 5000 kDa PEG, Laysan Bio Inc. Arab, USA). This reduces the grafting density of 'active' DNA linkers on the colloidal surfaces,

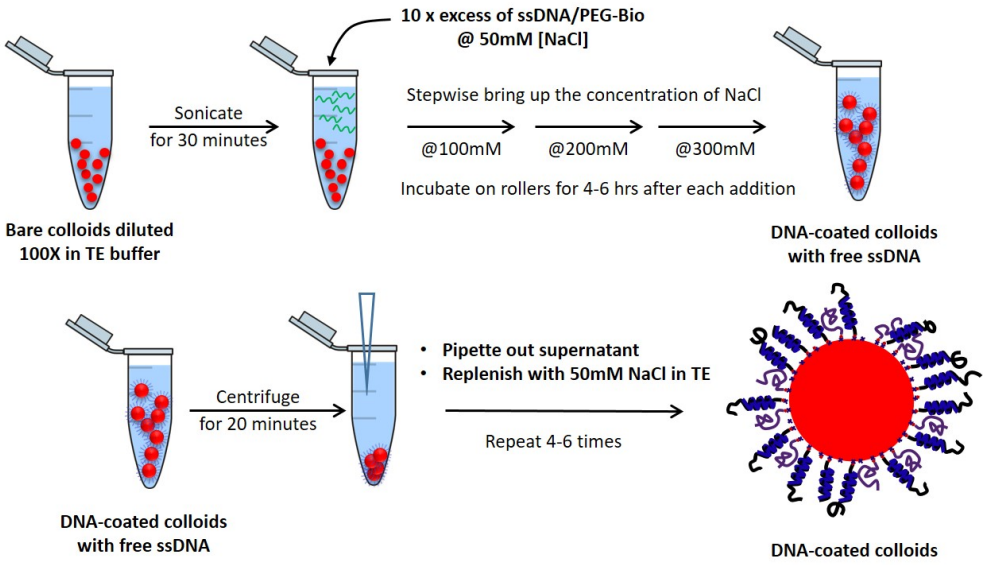

Fig. 3.2 Cartoon summarizing various stages of protocol for grafting biotinylated ssDNA to streptavidin functionalised polystyrene colloids.

thereby decreasing the melt temperatures. Because of its small radius of gyration (~ 3 nm) with respect to the lengths of the DNA constructs, PEG does not add to steric repulsion. The colloids are then pelleted using a microcentrifuge, supernatant is removed and the DNA coated colloids are then resuspended in 50 mM NaCl in TE buffer heated to 40 °C. This washing protocol is repeated $4-6$ times so as to remove the excess DNA and salt present in the system [8]. The washing protocol is done in 50 mM NaCl in TE buffer thereby ensuring steric stability of the DNA brush attached to the colloids. Depending on the requirements of the experiment, the PS colloids could be density matched ($\rho = \mathrm{g/cm^3}$) using sucrose solution. Fig 3.2 summarizes various stages of DNA functionalisation protocol for PS colloids.

3.2.3 Preparation of oil droplets (ODs)

Oil droplets are made by flowing a silicone oil with a dynamic viscosity of 50 cSt and an aquous solution containing 10 mM sodium dodecyl sulphate (SDS) (from Sigma Aldrich) into a microfluidic device. The device is plasma cleaned prior to use, filled with water immediately afterwards to slow down the loss of hydrophilicity of the device walls and

tested for leaks. The channels used are 20 µm wide and 25 µm high. Using syringe pumps (Harvard Apparatus, USA and Nemesys, Cetoni, Germany), we first flood the channels with 5 to 10 mM SDS solution by flushing it at a flow rate of 250 $\mu L\,h^{-1}$. Once SDS has filled the channel, we introduce the 50 cSt silicone oil (0.971 g/mL) at the rate of 25 $\mu L\,h^{-1}$ into the channels. Droplets are formed at the junction and are collected at the outlet (Fig 3.3). These are polydisperse ODs having diameters between 20-30 µm. ODs are stored in a 10 mM SDS solution and kept in the fridge at 4°C. They remained stable for a minimum of two years. All solutions were prepared in deionized water.

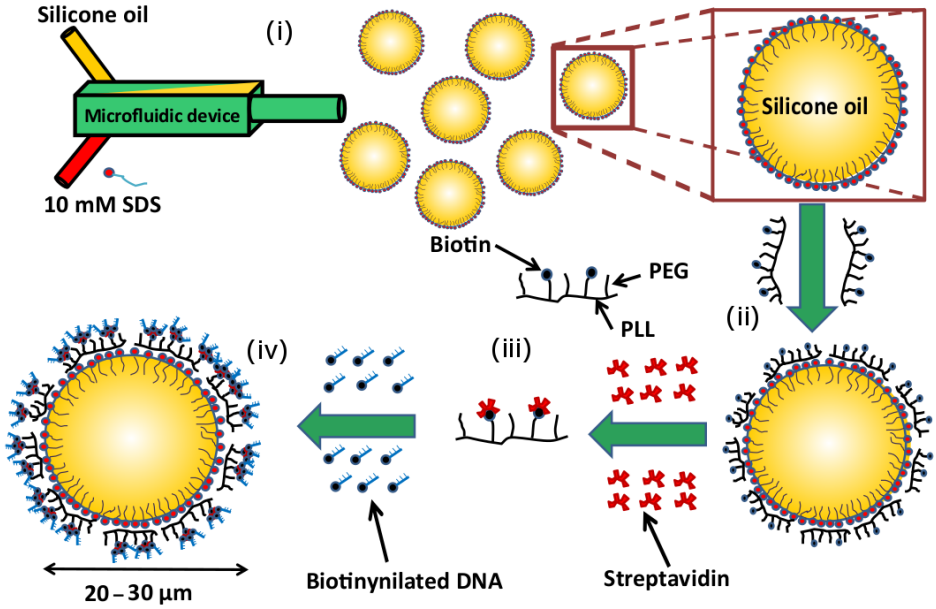

Fig. 3.3 Schematics showing various stages of functionalising oil droplets (ODs) with DNA (i) 10mM sodium dodecyl sulphate (SDS) and 50 cSt silicone oil are mixed in a microfluidic channel to prepare SDS stabilized ODs (ii) PLL-PEG-Bio adsorbs flat on the surface of ODs that are negatively charged due to the sulphate head group of SDS (iii) Texas Red labelled streptavidin linkers are then attached to the biotin heads on the ODs from solution, (iv) biotinylated ssDNA binds to the streptavidin linkers on the surface of ODs.

3.2.4 Functionalizing oil droplets with DNA

In order to achieve a similar DNA-binding capacity /µm^2 on the oil droplet as that on the colloids, 100 µL of the freshly prepared oil droplets stabilised in 10 mM SDS solutions

are taken from the creamed layer and mixed with 100 µl (1 mg/ml) of polylysine-g[3.5]-polyethyleneglycol-biotin (PLL-PEG-Bio) (from SuSoS AG, Switzerland). 1 M NaCl solution and 250 µl of 1 mM SDS solution in TE buffer is then added to establish an overall concentration of 50 mM NaCl and > 2 mM SDS. This mixture is then incubated on rollers overnight and washed twice with a wash solution (5 mM SDS, 50 mM NaCl in TE buffer), and then dispersed in a suspending solution (2 mM SDS, 50 mM NaCl in TE buffer). Since the droplets cream when the eppendorf is left vertical, we use a syringe to remove the buffer beneath the droplets. Further, 10 µl (1 mg/ml) of Texas Red labelled streptavidin (Sigma-Aldrich) per 100 µl of the droplets is added and they are incubated on the rollers for another hour. The droplets are then washed twice with the wash solution and suspended in suspending solution to remove excess streptavidin from the solution. This procedure provides oil droplets with approximately the same streptavidin coverage ($\sim 10^4$ µm^2) as that on the colloids. It is important to note that the droplets should not be left for incubation with streptavidin beyond 1.5 hrs. Doing so results in the bridging of oil droplets via streptavidin linkers and leads to coalescence. Streptavidin coated ODs are then mixed with the required biotinylated DNA having a hybridized S/S' spacer in a 10× excess. They are then allowed to incubate on rollers at a 50 mM NaCl and < 2 mM SDS. After 12 hours, the salt concentration is raised to 100 mM while maintaining the SDS concentration. After another 6 hours on the rollers, the DNA coated ODs are washed thrice using the wash solution and resuspended in the suspending solution to remove any unbound DNA. Fig 3.3 illustrates various stages of the protocol for introducing mobile DNA linkers on the ODs.

Depending on the experiment, DNA coated colloids and/or DNA coated ODs with complementary sticky ends are mixed to prepare the desired samples. Usually, the oil-colloid mixtures are allowed to bind overnight on the rollers. The final NaCl concentration used in all experiments is 50 mM. The desired SDS concentration is adjusted at this stage. Note while the colloids carried A_6' DNA, the ODs are functionalized with A_6 DNA.

Sample chambers

Capillary chambers purchased from CM scientific (0.2×4mm ID) were irradiated under a UV lamp for 30 minutes and then plasma cleaned in an oxygen plasma oven for 2 minutes (Diener Elecronics Femto). About 40 µL of the sample was filled into the capillary chambers using pipettes and then sealed and glued onto a glass slide using a two-component epoxy glue.

3.3 Observational Techniques

3.3.1 UV-Vis spectrophotometry

It is well known that DNA has a characteristic UV-Vis absorption peak at 260 nm. Hence, we utilize UV-Vis measurements for two important primitive quantifications in our experiments. Firstly, we use a Nanodrop 2000 (Thermo Scientific UK) spectrophotometer along with the sequence-specific extinction coefficients to carefully measure the amount of DNA supplied by the vendor (IDT). Secondly, we use a Cary 300 UV-Vis spectrophotometer (Agilent Technologies) with a Peltier temperature controller to record the absorption profile for hybridizing dsDNA spacer pairs for fixed excitation wavelength of 260 nm over a range of temperatures from 30-90 °C. Temperature is varied at the rate of at 0.25 °C/min, taking a measurement for each degree comprising of averaged absorption for a duration 20 seconds. These measurements allow us to obtain the melt temperatures for DNA pairs under varying solvent conditions (see Fig. 3.4).

3.3.2 Zeta (ζ) potential measurement

The ζ potential is defined as the electrostatic potential of the system at the shear plane, where counter-ions are no longer immobilized to the surface and hence don't experience a

synchronised transport with the moving particle. We have used a Zetasizer Nano ZS (Malvern Instruments) for measuring the ζ potential of our bare and DNA coated colloids. It is a dynamic light scattering setup that measures the mobility of particles undergoing stable motion in an electric field, hence providing a non-destructive method for probing the net resulting surface charge. The colloids used here were bought with predefined surface charge and streptavidin coating. Coating the surface of these colloids with DNA, which have a negatively charged backbone, results in a modification of the net surface charge. Prior to measuring, the particles are dispersed in 0.001 wt % solution in TE buffer at 50 mM NaCl.

3.3.3 Imaging and temperature cycling

Once the samples are prepared and sealed as described above, they are then transferred to an inverted epifluorescence microscope (Nikon Eclipse Ti-E) equipped with a CMOS sensor CCD camera (Grasshopper3, Point Grey Research Inc., Sony IMX174) for recording. Depending on the type of measurement we wanted to do, we use either a Nikon Plan Fluor E 40× NA 0.75 dry objective, or a 40× Plan Apo Lambda NA 0.95, or a Nikon Plan APO 60× NA 1.20 water immersion objective. A built-in perfect focus system in the microscope prevents the sample from going out of focus due to thermal or other drifts. A blue LED source (Cree XPEBLU, 485 nm) and a white lamp source is used to excite the fluorescence on the colloids and on the ODs. A home-made computer-controlled Peltier device is used to control and cycle the temperature of the system during measurements. A thermocouple, connected to the Peltier device is placed directly in touch with the sample chamber to measure the temperature of the sample. Samples could be heated or cooled at desired rates using the PID controller and videos recorded under red or green fluorescence and bright field. We also used a Leica TCS SP5 microscope equipped with HCX PL APO 40× /0.60 dry objective to image Z-stacks of the samples. Typical heating and cooing rates in our experiments were 1 °C/min. Image conversion and analysis were done using customised ImageJ and Matlab routines.

3.4 Results and Discussion

3.4.1 DNA functionalization of ODs and colloids

Before grafting the desired DNA construct (Table 3.1) to the surface of colloids or ODs, it is important to ensure that the dsDNA spacer pair S/S' has been assembled properly and will not fall apart duing thermal cycling meant for dissociating the sticky ends. The melt temperature (T_m) of a given pair, for instance S and S' is defined as the temperature at which half of all possible hydrogen bonds between the bases is formed, while the other half is still un-bound. T_m for a DNA pair depends on the number of bases that can bind and the solvent conditions. Since the S-S' spacer pair is much longer than the sticky ends (Table 3.1), for given solvent conditions, T_m for the dsDNA pair is expected to be much higher than that of the sticky ends used.

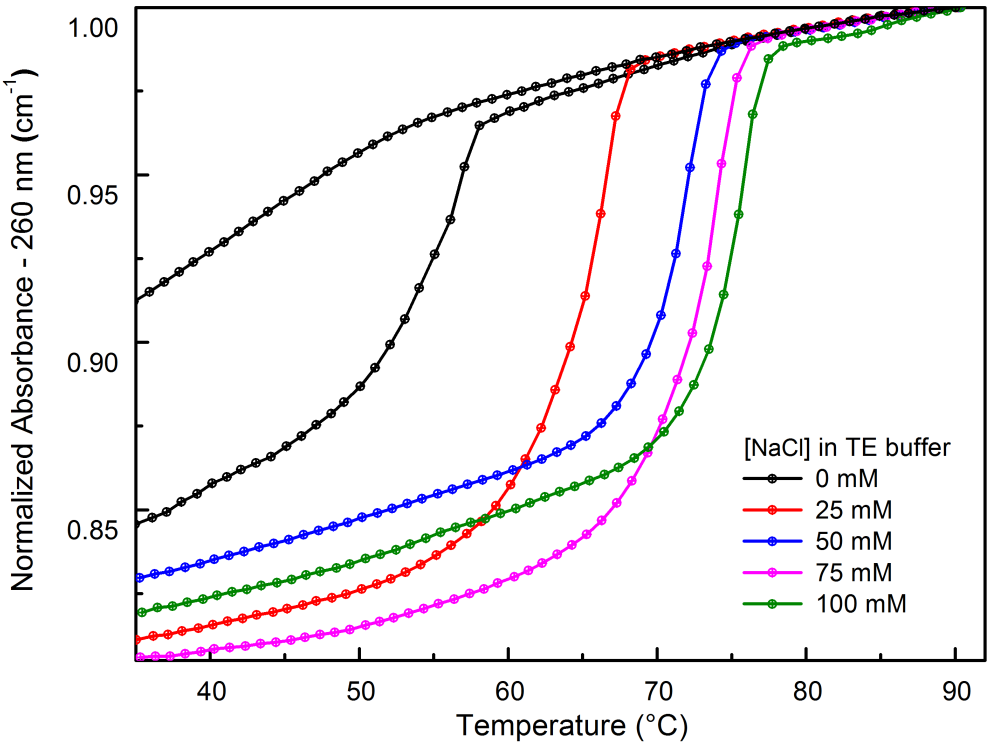

Fig. 3.4 Temperature dependence of absorbance at 260 nm for a mixture of A_6 and S' DNA at various salinities. A sharper decrease in absorbance at higher salinities shows the importance of added salt in facilitating a better hybridization of the S/S' duplex – the dsDNA spacer pair for A_6 DNA construct.

Fig 3.4 shows absorption profiles for a mixture of A_n and S' under various solvent conditions in the temperature range 30-90 °C. We observe a plateau at higher temperatures (all strands are unbound), followed by a decrease in absorbance over a temperature range which again saturates at lower temperatures (All pairs have formed). This decrease marks the transition of S/S' pair from a fully dissociated (higher temperatures) to mostly hybridized (lower temperatures) state. This is because the absorption of ssDNA at 260 nm is greater than the net absorption of the hybridized dsDNA. The presence of counter ions in the solvent shields the charges along the DNA-backbone and facilitates a close proximity required for stronger hybridization of ssDNA into duplexes. With an increase in the amount of added salt, the melt temperatures shift to higher values and the transition becomes sharper - indicating a stronger binding in the DNA duplexes. Hence, to ensure the stability of long dsDNA spacer during our experiments, we always maintain a minimum of 50 mM concentration of NaCl in our samples. It should be noted that slow cooling and heating curves lie on top of each other (except for the case of no added salt), reflecting the equilibrium nature of the hybridization process. In the absence of added salt, repulsion between the highly charged DNA-backbones hinders a proper hybridization of DNA duplexes.

Geometry of the PLL-PEG-Bio chain at the oil-water interface

Fig 3.5 shows a schematic representation of polylysine-g[3.5]-polyethyleneglycol-biotin (PLL-PEG-Bio), a comb-like polyelectrolyte, arranged on the surface of sodium dodecyl sulphate(SDS) stabilized oil-droplets. SDS is a negatively charged surfactant with an effective head-group size of roughly 50 Å^2 corresponding to a radius of about 0.3 nm [52]. PLL-PEG-Bio has a 20 kDa poly-lysine backbone comprising of 137 repeat units. To every third to fourth lysine repeat unit a 2 kDa PEG chain or 3.5 kDa PEG-Bio chain is attached. While a lysine monomer carries one positive charge on the amino group, the repeat-units linked to a PEG chain via that amino group are neutral. Hence, each PLL backbone made of 137

repeat units will carry ∼40 positive charges [53], allowing the backbone to adsorb flat on the negatively charged SDS head-groups at the OD-water interface. The radius of gyration of a

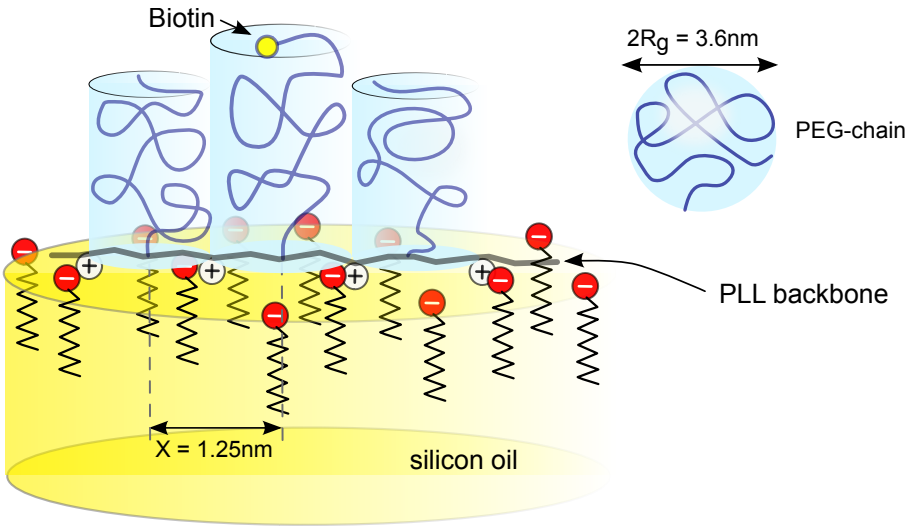

Fig. 3.5 Schematic illustration of a part of the PLL-PEG-Bio chain adsorbed to the oil-water interface through the Coulomb attraction between the positive charges on the polylysine backbone and the negatively charged head groups of the SDS surfactant. At approximately every 3.5 lysine repeat units a PEG chain is attached, half of them with molecular weight of 2 kDa and the other, holding a biotin end, with 3.5 kDa. The lysine monomer is 0.355 nm long. The radius of gyration, R_g, of the unbound PEG(2 kDa) chain is ∼1.8 nm.

free 2 kDa PEG chain in good solvent conditions is about 1.8 nm [54]. However, a PEG chain achored at every 3.5 repeat lysine unit on average corresponds to an inter-anchor spacing of about 1.5 nm. Half of the roughly 40 PEG chains per PLL backbone carry a biotin group. The 3.5 kDa chains carrying the biotin ends will have an even larger R_g. This means that the PEG chains must be in a comb-like configuration when the PLL is lying flat on the OD surface, as the osmotic pressure building up between the PEG chains will force the PLL chain to be in a stretched configuration. Hence, the hydrophilic, uncharged and flexible PEG side chains align perpendicular to the interface forming a comb-like geometry [55, 53]. Also, since the PEG-Bio chains (3.4 kDa) are longer than the other ones, it makes biotin accessible for attaching streptavidin from the solution.

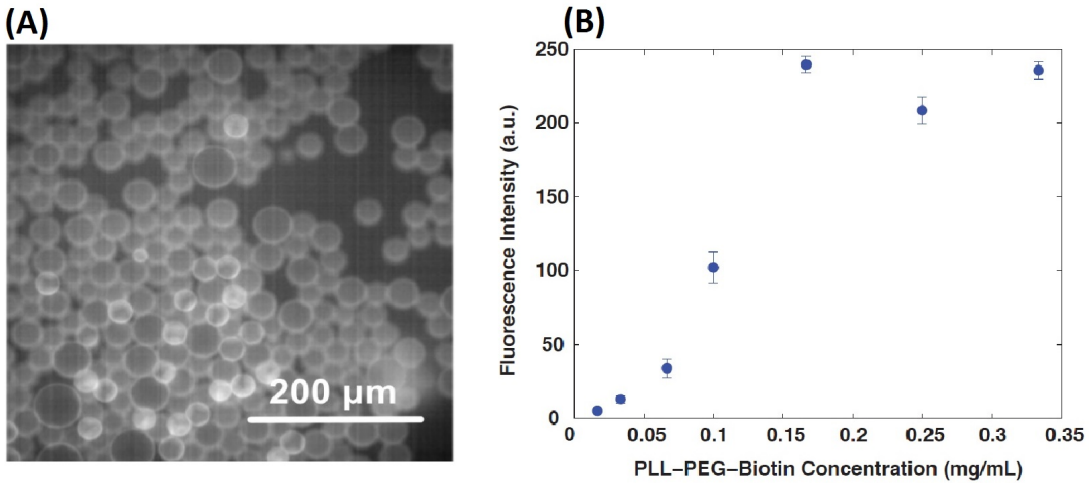

Fig. 3.6 Surface coverage of ODs with PLL-PEG-Bio. (A) Fluorescence image of the oil droplets after attaching Texas Red labelled streptavidin from solution, indicating presence of surface bound streptavdin and (B) Calibration curve for the surface coverage of PLL-PEG-Bio, obtained by titrating a fixed volume of ODs (25 µL) in suspending solution (2 mM SDS, 50 mM NaCl) with a solution of PLL-PEG-Bio in an overall volume of 300 µL. Fluorescence intensities of the Texas Red labelled streptavidin, extracted by averaging on the contour of the droplet, were used as a measure for the approximate surface coverage of PLL-PEG-Bio on the ODs. The error bars are the standard error of the mean for each concentration (experiments done in collaboration with Dylan Bargtail, NYU).

PLL-PEG-Bio adsorption on the surface of oil droplets

In Fig 3.6 we show a calibration curve for the adsorption of PLL-PEG-Bio on the SDS stabilized ODs. The coverage of PLL-PEG-Bio on the OD was tested by binding fluorescently labelled streptavidin to the biotinylated PEG ends (Fig 3.6). After removing excess PLL-PEG-Bio from the OD solution Texas Red labelled streptavidin was added adsorbing readily to the biotinylated PEG end groups. The clearly visible fluorescence on the OD surfaces (Fig 3.6 A) supports the assumption that the PLL-PEG-Bio chains are located at the oil-water interface. We used fluorescence intensity measurements to estimate the maximum PLL-PEG-Bio grafting density for a fixed volume of ODs (Fig 3.6 B). All experiments presented in this thesis were performed at the onset of the saturated grafting regime to avoid free, unbound chains in solution. An increase in fluorescence intensity by several orders of magnitudes was observed, in comparison to that of biotinylated lipid-monolayer stabilised droplets reported earlier [10]. Here, we obtained a higher coverage of streptavidin linkers ($\sim 10^4\ \mu m^{-2}$) on the

OD surface, which corresponds to an average distance of < 10 nm between biotin-streptavidin ends.

After removing excess streptavidin from the continuous aqueous phase, we grafted biotinylated ssDNA, A_6, to the OD-solution—again any unbound DNA was removed before adding 0.52 µm, green fluorescent PS colloids coated with A_6' DNA. For the DNA coated colloids, ζ potential measurements provide a non-destructive method to probe and quantify the presence of surface grafted DNA. For 0.52 µm polystyrene colloids, ζ potential changes from (-32.03 ± 0.72) mV to (-47.5 ± 1.5) mV and for 1.2 µm colloids it goes from (-43.06 ± 1.15) mV to (-49.8 ± 0.9) mV for bare and DNA coated colloids respectively. This significant change in ζ potential indicates an enhanced stability of the colloids due to an additional negatively charged DNA brush on the surface of the colloids. Final aqueous conditions are maintained at an added NaCl concentration of ∼50 mM. After incubating the samples overnight for DNA equilibrium-hybridization, the samples are then studied using epifluorescence video microscopy. In most samples we use colloidal bulk volume fractions of $\Phi_c \leq 0.05\%$. Looking at (Fig 3.7) it is evident that the PS particles have hybridized to the ODs, while a considerable fraction of the colloids remained in the aqueous bulk phase. Since the ODs cream and touch the upper wall of the sample chambers, proximity of wall will affect the behaviour of colloids bound to ODs in that region. Hence for our analysis, we focus on the area around the'south pole' of the ODs, away from the wall.

Further proof that our colloids were indeed anchored to the OD-surfaces purely via DNA-hybridization and not due to surface tension effects like in Pickering-Ramsdon emulsions[56] or other non-specific interactions came from several different control experiments. In the first one, we mixed our ODs having A_6 DNA with colloids coated with non-complementary B DNA, using the standard solvent conditions with SDS concentration of ∼2 mM. No colloidal adsorption to the ODs was observed, even after a week. In the second control sample we replaced the A_6' DNA on the colloids by PEG-Biotin that formed a similar steric stabilization

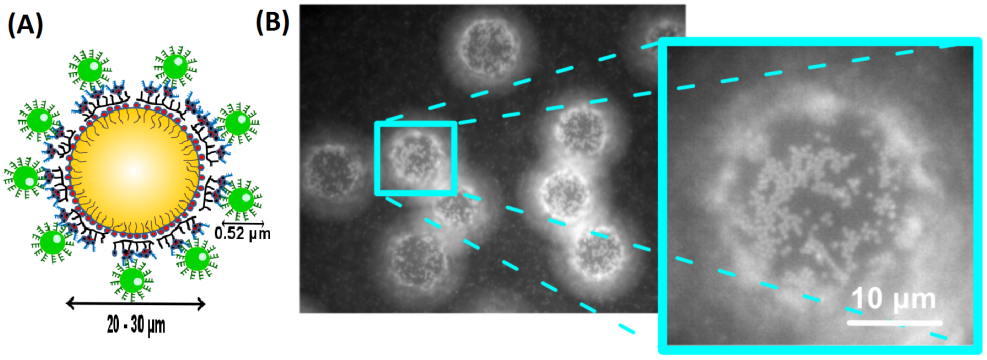

Fig. 3.7 Polystyrene colloids hybridize to oil droplets. (A) Artistic representation and (B) typical epifluorescence image showing 0.52 µm fluorescent colloids hybridized to the OD surfaces with a zoom onto the *'south pole'* of the droplet

layer as the DNA linkers, while the ODs were either grafted with A_6 or B DNA. These samples also did not show any signs of binding between the ODs and the colloids. Even the mixtures of DNA-coated colloids and bare SDS-stabilised ODs did not display any colloidal adsorption on the oil-water interfaces at all bulk SDS-concentrations used. Hence, these control experiments proved that the binding between the colloids and the ODs are the strictly mediated through 'active' DNA linkers.

3.4.2 Thermoreversibility: melting-off colloids from the ODs

After confirming that the attachment of colloids to ODs is mediated via the hybridization of ssDNA sticky ends, we move on to verify whether it is possible to remove the colloids from the OD-water interface by heating the sample well above the hybridization ('melt') temperature for the sequence used here. The width of the melt region for complementary ssDNA free in solution is typically $\Delta T \sim$ 10-20 °C, depending on the solvent conditions and the DNA concentration [57], but it narrows down to $\sim$1 °C when the same DNA strands are attached to colloids only [6]; moreover T_m shifts to higher values. In a control experiment in which we mixed 0.52 µm particles half functionalized with A_6 and the other half with A_6', using the same solvent condition as those used in the OD experiments, we measured $T_m \simeq$ 35 °C (Fig 3.9).

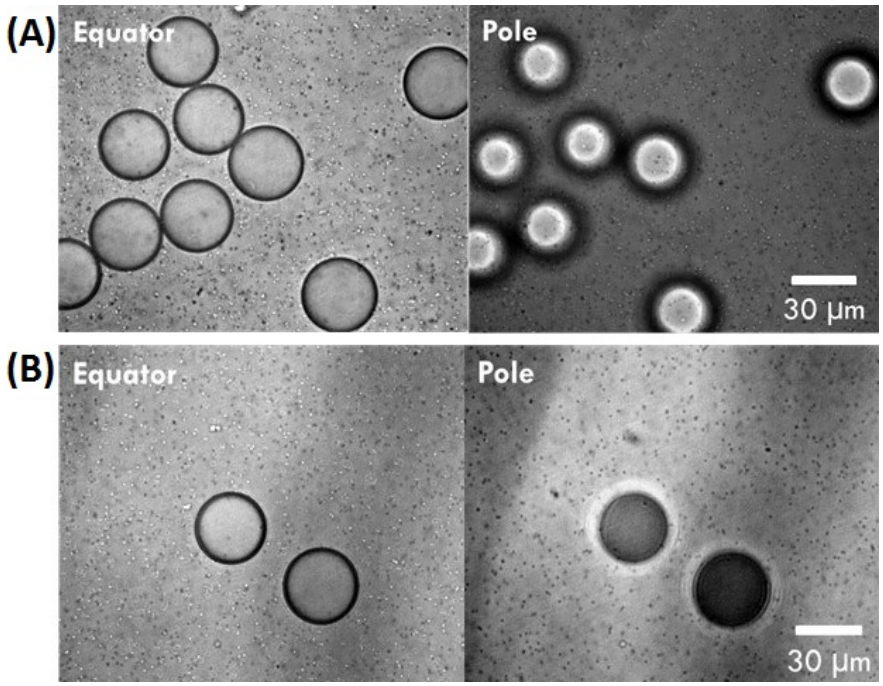

Fig. 3.8 Switching off active DNA 'glue' - A) Control Sample 1: ODs are coted with A_6 DNA while the 0.52 µm fluorescent colloids are coated with a non-complementary DNA strand B, B) Control Sample 2: ODs are coated with A_6 while the streptavidin sites on the 0.52 µm fluorescent colloids are passivated by PEG-Bio. In both cases colloids did not attach to ODs at all, affirming that the ODs and colloids strictly interact via complemetry DNA hybridization.

After mixing A_6'-functionalized 0.52 µm particles with the A_6-coated ODs ($\sim$2 mM SDS, 50 mM NaCl in TE buffer) we let the colloids hybridize to the ODs overnight at room temperature. The fluorescence images in Fig 3.10 show that at room temperature, liquid colloidal islands coexist with non-aggregated colloids hybridized to the interface. As we increased the temperature (using a computer-controlled piezoelectric heating stage on the microscope) these islands became smaller and more mobile, but even when heating beyond 35 °C most colloids did not detach from the droplet surface – rather, the particles diffused ever faster. Even after heating to 80 °C, very few particles came off. We hypothesize that the reason for the strong binding of the colloids is the mobile anchoring of DNA on the ODs. Since the A_6 DNA bound via PLL-PEG is mobile, the moment a colloid lands on the ODs surface, A_6 DNA will accumulate in the contact region and hence the binding strength will increase with time. Consequently the final number of A_6-A_6' bonds in the contact region will

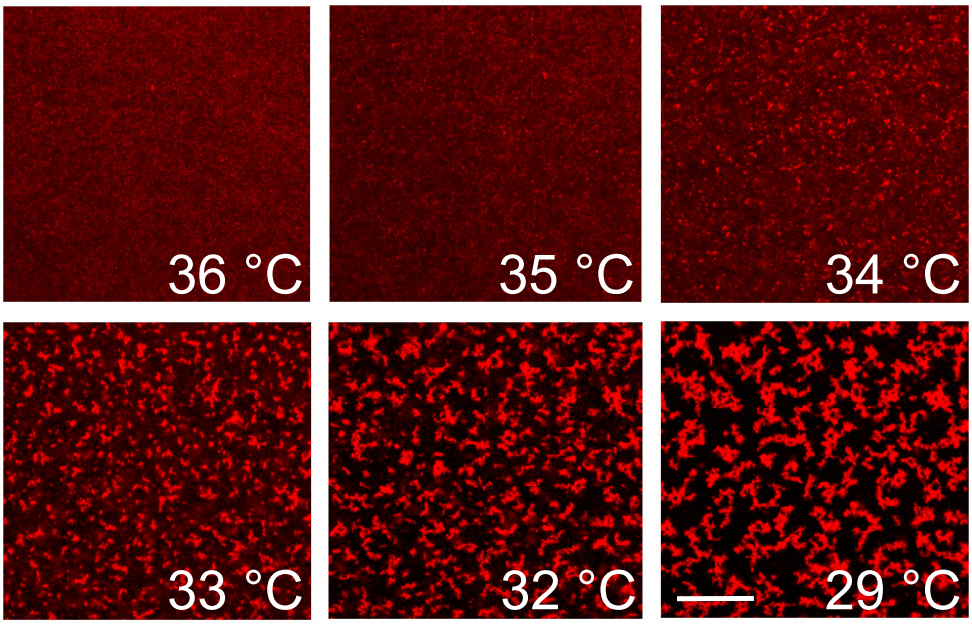

Fig. 3.9 Phase transition of the DNA-functionalized PS spheres. Fluorescence-microscopy images showing the transition from a high temperature uniform gaseous phase to a low temperature gelled phase (upon cooling) in a single component system of red fluorescent 0.52 µm large colloids, where half of the colloids were coated with ssDNA, A_6, and the other half with A_6' DNA, in 50 mM NaCl in TE buffer. The scale bar is $\sim$ 50 µm.

be in this case larger (and T_m will be higher) than that for the contact region between two hard spheres where the A_6 DNA is fixed. This effect will be enhanced by the fact that the effective contact region between colloids and ODs is larger than that between two colloids with the same curvature.

However, reducing the overall 'active' DNA bridges should result in a reduction in binding strength and consequently lowering of the T_m. To test this hypothesis we reduced the total number of A_6' strands on the PS particles by replacing 70% of the A_6' strands by non-complementary B strands. The images for increasing temperatures in Fig 3.10B show that now particles start to melt off the surface at $\sim$56 °C; at $\sim$66 °C almost all bound particles have left the OD surfaces. This supports our assumption that the colloid-OD binding is due to DNA hybridisation and that the very strong binding experienced by colloids with a dense A_6' coating is due to the accumulation of complementary, PLL-PEG bound DNA in

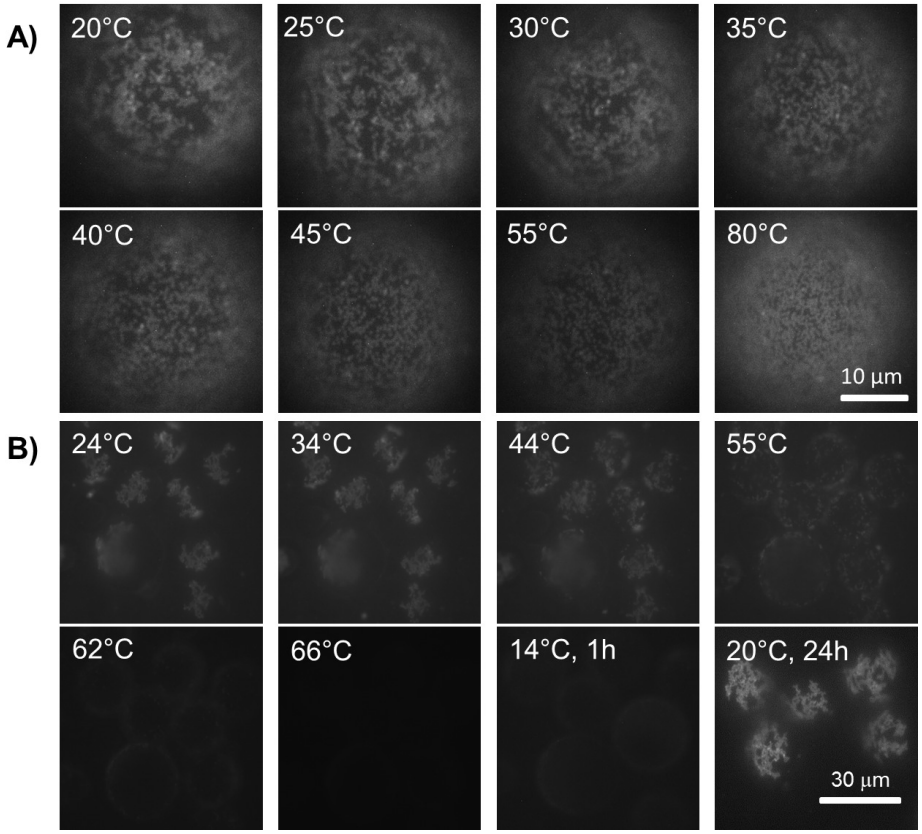

Fig. 3.10 Thermal recyclability of colloidal binding at the interface. Sequence of fluorescence images showing heating of a sample of 0.57 µm colloids grafted to ODs using colloids A) fully covered with A_6' DNA (∼1.5 mM SDS and 50 mM NaCl concentrations); and B) where 3/4 of the A_6' DNA are replaced by non-binding B (∼2.5 mM SDS and 50 mM SDS) . In all images we focus on the *south pole* of the ODs using the same illumination and exposure time. A) For full coverage most colloids remained on the OD surface even when heating to 80 °C, though they became increasingly more mobile, which is expressed in the increasingly more blurry appearance of the images. B) For samples with reduced number of binding sites on the colloids melting set in at ∼56 °C, and at ∼70 °C almost all colloids have come off the ODs. The image taken shortly after cooling the sample (over a period of 1 h) to 14 °C showed only few colloids bound to the ODs. The same sample recovered similar coverage and aggregation state as the initial samples after 1 day (bottom most right image)

the contact region. We also note that the melting region is not as sharp as for hard particles, although a larger number of binding DNA in the contact area would suggest a narrowing of the melt region. This widening can be understood by considering that the distribution of PLL-PEG bound DNA over the different colloidal contacts is determined by kinetics: some colloids will accumulate more than others. However, once bound, redistribution of PLL-PEG-DNA domains over different colloidal contacts is very slow. Hence, some colloids are more strongly bound than others. This broadening will only occur if the deposition of colloids on the ODs is relatively fast. Otherwise, every colloid that lands on the surface has time to accumulate its full share of PLL-PEG-DNA. But of course, this also means that less PLL-PEG-DNA remains for any subsequent colloids.

Note that after melting off the particles the initial particle grafting density on the OD's is recovered upon cooling back to 20 °C, be it that the process is very slow. An hour after cooling initially to 14 °C few colloids have hybridized back to the ODs, and only after 1 day at room temperature we recover the initial colloid density (Fig 3.10B).

3.4.3 Conclusion

We have demonstrated a novel approach for functionalizing oil droplets with DNA. This simple approach results in a relatively higher grafting density of DNA at the interface compared to those using expensive biotinylated lipids. Moreover, polystyrene colloids coated with complementary DNA strands could be attached to these ODs. Various control experiments show that the colloids are grafted to the interface via the DNA mediated interactions only, which are highly specific and thermally reversible in nature. Hence, we could release these colloids from the surface of ODs with an increase in temperature and reattach on cooling. This system with tunable functionality is stable over several heating-cooling cycles and also does not show any coalescence of ODs for well over a year. It is intriguing to note that the colloids bound to the surface of the oil droplets sometimes exist freely and in some cases

aggregate and form colloidal *islands* that also move around albeit much slower. Tuning the interaction potential of colloids at the interface, we can use this as a model system for studying the self assembly of DNA coated colloids in a quasi-2d setting. This will be discussed in the forthcoming chapters.

Chapter 4

Kinetic Control of the Coverage of Oil Droplets by DNA-Functionalized Colloids

Building on our strategy introduced in chapter 2 to reversibly bind PS colloids at a liquid-liquid interface, we explore the dynamics and the unexpectedly rich quasi two-dimensional phase diagram of colloidal aggregation that this system exhibits. We make two important observations. Firstly, because of the mobility of the DNA attached to the oil-water interface, the resulting binding density of the colloids becomes dependent on the total colloidal volume fraction in bulk. Secondly, once colloidal adsorption is saturated, a rich phase diagram of colloidal aggregation emerges, which is controlled by the excess concentration of the added surfactant micelles inducing depletion interactions. Varying the micelle concentration in the aqueous phase, a purely entropic transition from a fluid-like phase to a more compact packing of the solid colloids at the interface is observed.

4.1 Introduction

As children, our imagination is set on fire while looking at surfaces of soap bubbles or foams. These omnipresent surfaces which form interfaces between different phases of liquids, gases or solids have also captured the fascination and scientific curiosity of researchers across various disciplines for their importance in day-to-day life and industrial processes. For instance, in biology, cell walls present a complex interface between the outside and inside of the cell, the fundamental unit of all living organisms. Many industrial and technological products such as cosmetics, paints, agrochemicals, medicines, petrochemicals, food, and energy harvesting and storage devices derive their function from interfaces. 'Predictive capability' for governing the self-assembling behaviour of macromolecules and mesoscopic particles into ordered structures and their controlled release at the aforementioned interfaces could pave the way for development of newer and better industrial formulations with end-user functionalities such as personalized medicines and smart drug delivery systems.

However, one of the key challenges in complex self-assembly is the creation of ordered, quasi-2d patterns of many distinct colloids or nano-particles. To achieve this objective, it is important that the substrate is smooth and clean, and that different species of colloidal particles can bind independently and reversibly to the surface. Further, the surface-bound particles should be sufficiently mobile to ensure that the structure that is most stable is also kinetically accessible. Most solid substrates are less than ideal for this purpose: the surfaces often contain defects or impurities that trap colloids and, in addition, bound colloids diffuse slowly on such surfaces. Liquid interfaces would be less susceptible to the above problems. But, the strength with which colloids bind to liquid-liquid interfaces – through the Pickering mechanism [56], are nearly a hundred or thousand times stronger than the thermal energy. As a consequence, controlled and reversible adsorption of different species is difficult to achieve at liquid-liquid interfaces [58, 59]. The dominance of long-ranged capillary forces [60–62] also makes it difficult to control the interactions between surface-incorporated

colloids. Renewed interest in the recyclability and controlled stability[63, 64, 59] of Pickering emulsions over the past decade have opened doors to a plethora of applications. For instance in utilizing them as 'reactors' for building complex templates for new colloidal materials such as colloidosomes [65] and patchy particles [66] or bijels [67] in which phase-separating fluid mixtures are dynamically arrested. Studies of particles at flat interfaces also show a rich two-dimensional (2D) phase behaviour that can be influenced not only by the interactions between the typical colloid-colloid interactions such as van der Waals and Coulomb, but also by the long-ranged deformation of the contacting interface and capillary actions [60, 62].

In this chapter, using our new approach for functionalizing oil droplets with DNA and reversibly adsorbing polystyrene colloids onto them, we show that it is possible to control the amount of colloids that hybridize to the surface of oil droplets. In other words, we can control the surface coverage of colloidal particles on the oil droplets. By exploiting the fact that during slow adsorption, compositional arrest takes place well before structural arrest occurs, we can prepare colloid-coated oil droplets with a 'frozen' or pre-defined degree of colloidal coverage, but with fully ergodic colloidal dynamics on the droplets. We illustrate the equilibrium nature of the adsorbed colloidal phase by exploring the quasi two-dimensional (2d) phase behaviour of the adsorbed colloids under the influence of depletion interactions.

4.2 DNA Functionalisation

The oil droplets and colloids are functionalised as per protocols described in chapter 2. The concentration of NaCl was fixed at $\sim$50 mM for all experiments. The desired concentration of SDS was optimized while mixing DNA coated colloids and ODs. Two different sizes of PS colloids, d_s=0.527 µm and d_l=1.2 µm with either green or red fluorescence (Microparticles GmbH) were used. For ease of tracking particles on the surface of ODs and in the solution we use large particles (d_l=1.2 µm). For all other experiments we use the small particles (d_s=0.527 µm).

4.3 Image analysis and diffusivity measurements

Image conversion and analysis were done using customised ImageJ [68] and Matlab routines. Single particle diffusivity movies were analysed and tracks were generated using the ANALYSE subroutines of ImageJ. These tracks were subsequently analysed using custom Matlab routines generating mean-squared displacements and calculating diffusivities. Several bright-field time series of 1-2 minute durations were recorded and evaluated using a Matlab routine for DDM analysis developed by S. H. Nathan [69]. In DDM, bright field (or fluorescence) microscope images separated by a given time lag are subtracted such that only the dynamic information due to colloid motion remains. Fourier transforming these difference images for varying time lags and correlating them provides the the charecteristic relaxation times for the system, $\tau = (Dq^2)^{-1}$, as function of the scattering wavelength q .

4.4 Results and discussion

4.4.1 Controlling degree of colloidal adsorption on the ODs

One of the most striking features of the colloid-OD system is the ability to control the extent of coverage of oil droplets by colloids. The total colloidal volume fraction(Φ_{bulk} or Φ_b) controls the rate and amount of colloids hybridizing to the surface of ODs. We first mix A_6'-functionalized d_s=0.52 µm particles with the A_6-coated ODs ($\sim$2 mM SDS, 50 mM NaCl in TE buffer). For a fixed amount of ODs and a constant overall volume, we vary Φ_b as - 0.001, 0.005, 0.01, 0.02 and 0.05 wt% of PS colloids. Fig 4.1(A) shows the difference in coverage of ODs by PS colloids for various volume fractions. Fig 4.1(B) shows the surface coverage or surface fraction, $\Phi_{surface}$ as a function of Φ_{bulk} upto 0.02 wt%. The error bars are standard deviation of the average coverage per droplet. Starting with a $\Phi_b \simeq 0.05$ wt %, which corresponds roughly to a full DNA coverage of the ODs in solution, we obtain a relatively high colloid coverage (Fig 4.1(A)), but still a number of colloids remain free in

the bulk solution. Using a ten times lower Φ_b, we observe much fewer colloids on the OD surfaces. Further, when we go down to Φ_b = 0.001 wt% for tracking purposes, we see only one or two particles binding to the ODs. For samples with lower bulk volume fractions Φ_b (between 0.0001 – 0.01 wt%) $\Phi_{surface}$ is estimated by manually counting the number of colloids attached to a given oil droplet and the dividing it with the total surface area of the spherical droplet. For higher coverages, $\Phi_{surface}$ is estimated by counting the number of particles attached near the southern hemisphere and dividing it with the surface area of the corresponding hemispherical cap. For full coverages, due to close proximity of particles, it is difficult to count them. Hence, the adsorption curve presents data of $\Phi_{surface}$ vs Φ_{bulk} only up to 0.02 wt%.

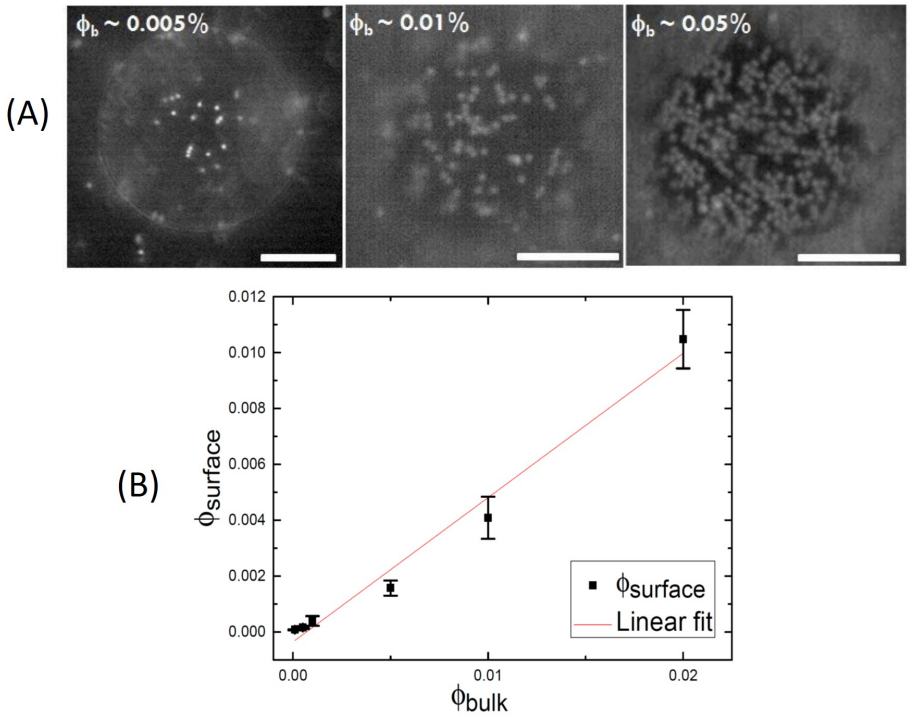

Fig. 4.1 Controlling the coverage of ODs by DNA coated colloids. (A) Fluorescence micrographs (under GFP illumination) showing change in the coverage of ODs by DNA coated PS colloids as a function of total bulk colloidal volume fraction, Φ_b or Φ_{bulk}. (B) Colloidal volume fraction on the surface of ODs, $\Phi_{surface}$ as a function of Φ_{bulk} . The error bars are standard deviation of the average coverage per droplet. In all OD-colloid mixtures, irrespective of Φ_b, a large number of colloids remain free in solution. All the scale bars are 10 µm.

It is also observed that in all OD-colloid mixtures, irrespective of Φ_b, a large number of colloids remain free in solution. Even though the colloids on the ODs are highly mobile, this protocol dependence is due to the fact that during slow deposition (lower Φ_b), colloids have more time to 'collect' the PLL-PEG-DNA 'receptors' than during fast deposition (higher Φ_b). In fact, during slow deposition, the bound colloids deplete the remaining PLL-PEG-bio domains from the interface, so that no further colloids can bind. We propose that the amount of colloids hybridized to the ODs depends on the total colloid volume fraction Φ_b. Since the DNA on the surface of ODs is mobile, we argue that most of the A_6 DNA bound via the PLL-PEG-bio chains is recruited by the hard colloids forming small rafts of several chains in the contact region. However, when using higher initial colloid concentrations, these rafts would be smaller. Every colloid that lands on the surface has time to accumulate its full share of PLL-PEG-DNA. But of course, this also means that less PLL-PEG-DNA remains for any subsequent colloids. Once all A_6 DNA is bound, no further colloids can bind to the oil-water interface. The interfacial regions free of colloids can thus be thought of as regions purely stabilised by SDS. Or in other words, the colloidal hybridization leads to segregation into regions of a pure SDS monolayer and others holding the PLL-PEG-bio with the DNA (Fig 4.2). Because of the fluorescence of the streptavidin attached to the biotins on the PLL-PEG was much weaker than that on the colloids, we could not observe this segregation in experiments. However, simulation studies by our collaborators strongly support our assumptions and are described in the following section [42]. Also, this distribution in the number of PLL-PEG-DNA rafts over different colloidal contacts is what we atrributed to an unexpectedly broad melt region for colloids bound to ODs in chapter 2. When starting with a high Φ_b, there is no time for the colloids to collect their share of PLL-PEG-DNA as many more colloids land on the surface of the ODs simultaneously. Hence many colloids recruit their share of rafts at the same time. Indeed, if we start with a high Φ_b, a higher density of

colloids on the ODs is observed, which automatically leads to fewer DNA bridges between any given colloid and the OD, and therefore to a reduced T_m.

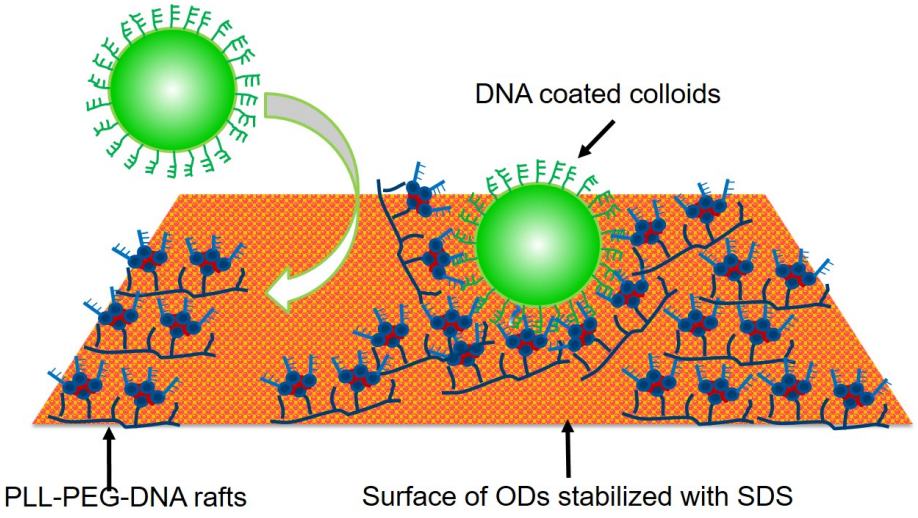

Fig. 4.2 Not to scale artistic representation of PLL-PEG-DNA rafts being recruited by impinging colloids on the surface of ODs. Since the diameter of ODs are much large compared to the size of PS colloids used, they do not see the curvature of the ODs. Colloids landing at first deplete PLL-PEG-DNA domains from the interface, making them less availabe for any further incoming colloids (marked by the arrow). This leads to a distribution in the number of PLL-PEG-DNA domains per colloid and hence a Φ_b dependent coverage of ODs by colloids and a broader melting transition for the OD-colloid system.

4.4.2 Comparing dynamics of colloids bound to the interface and free in solution

To understand how binding to the OD interface affects the dynamics of the colloids compared to motion of free particles in the bulk, we performed particle tracking and Differential Dynamic Microscopy (DDM) measurements. For particle tracking, we used 1.2 µm PS colloids coated with a grafting density of A_6' DNA comparable to the one used on the smaller particles. We also lowered the overall added colloid concentration to $\Phi_b = 0.001$ wt%, thus assuring only a few particles binding to the surface of the OD. We only track trajectories close to the south pole such that the particles move mostly in a plane perpendicular to the viewing

direction. We study root mean-square displacements that are much smaller than the radius of the OD and hence we assume that the curvature of the ODs can be neglected in the analysis of the diffusive motion (Fig 4.3). The averaged diffusion coefficient, $D_{\mathrm{OD}} \sim 4.0 \times 10^{-14}\,\mathrm{m^2\,s^{-1}}$, obtained for 1.2 µm colloids bound to the ODs is found to be reduced by one order of magnitude compared to that of free particles in solution, $D_{\mathrm{sol}} \sim 3.37 \times 10^{-13}\,m^2 s^{-1}$. The value of diffusion coefficient for particles free in solution is close to the theoretical estimate $D_{\mathrm{theo}} = 4.11 \times 10^{-13}\,\mathrm{m^2\,s^{-1}}$ (Fig 4.3B). Particle tracking of free PS particles is done in the absence of ODs, but under equivalent solvent conditions and temperature. Feeding the displacements extracted from the same particle tracks into an in-situ analysis program detailed here [70], we also extract the effective viscoelastic properties the bound colloids experience. These suggest that the colloids experience a viscosity of 9.5 ± 0.6 mPa s, which is roughly 10 times larger than that of water.

For samples with only 0.52 µm particles attached to ODs, we used DDM to extract the particle diffusivities on the ODs and in bulk [69, 71, 72]. Similar to the larger particles a considerable reduction in the diffusivity ($\sim 2.4 \times 10^{-13}\,\mathrm{m^2\,s^{-1}}$) of bound colloids is found, while the value D_{sol} $\sim 9.52 \times 10^{-13}\,\mathrm{m^2\,s^{-1}}$ measured for the free particles is again similar to the theoretical one (Fig. 4.3). Note, the DDM results for the particles on the OD surface have a larger error because of the reduced statistics as we limited the sampling to the small region on the south pole to avoid systematic errors due to the curvature of the droplet.

The strong slowing down of the colloidal diffusion on the ODs also supports our hypothesis that several mobile PLL-PEG-bio chains form rafts. It appears that the measured colloidal diffusion coefficients are dominated by the diffusion coefficient of the rafts. We have shown that the diffusion coefficient of colloids sedimented onto either a 'soft' cross-linked polymer surface or a 'hard' sterically stabilised support surface does not deviate more than some 10% from their bulk diffusion value [73], while here we observed a reduction of one order of magnitude.

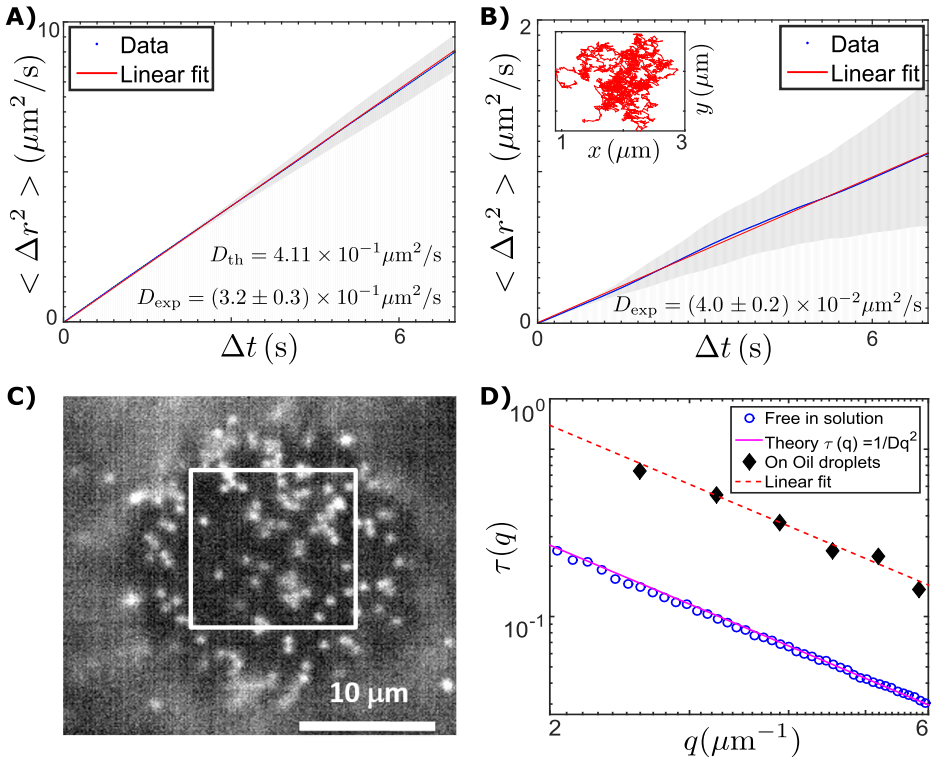

Fig. 4.3 A) Mean square displacement versus delay time for 1.2 µm colloids diffusing free in solution, and B) for DNA-bound colloids diffusing on the OD surfaces averaged over 5 tracks. The inset shows a typical single-particle track. C) Microscope image of 0.57 µm colloids bound to an OD surface focusing on its *south pole*. The square selection was used for DDM analysis. D) Decay time $\tau(q)$ as a function of the scattering vector q extracted from DDM analysis for both colloids diffusing on OD surfaces (as shown in C) and from microscope movies taken from free colloids in solution; the theoretical line passing through the data for the free colloids were obtained assuming a colloid diameter of 0.57 µm, a viscosity of buffer solution of 0.9 mPa s, and RT.

Saffman and Delbrück [74] recognized early on that the Brownian motion of proteins attached to a lipid bilayer can be expressed in form of the Stokes-Einstein relation of the translational diffusion coefficient, $D = k_{\rm B}Tb$, where $k_{\rm B}$ is Boltzmann's constant, T the temperature and b the mobility of the protein (for a free sphere in solution $b = (6\pi\eta R)^{-1}$, with η being the viscosity and R the radius of the particles). However, this mobility will be dominated by the viscoelasticity of that layer. They derived an analytical expression for a modified mobility of a cylindrical disk embedded in the double-layer. Their work was extended to monolayers separating two phases by Fisher *et al.* and by others, deriving complex expressions and verified in part by simulations [75, 76]. Sickert and Rondelez

reported experimental results on the diffusion of colloidal particles located at the water-air interface separated by lipid monolayers of different densities [77]. They found a reduction in the colloid's translational diffusion coefficient by one to two orders of magnitude.

Here we give a rough estimate of the diffusivity of the PLL-PEG-bio rafts. We argue that the PLL chains are in a rather stretched configuration on the surface (as seen in chapter 2) due to steric hindrance between the PEG chains [53, 54]. The positively charged polylysine will be bound to the SDS surfactants at the water-oil interface, where the hydrophobic tails of the surfactants extend into the roughly 50 times more viscous oil phase. We can estimate the mobility of such a chain by $b = (6\pi(\eta_{\text{oil}} + \eta_{\text{water}})R)^{-1}$, where the length of the stretched PLL chains is $\sim$48 nm, assuming that the length of a lysine monomer is $0.355\,nm$ [53]. This gives us a translational diffusion coefficient of $D_{\text{PLL}} \simeq 1.8 \times 10^{-13}\,m^2 s^{-1}$, which is about a fifth of that of the free 0.52 µm particles (D_{sol} =$9.52 \times 10^{-13}\,\text{m}^2\,\text{s}^{-1}$) and surprisingly close to those bound to the surface ($D_{\text{OD}} \sim 2.4 \times 10^{-13}\,\text{m}^2\,\text{s}^{-1}$). A slightly larger reduction is observed for the 1.2 µm particles, which is in agreement with our assumption that a larger raft of several PLL-PEG-bio chains may be bound in the contact region. Hence the colloid motion is dominated by the viscous drag of the monolayer-raft with the oil. This finding is in agreement with the microrheology data, which suggest that the larger colloids experience an apparent viscosity of about 9.5 mPa s, while we extract a viscosity of $\sim$3.5 mPa s from the DDM measurements of the bound smaller colloids.

4.4.3 Colloidal 2d-aggregation at the oil-water interface

Another striking feature that this system exhibits is that once colloidal adsorption is saturated (for Φ_b = 0.05 wt%), a rich phase diagram of colloidal aggregation emerges, which is controlled by the excess concentration of the added surfactant micelles inducing depletion. While keeping the PLL-PEG-bio and A_6 DNA coverage approximately constant for all experiments we studied the effect of varying the SDS concentration on the aggregation

behaviour of the PS-colloids hybridized to the ODs (Fig 4.4). As we increased the excess SDS concentration in bulk, we observed a transition from a gas-like distribution of hybridized PS-colloids (SDS concentrations <2 mM) to the formation of 2d 'continents' with crystalline order at higher concentrations of SDS (5 mM; SV 2). Between 2 mM and 4 mM SDS concentrations, a two-phase region was observed, where individual hybridized colloids coexisted with more disordered 'fluid-like' colloidal islands containing more than just a few colloids (Fig 4.4). We attribute this behavior to depletion attraction induced by SDS micelles. All samples show a considerable fraction of free, non-hybridized colloids in solution. These did not aggregate because of the steric stabilization provided by the A_6' DNA brush on the colloids. However, at SDS concentrations above 2 mM, we also observed weak colloidal aggregation in the bulk, again presumably due to depletion forces.

4.4.4 Simulations

As it is difficult to probe the distribution of colloid-OD bonds directly in experiments, we used kinetic Monte Carlo simulations ([42]) to investigate the factors that affect the protocol-dependent OD-colloid binding. For KMC simulations we collaborated with Dr Nuno in A. M. Araújo's group at the Universidade de Lisboa. Complete details of the simulation can be found in the main text and SI information of our paper [42]. In these simulations, the interface is described as a 2d discrete square-lattice with a given density of square patches, ρ_{p}. A patch represents a single DNA-functionalized PLL-PEG-biotin chain of length l_{p}, in units of lattice sites, and an interfacial diffusion coefficient D_{p}. The contact region of the colloids with the interface is represented by a square of length l_{C}. The number of colloids that arrive per unit time at the oil-water interface is denoted by F (the 'flux'). F increases monotonically with the bulk concentration Φ_b . In is assumed that the colloids bind irreversibly if they overlap with at least one site of the patch. Both colloids and patches are assumed to be impenetrable. Since we are interested in the initial stage of binding, we ignore the diffusion of

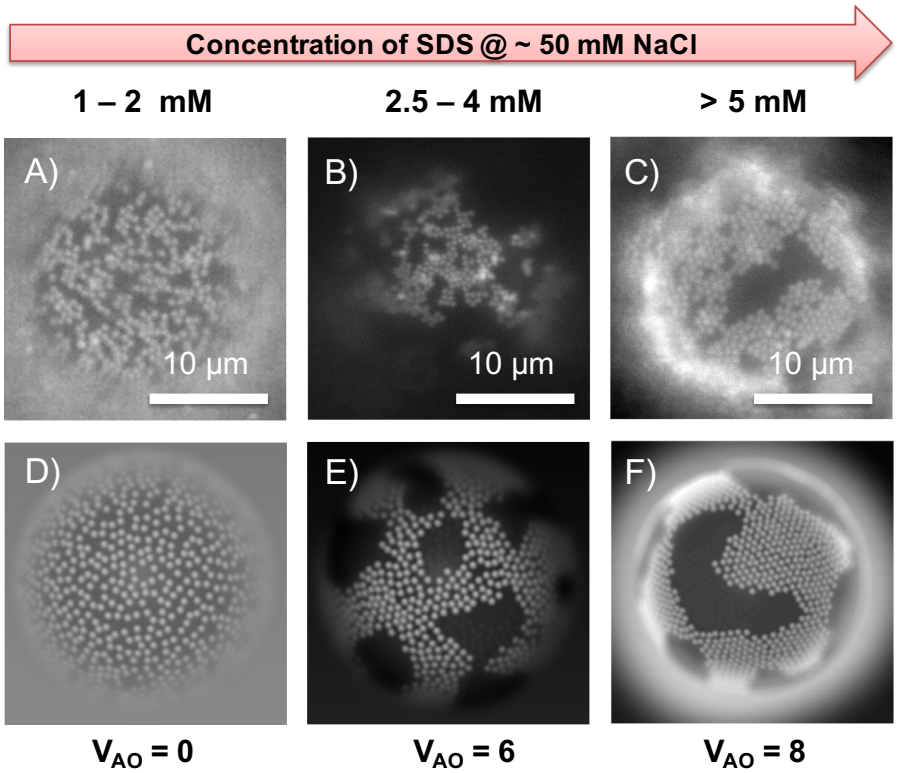

Fig. 4.4 Various phases of colloidal assembly at the interface with comparison between experimental (Top Row) and numerical results (Bottom Row)being shown. *Top row*: Fluorescence micrographs (under GFP illumination) showing change in the packing of the 0.52 µm polystyrene colloids on the surface of ODs as a function of SDS concentration in the bulk of the sample. The colloids go from A) a colloidal gas-like phase to B) a liquid-like cluster to C) well aligned hexagonal packing at the interface. *Bottom row*: Snapshots for different strengths of the Asakura-Oosawa potential: D) $V_{\mathrm{AO}} = 0$, E) 6, and F) 8 (simulation details in Joshi *et al.* [42]). These images were modulated with a Gaussian blur emulating the experimental situation.

colloid-patch complexes. However, free patches can diffuse and thus accumulate in accessible sites underneath a colloid-patch complex forming a raft. The simulations confirm that as F decreases, the limiting density of surface bound colloids decreases, due to the depletion of accessible patches [42]. We also used numerical simulations to study the 2D-aggregation behaviour of the bound colloids on the SDS concentration. To this end, we used Brownian dynamics simulations on a curved interface describing the pair-wise colloid interactions by the superposition of a repulsive Yukawa and the short-ranged, attractive Asakura-Oosawa (AO) potential (see SI of [42] for further details). Keeping the fraction of bound colloids per

OD constant, we increased the strength of the attraction – it scales linearly with the micelle concentration. Fig 4.4D-F show snapshots for different strengths of the AO potential. As observed experimentally, by increasing the density of depletant we observe a transition from a fluid-like structure to crystalline-like order (Fig 4.4A-C).

Our results presented in Fig 4.4 demonstrate that the surfactant concentration is an important ingredient in our systems aggregation behaviour. In the final OD-colloid mixture we adjust the SDS concentration in the aqueous bulk. For the buffer solution with 50 mM added NaCl concentration a minimum of 1-2 mM SDS concentration was required in order to prevent coalescence of the oil droplets. This SDS concentration is just below the Critical Micelle Concentration (CMC) for SDS, which is around 2.5 mM for the ionic strength used in our experiments. Hence, at higher SDS concentrations we create more and more micelles, which induce increasingly stronger depletion attraction between the DNA-stabilised colloids that do not aggregate in the same salty buffer solution but in absence of a surfactant. Depletion attractions between large colloids in bulk solution, induced by small colloids or polymers, have been studied extensively in theory, simulations and experiments [78–81]. Fewer studies used charged surfactant micelles as the depleting agent. Iracki *et al.* observed the aggregation behavior of 'hard', negatively charged silica beads sedimented onto a non-sticking glass surface in the presence of SDS [82]. Similar to our experiments they showed that below the CMC hard sphere repulsion dominated, while an increasingly deeper attractive minimum emerged as the SDS concentration increased beyond the CMC. Again, the simulation results confirm that scenario [42].

Also, when we go to higher SDS concentrations we see ordered 2d crystals with faceted boundaries. Similar to the observations by Meng et al [83] made on depletion driven colloidal aggregation on the inside of emulsion droplets these crystals remain finite size and 'fracture'. This is due to the competition between the elastic deformation of the 2d crystals that prefer a flat arrangement and the binding strength of the colloids to the interface via DNA. As the

melting experiments demonstrate, any clusters formed at room temperature will become smaller and more mobile upon heating. To summarize, we have introduced a new colloid aggregation mechanism on emulsion droplets that explain the reversible detachment from the OD surface in a controlled manner using DNA hybridization. The fact that the hybridization recruits the mobile linkers between the colloids and the OD may be used as model system to understand and study the dynamics of particle or protein adsorption to biological molecules in a crowded environment. The very slow dynamics of the aggregation process may help understand how this aggregation can be controlled [84, 55].

4.5 Conclusion

We have demonstrated that it is possible to control the surface coverage of oil droplets by colloidal particles, by exploiting the fact that during slow adsorption, compositional arrest takes place well before the structural arrest occurs. As a consequence, we could prepare colloid-coated oil droplets with a 'frozen' degree of loading, but with fully ergodic colloidal dynamics on the droplets. However their diffusivities were found to reduce by atleast a fifth compared to their free counterparts in solution. Depending on the solvent conditions, our seemingly simple system exhibits an unexpectedly rich quasi-2d phase diagram of colloid aggregation. We illustrated the equilibrium nature of the adsorbed colloidal phase by exploring the quasi-2d phase behaviour of the adsorbed colloids under the influence of depletion interactions. As the concentration of the free surfactant in solution is increased, the colloids bound to oil droplets undergo a purely entropic transition from a fluid like phase to a compact crystalline packing of colloids at the interface forming colloidal 'islands'. This transition is attributed to the depletion interaction caused by the excess surfactant micelles in the system. I also briefly report the simulation studies from our collaborators from Lisbon that reaffirm the experimentally oberved phase behaviour. These simulations of a simple model system illustrate the nature of the compositional arrest and the structural ergodicity

observed in our experiments. The findings summarized in chapter 3 and 4 are published in Joshi *et al.* [42].

Chapter 5

Binary Mixtures of DNA-Coated Colloids in a Quasi 2 Dimensional Environment

Having devised an approach for kinetically controlling the coverage of oil droplets (ODs) by colloids using DNA linkers (described in Chapter 3 and 4), this method is extended to bind different colloidal species at the interface. This chapter summarizes some preliminary results on the dynamics and phase behaviour of binary colloidal mixtures at the oil/water interface. These results present an exciting opportunity for designing recyclable bi-dispersed systems.

5.1 Introduction

Food, cosmetic and pharmaceutical formulations frequently contain more than one kind of active ingredients dispersed at oil-water interfaces. A controlled release of active ingredients from the interfaces under external triggers such as temperature, shear, or change in pH adds extra functionality to these formulations. Hence, for designing formulations that are selective in nature, such that they could adsorb one kind of species more than others and later

sequentially release them – it is rather important to understand the kinetics, dynamics and phase behaviour of multi-component systems.

Our approach for kinetically controlling the coverage of oil droplets by colloids using DNA linkers (described in Chapter 3 and 4) enables us to bind different kinds of colloidal species at the interface. Further tuning the bulk colloidal volume fractions Φ_b, it is also possible to control the composition of bound colloidal mixtures. We bind large (1.2 µm) and small (0.5 µm) polystyrene colloids to ODs in various ratios of large to small colloids at varying solvent conditions. Despite mobile anchors holding colloids at the interface, which in principle, could permit rearrangement of the colloids at the interface, we do not observe any phase separation between the different colloidal species. It is also observed that the presence of larger colloids forces small colloids to aggregate at the interface at concentrations of SDS much lower than the critical micellar concentration (CMC). This behaviour is rather contrary to that observed in chapter 4, where the onset of aggregation of colloids bound to the surface of ODs is marked at the CMC of SDS. For concentration of SDS below the CMC, these surface bound colloids exist in a freely moving gaseous phase. Note that the CMC of SDS for 50 mM NaCl is is about 2.5 mM.

5.2 Experimental methods

Following the protocols listed in chapter 2 [42], we prepare oil droplets coated with A_6 DNA and coat1.2 µm and 0.5 µm polystyrene (PS) and 0.2 µm PMMA colloids with A_6' DNA. These colloids are either green (G) or red (R) fluorescent. For grafting DNA to the surface of SDS-stabilized oil droplets, we first adsorb PLL-PEG-Biotin on the negatively charged SDS head groups. PLL-PEG-Biotin has a highly negatively charged backbone that adsorbs flat on the surface of the oil droplets, while the PEG-bio overhangs protrude into the water phase. These PEG-bio overhangs are then functionalized with streptavidin. Single stranded (ss)DNA with a biotin functionalization later attaches to these streptavidin sites on the oil droplet.

Keeping the overall volume fraction of colloids, $\Phi_b \sim 0.06$ wt% of polystyrene, ratio of large (1.2 µm) to small (0.5 µm) colloids is varied across various samples. Three different volume ratios of large to small colloids (1:5, 5:1 and 1:1 μl) are used from concentrated (1 wt%) suspensions of the DNA coated colloids. The salinity of the system is maintained at 50 mM of NaCl for all experiments. For each composition of the colloidal mixtures two samples are prepared, one having surfactant concentration adjusted above (5 mM) and another one below (1 mM) the CMC (2.5 mM) of SDS. Once the samples are prepared, they are imaged under a Nikon TI-E epifluorescence micrioscope equipped with a CMOS camera. For ease of visualization the small colloids were chosen with red fluorescence and the large ones with green. False colour overlay images are later generated by using ImageJ for data analysis.

5.3 Results and Discussion

Chapter 2 of this thesis presented a new approach for functionalizing SDS stabilized oil droplets with DNA. When colloids coated with complementary ssDNA are mixed with these DNA functinalized oil droplets, they bind reversibly to the surface of ODs via DNA hybridization. The colloids remain mobile and their diffusivities are reduced nearly by a factor of five for the small colloids and an order of magnitude for the large ones, compared to their counterparts moving freely in the bulk. Further, because of the mobility of the DNA attached to the oil-water interface the resulting binding density of the colloids becomes dependent on the colloidal concentration in bulk. Once colloidal adsorption is saturated a rich phase diagram of colloidal aggregation emerges, which is controlled by the excess concentration of the added surfactant micelles inducing depletion. Varying the micelle concentration in the aqueous phase, a purely entropic transition from a fluid-like phase to a more compact packing of the solid colloids at the interface is observed. Following up on this interesting phase transition, we decided to study the phase behaviour of a binary mixture of DNA coated polystyrene colloids at the interface. These are only preliminary results and

detailed experimental and simulation studies to clearly understand the phase behaviour of colloidal mixtures in this quasi-2d environment are underway.

We functionalized 1.2 µm and 0.5 µm colloids with A_6' DNA and the oil droplets with A_6 DNA. In control experiments both colloidal species are seen to bind with the ODs. However, the droplets coated with only 1.2 µm colloids demonstrate a transition into a colloidal crystalline phase at much lower SDS concentrations compared to the 0.5 µm colloids bound to ODs. The large colloids demonstrate a nice 2d crystalline packing at the oil/water interface at SDS concentrations as low as 3 mM as opposed to the 0.5 µm particles that undergo a crystalline transition only at SDS concentrations above 5 mM. Below the critical micellar concentration of SDS, the 0.5 µm colloids exist freely as a colloidal gas for months after preparation. Whereas the 1.2 µm colloids are mobile to begin with but, if left undisturbed, they aggregate into random clusters after around 24 hours (Fig 5.1). We suspect this difference of behaviour might be due to the extra drag the larger colloids experience because of a larger size and hence a higher number PLL-PEG-DNA rafts that they can recruit at the interface. Further we suspect that due to their size, gravity may also be playing a significant role in forcing them to aggregate.

In chapter 4 we observed that as we increase the concentration of of SDS beyond the CMC, we create more and more micelles, which induce an increasingly strong depletion attraction between the DNA-stabilised colloids that do not aggregate in the same salty buffer solution, in absence of a surfactant [42]. We observed that below the CMC hard sphere repulsion dominated, while an increasingly deeper attractive minimum emerged as the SDS concentration increased beyond the CMC. On going to higher SDS concentrations, we observed ordered 2d crystals with faceted boundaries [42].

Having studied the kinetics and phase behaviour of colloidal adsorption on the surface of ODs, we decided to dope the system with a small amount of large 1.2 µm colloids. An overall bulk volume fraction (Φ_b) of the polystyrene colloids > 0.05 wt% corresponds to

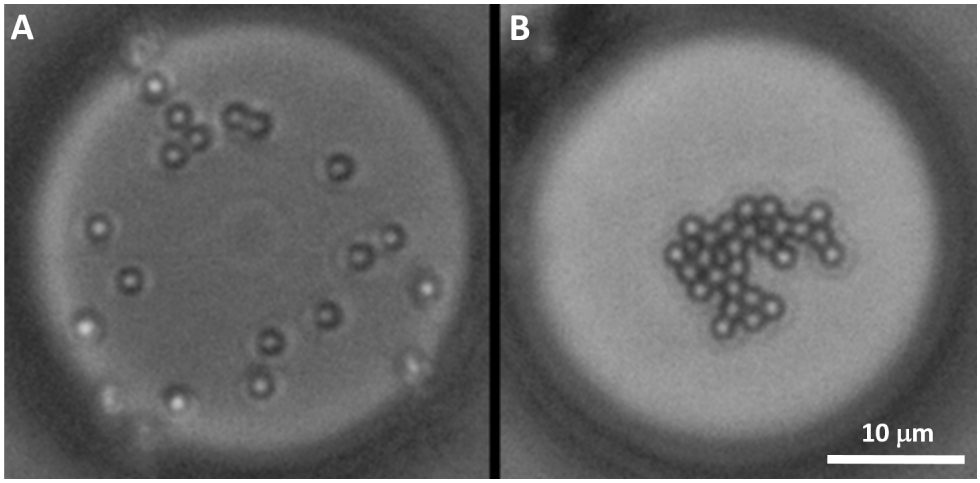

Fig. 5.1 Bright field images of 1.2 μm green (G) fluorescent polystyrene (PS) colloids with A_6' DNA hybridized to the oil droplets having A_6 DNA. (A) As prepared samples show the large 1.2 μm colloids moving in a well dispersed and freely moving gaseous phase (B) If the sample is left undisturbed for 24 hrs, bound colloids aggregate into random clusters as opposed to their 0.5 μm, where the gaseous phase is stable for well over several months. Scale bars are 10 μm.

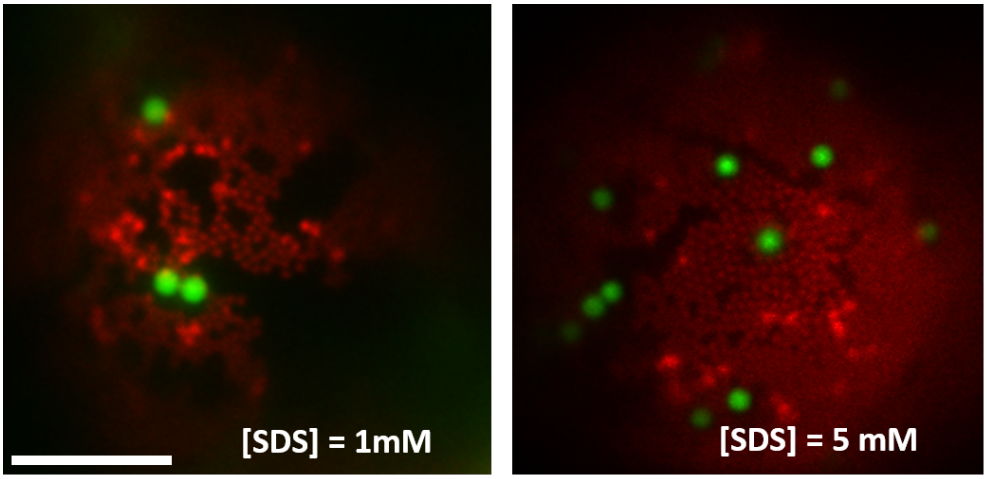

Fig. 5.2 Fluorescence images of 1.2 μm green (G) fluorescent and and 0.5 μm red (R) fluorescent colloids with A_6' DNA hybridized to the oil droplets functionalized with A_6 DNA when the colloids are mixed in a 5:1 wt% ratio of small (R) to large (G) colloids(A) below the CMC of SDS (B) above the CMC of SDS. It can be seen that the presence of large colloids forces the small colloids to aggregate well below the CMC of SDS. However, above the CMC of SDS, the small colloids show a more compact packing at the interface. False colour overlay is utilized to clearly visualize the arrangement of both types of colloids at the interface. Scale bars are 10 μm.

a full coverage of the ODs by colloids. Keeping the overall Φ_b constant, we replace one in six parts of the 0.5 µm (small) DNA coated colloids with 1.2 µm (large) colloids. We prepared two samples, with concentration of SDS set to 1 mM in the first one and 5 mM in the other, with each having a 50 mM concentration of NaCl. Note that the critical micellar concentration of SDS for 50 mM NaCl is about 2.5 mM.

We see a good coverage of the ODs with small colloids and a few occurrences of the large colloids bound to the surface of the ODs (Fig 5.2). This was rather expected as the bulk concentration of colloids controls the kinetics of their adsorption to the surface of ODs. However, contrary to our earlier observations from chapter 4, we observed that the small colloids aggregated into random clusters on the surface of ODs at concentration of SDS much lower than the CMC. For concentration of SDS above the CMC, we observe a compact crystalline packing of the small colloids at the interface with large colloids embedded at in matrix of small colloids. Intrigued by these observations, we decided to vary the proportions of large to small colloidal mixtures.

Further, we prepared another sample with an overall bulk volume fraction (Φ_b) of the polystyrene colloids $\sim$0.05 wt% having five parts of the large colloids and one part of the small colloids. To our surprise, despite having a low Φ_b of the 0.5 µm colloids, this sample still had a significant amount of small colloids bound to the oil droplets as opposed to a scarce presence of large colloids in the previous case (Fig 5.3). This can be attributed to the fact that the small colloids are far more diffusive compared to the larger colloids. Hence, despite having a smaller concentration in the bulk, they collide more often with the ODs and a significant number of them end up binding to the surface of ODs. For both samples, we also notice that occasionally the small colloids like to wrap themselves around the large ones. Again, it can be seen that the presence of large colloids forces the small colloids to aggregate well below the CMC of SDS. Further, for the sample having a higher concentration of SDS

(5 mM), we observe a more compact packing of the smaller colloids and the large colloids are occasionally embedded in the matrix.

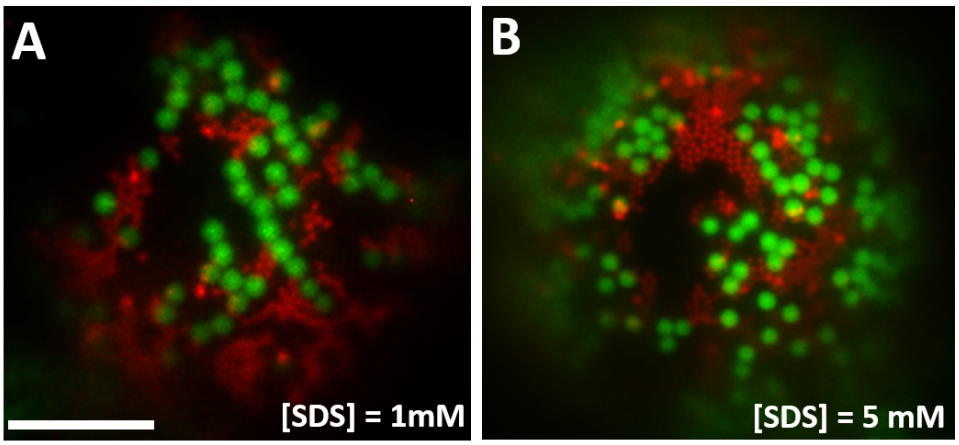

Fig. 5.3 Fluorescence images of 1.2 µm green (G) fluorescent and and 0.5 µm red (R) fluorescent colloids with A_6' DNA hybridized to the oil droplets functionalized with A_6 DNA when the colloids are mixed in a $1:5 wt\%$ ratio of small (R) to large (G) colloids (A) below the CMC of SDS (B) above the CMC of SDS. False colour overlay is utilized to clearly visualize the arrangement of both types of colloids at the interface. Scale bars are 10 µm.

Finally, we prepared a sample with equal portions of the large to small colloids, keeping the overall bulk volume fraction (Φ_b) of the polystyrene colloids > 0.05 wt%. We again observe a higher number of small colloids binding to the oil droplets compared to the large colloids (Fig 5.4). This may be attributed to their higher diffusivity. Also the small colloids aggregate into loose random aggregates and wrap around large colloids at lower SDS concentrations and demonstrate a compact packing at the higher SDS concentration.

Further, we prepared another sample with 200 nm, PMMA and 500 nm PS colloids in equal proportions and observe a similar trend. The PMMA colloids being more diffusive are present in larger numbers at the oil/water interface. Presence of the 500 nm colloids again causes them to aggregate albeit in smaller clusters. Due to the limitation of resolution of our imaging setup, good resolution images for this system could not be obtained. We are collaborating with groups from the Chemical Engineering department to produce high resolution images of this system and study it in great detail. This is work in progress. Further

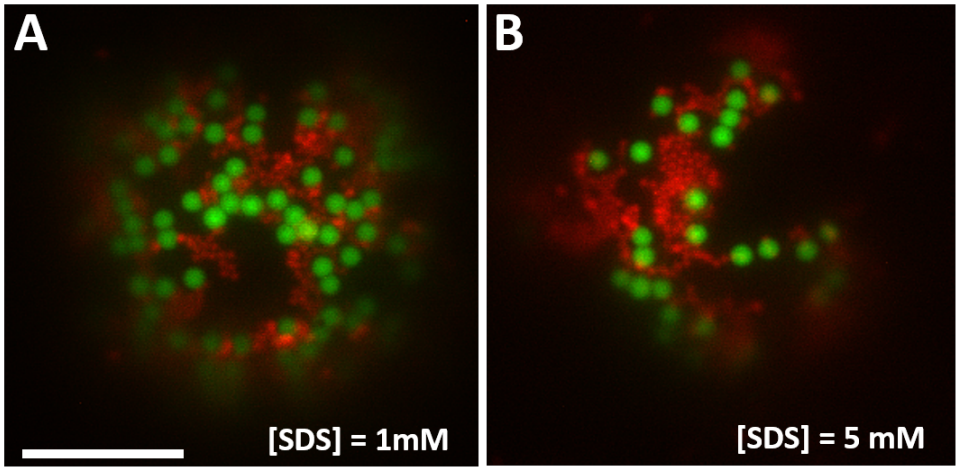

Fig. 5.4 Fluorescence images of 1.2 µm green (G) fluorescent and and 0.5 µm red (R) fluorescent colloids with A_6' DNA hybridized to the oil droplets functionalized with A_6 DNA when the colloids are mixed in a 1 : 1 wt% ratio of small (R) to large(G) colloids (A) below the CMC of SDS (B) above the CMC of SDS. False colour overlay is utilized to clearly visualize the arrangement of both types of colloids at the interface. Scale bars are 10 µm.

we also plan to do *g(r)* - radial distribution function, analysis for samples with various proportions of small to large colloids at different concentrations of SDS to quantify the colloidal packing of small colloids around the large ones. The *g(r)* analysis enables us to quantify how the packing density varies as a function of distance from a reference particle.

5.4 Conclusions

We successfully prepared oil droplets coated with binary colloidal mixtures using DNA linkers. Owing to the kinetics of the system, we could control the proportions of colloidal mixtures at the interface. For all wt% ratios of small (0.5 µm) to large (1.2 µm) colloids, we see a significant amount of small colloids bound to the ODs. This can be attributed to a higher diffusivity of smaller colloids because of which they have a higher collision frequency with the ODs and hence bind in higher numbers. Further, we observe that the small colloids in the binary mixtures aggregate at SDS concentrations much lower than the the CMC of SDS. This is contrary to our observations in chapter 4, where we established that the presence

of SDS micelles causes an attractive depletion interaction for otherwise sterically stabilized DNA coated colloids. Further, we did not observe any phase segregation for either SDS concentrations or the composition of binary mixtures. However, small colloids are seen to wrap around the large colloids and aggregate in irregular clusters below the CMC of SDS and into compact packing above the CMC of SDS. This suggests that the larger colloids are acting as nucleation points for smaller colloids. We believe that this observed aggregation below the CMC might be due to bridging by PLL-PEG-DNA rafts. Once a large colloid recruits PLL-PEG-DNA rafts, due to geometric constraints another large colloid can not be accommodated on the free biotin heads in these rafts. However, small colloids slip into the void and recruit additional biotin anchor points on the PLL-PEG-DNA rafts. Many small colloids sharing several such rafts with a large colloid can lead to local distribution in the number of small colloids on the surface of the ODs. Hence, the reason for observed aggregation and wrapping of small colloids around the large colloids. Results presented in this chapter are only in the primitive stages of investigation for this system. Further careful experiments and detailed analysis of these observations are underway.

Chapter 6

Magnetic Field Directed Assembly of DNA Coated Colloidal Superstructures

In this chapter we discuss an approach for directing the assembly of a multi-component system of DNA-coated colloids (DNAcc) via an externally applied magnetic field. Using the right combination of DNA it is possible to tune the sequential interactions for this multi-hierarchical system while ensuring thermoreversibility of the assembled superstructures. Colloidal superstructures with topological complexity such as 'raspberry' like and long coaxial skeletons of smaller colloids around larger superparamagnetic cores are demonstrated in a two component system. Self-assembly of these long, straight, mesoscopic scaffolds of colloids can be utilised as a primitive for building more complicated structures. This work was done in collaboration with Mykolas Zupkauskas, Dong Ok Kim and Simon Nathan in the Eiser group.

6.1 Introduction

Owing to the thermally-reversible and highly specific binding between two complementary single strands of DNA linkers, various theoretical studies have demonstrated the possibility

of readily assembling DNA coated colloids into various lattice forms and complex mesocopic structures [85, 86, 36]. However, their experimental realization has proven to be more difficult than originally envisaged. This difficulty is attributed to the nature and strength of DNA binding. Single stranded DNA attached to hard colloids acts as a molecular velcro making it diffciult for the colloids to relax into the crystalline equilibrium structure upon binding. Moreover, the binding strength between DNA coated colloids can be several orders of magnitude higher than that of free strands in solution. This results in a sharp melt transition over a narrow temperature range [6]. Such a sharp binding transition between freely moving colloids and the aggregated phase along with their inability to reorient makes it difficult for the system to anneal into equilibrium structures. As a result, DNA coated colloidal clusters get trapped into dynamically arrested states lacking long-ranged order or structure control even under conditions when a highly ordered phase is thermodynamically more favoured [45, 34]. A number of strategies including using mobile DNA linkers [42, 10, 43], grafting both DNA and an inert polyemer to the colloidal particles [34] and using nanoparticles instead of micron-sized colloids [36, 44] have been proposed to overcome these kinetic barriers. Despite these attempts, only a handful of DNA coated colloidal systems have been successful in realizing various crystal structures [36, 6, 44–46]. However, a full control over the programmability to direct these systems into topologically complex structures is yet to be established .

When thermodynamic pathways for relaxation into equilibrium structures are extremely slow or hindered greatly by kinetic barriers, externally applied force fields such as gravity, compressive or shear stress, electric and/or magnetic fields can be used to direct the assembly of micron sized building blocks into well defined complex structures [47, 16]. Since it is more difficult to thermally organize larger particles(>1.0 μm) into ordered assemblies, these methods can play a crucial role in engineering their self-assembly.

Magneto-responsive colloidal particles can be self-assembled into field-controllable structures. Magnetic forces arising both internally due to interactions between neighbouring colloids and due to externally applied magnetic field that drive the particles to self-assemble via the alignment of their magnetic diploes [16]. These field assisted methods are unique and effective because of their ability to manipulate particle-particle interactions in real time. Studies on directing the assembly of magneto-responsive colloidal systems – colloids dispersed in a ferrofluid (Fe_3O_4), have already demonstrated linear and zigzag chains [87, 16], two-dimensional (2-d) arrays [88], superstructures with multipole symmetry [89], a number of complex structures (rings, chains and tiles) [90], and chiral structures with controlled helicity [91]. These assembled structures can be recycled into their building blocks or reconfigured into a different state by tuning the magnetic field or applying a remote demagnetizing field. Further, some groups have explored the possibility of creating 'materials with a reconfigurable responsive structural arrangement' by using magnetic Janus particles [92] or by introducing magnetic patches on spherical colloids [93]. These anisotropic colloids spontaneously self-assemble into clusters in the absence of external magnetizing fields. Applying a field externally allows the clusters to reconfigure themselves by unbinding or slight geometrical relaxations [93, 92].

One of the disadvantages of using ferrofluids for designing 'macrocolloidal superstructures' is that it is difficult to separate the assembled superstructures from the continuous ferrofluid phase which have substantial remanent magnetizations i.e. they retain a finite degree of magnetization even when the applied magnetic filed is swittched off. Hence, it becomes very difficult to employ these structures for practical purposes including recyclable and reconfigurable assemblies. Employing superparamagnetic colloids becomes more advantageous for they align and form chains or columns at high field strength and revert to an isotropic suspension when the field is removed. Using polymer bridges, long, stable, extremely regular and permanent chains of superparamagnetic colloids were formed [94].

Using DNA instead of the polymer bridges allows creation of flexible and semiflexible chains of these superparamagnetic colloids with short persistence lengths [95–98].

Here we describe our approach to create magneto-responsive, multi-hierarchical colloidal superstructures with topological complexity such as 'raspberry' like [99] and long coaxial skeletons of smaller DNA coated colloids around larger superparamagnetic cores. Proof of concept is demonstrated for further stabilizing these structures by adding a suitably functionalized third component. Tuning the sequential interactions for these systems, recyclable novel superstructures such as a mesoscopic straight coaxial scaffolds with a bilayer of different colloids attached could be realized. The length of these 'coaxial' colloidal cables can be tuned from a few microns to a few hundreds of microns by changing the strength of the applied magnetic field, ranging from 1.8 - 30 mT.

6.2 Experimental Methods

6.2.1 Grafting DNA to colloids

Commercially available streptavidin functionalized colloids are coated with DNA as per the protocols detailed in Chapter 2. The concentration of added NaCl was fixed at $\sim$50 mM for all experiments. Table 6.1 lists various colloidal species used and the corresponding DNA they are functionalized with.

Table 6.1 Various colloidal species and corresponding DNA constructs with sticky ends.

Colloids	Diameter(μm)	Composition	Supplier	DNA	Sticky end
M_1	2.8	PS	Dynabeads ThermoFisher	A_7	CCC GGC C
M_2	1.5	PS	Microparticles GmbH	A_7	CCC GGC C
M_3	1.0	PS	Dynabeads ThermoFisher	A_7	CCC GGC C
G_1	0.5	PS	Microparticles GmbH	A_7'	GGC CGG G
G_2	0.2	PMMA	Microparticles GmbH	A_7'	GGC CGG G
R_1	0.5	PS	Microparticles GmbH	A_6	CCG GCC

6.2.2 Imaging, temperature cycling and applying magnetic fileds

Once the samples are prepared and filled into sample chambers, they are then imaged (as described in chapter 2) with a Nikon Eclipse Ti-E epifluorescence microscope. For these measurements, we use a home-made sample stage equipped with a pair of Helmholtz coils and a computer-controlled Peltier cooler. The Helmholtz coils are connected to a DC power supply. The position of sample on the stage is fixed such that it lies in the plane of uniform magnetic field for the coil pair (Fig 6.1). A thermocouple, connected to the Peltier device is placed directly in touch with the sample chamber to measure the temperature of the sample. Samples could be heated or cooled at desired rates using the PID controller and videos recorded under red or green fluorescence and bright field.

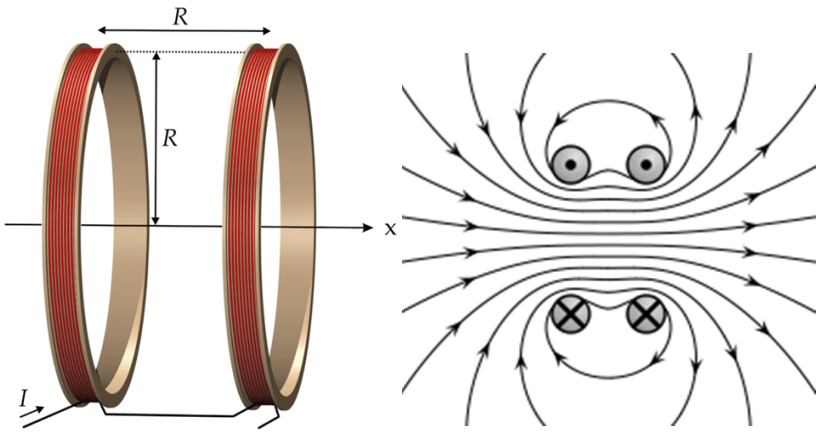

Fig. 6.1 Schematic drawing of a Helmholtz coil pair and the magnetic field lines along the plane of the sample stage. This plane bisecting perpendicularly the coil pair has a nearly uniform distribution of magnetic field lines between the coils (image taken from Wikipedia).

6.3 Results and Conclusions

6.3.1 Binding rules and control experiments

In order to design hierarchical assembly in multi-component systems it is important to have highly specific interactions that can be switched on or off sequentially along the temperature

axis. Hence to tune the melt transitions and choose suitable DNA linkers, we first study the change in melt temperature (T_m) as the length of the sticky end is shortened by one base pair. Following the protocols listed in Chapter 2, we prepare two sets of single component gels of 0.5 µm R_1 colloids one with $A_7 - A_7'$ and the other with $A_6 - A_6'$ pairs grafted in a 1 : 1 ratio. DNA binds to the colloids via a streptavidin-biotin chemistry. For the $A_7 - A_7'$ pair the T_m is measured to be 48 °C whereas for an $A_6 - A_6'$ pair it is measured as 34 °C while cooling from an ispotropic colloidal gas phase above the melt temperature.

6.3.2 Two component system

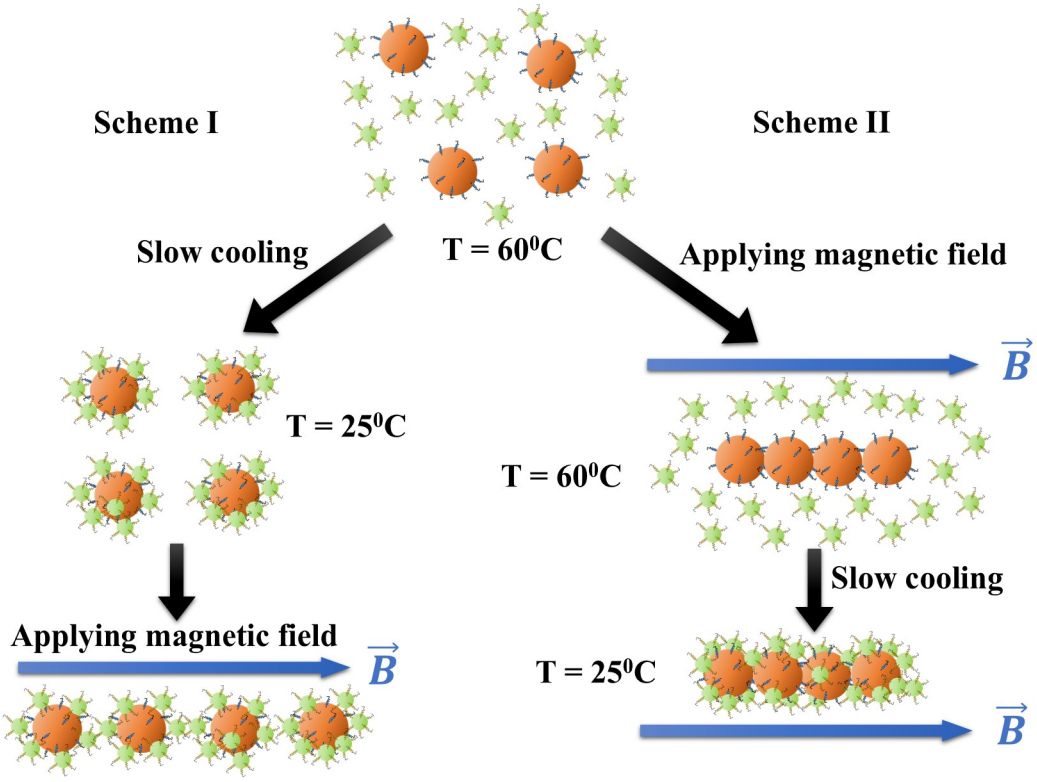

Fig. 6.2 A not to scale schematic describing the strategy for assembling 'raspberry' like and coaxial scaffolds in a two component system. Switching on magnetic field at different stages determines the final assembled superstructure. 'Raspberry' like superstructures are formed when the system is cooled slowly in the absence of magnetic field (scheme (I)). These colloidal raspberries can then be aligned into chain like structures by applying a magnetic field and are redispersed when the magnetic field is switched off. If the field is switched on at $T > T_m$ and the system is cooled slowly in the presence of magnetic field, linear coaxial scaffolds with a superparamagnetic core are formed (scheme (II)).

For a two component system strategies for assembling colloidal superstructures with topological complexity such as raspberry like and long coaxial skeletons of smaller colloids around superparamagnetic colloids are described in Fig 6.2. Binding rules for the multi-component system strictly prohibit binding between the colloids of the same kind. A mixture of superparamagnetic (M) colloids and the second colloidal component of desired size (depicted green (G) in this cartoon) coated with complementary DNA linkers are first heated to 60 °C ($T > T_m$) to make sure all the components are diffusing freely in a homogenous gaseous phase. When the system is cooled very slowly (over 6 hrs) to 40 °C, 'raspberry like' colloidal superstructures of the small colloids around the large superparamagnetic colloids are formed by DNA hybridization as depicted in scheme (I). These colloidal raspberries are aligned into chain like structures by applying a magnetic field and are redispersed when the magnetic field is switched off. However, if the magnetic field is switched on while the system is in gaseous phase, superparamagnetic colloids are pushed together forming long chains as their magnetic dipoles align in the direction of applied magnetic filed. Since these colloids are sterically stabilized with a DNA brush on their surface, they do not bind or stick to one another. The G beads stay in the gas phase unaffected by the applied field. If we start reducing the temperature of the system at this stage, these chains of superparamagnetic colloids are bridged and stabilized by the secondary colloidal component present (G). This results in the formation of long colloidal wires having a superparamagnetic (M) core ideally covered with G colloids (scheme (II)). These chains are stable even after the field is switched off. It is also observed that the formation of these 'raspberry' colloids and linear coaxial scaffolds is recyclable over temperature cycling. Using this scheme we have assembled 'raspberry' colloids of various size ratios and the results are summarized below. Note, because of their size and higher density the superparamagnetic beads always settle to the lower surface of the sample chambers, making it easy to image them.

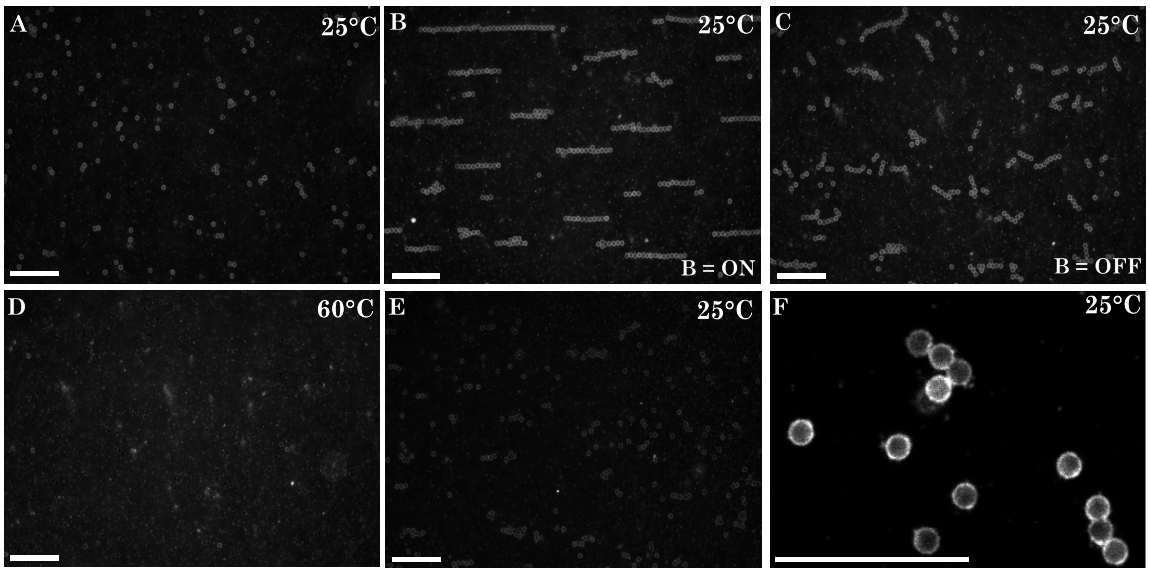

Fig. 6.3 A two component system composed of2.8 µm PS superparamagnetic colloids (M_1) coated with A_7 DNA and 0.5 µm green fluorescent PMMA colloids (G_2) coated with A_7' DNA. Green fluorescence images show locations of small colloids bound to the superparamagnetic colloids. (A) As-prepared samples at room temperature showing the formation of 'raspberry' like superstructures of M_1 beads coated with small G_2 beads. (B) These colloidal raspberries align into straight chains when an in-plane magnetic field is applied. (C) These chains of colloidal raspebrries fall apart upon removal of the magnetic field. (D) Both M_1 and G_2 colloids redisperse into a gaseous phase when heated to 60 °C, which is well above the melt temperature (T_m) for the $A_7 - A_7'$ DNA pair. (E) The 'raspberry' like superstructures are recovered by cooling slowly to room temperature in the absence of magnetic field. (F) Shows a zoom of the colloidal 'raspberries', clearly showing the surface bound green fluorescent PMMA (G_2) particles. Scale bars are 30 µm

Firstly, 2.8 µm superparamagnetic polystyrene (PS) beads (M_1) coated with A_7 DNA and 0.5 µm green fluorescent PMMA colloids (G_2) coated with A_7' DNA are mixed in a 1:5 ratio, keeping an overall volume fraction of ∼0.01 %vol. They are allowed to incubate on rollers for an hour before injecting them into the sample chambers. Fig 6.3 shows images of the sample under green fluorescence. Fluorescence imaging helps in locating the positions of small colloids bound to large superparamagnetic colloids (non-fluorescent) or those free in solution. Looking at as-prepared samples under green fluorescence we see that G_2 colloids have indeed hybridized to M_1 colloids via DNA linkers. Both M_1 and G_2 colloids can be redispersed into a gaseous phase when heated to 60 °C, above the melt temperature (T_m) for the $A_7 - A_7'$ DNA pair. Further, the 'raspberry' like superstructures are recovered by

cooling slowly to room temperature in the absence of a magnetic field (scheme(I)). This is reproducible over several cycles of temperature cycling from room temperature to $T > T_m$. When an in-plane magnetic field is applied after the sample is cooled to room temperature, these colloidal 'raspberries' align into straight chains in the direction of the magnetic field. This happens as consequence of the reorientation of magnetic moments on M_1 in the direction of applied field. These chains stay assembled as long as the magnetic field is on and fall apart into individual raspberries due to thermal motion soon after removing the field. If a very strong magnetic field (>20 mT) is applied, these colloidal raspberries may aggregate irreversibly through non-specific interactions owing to the high surface roughness of the M_1 colloids.

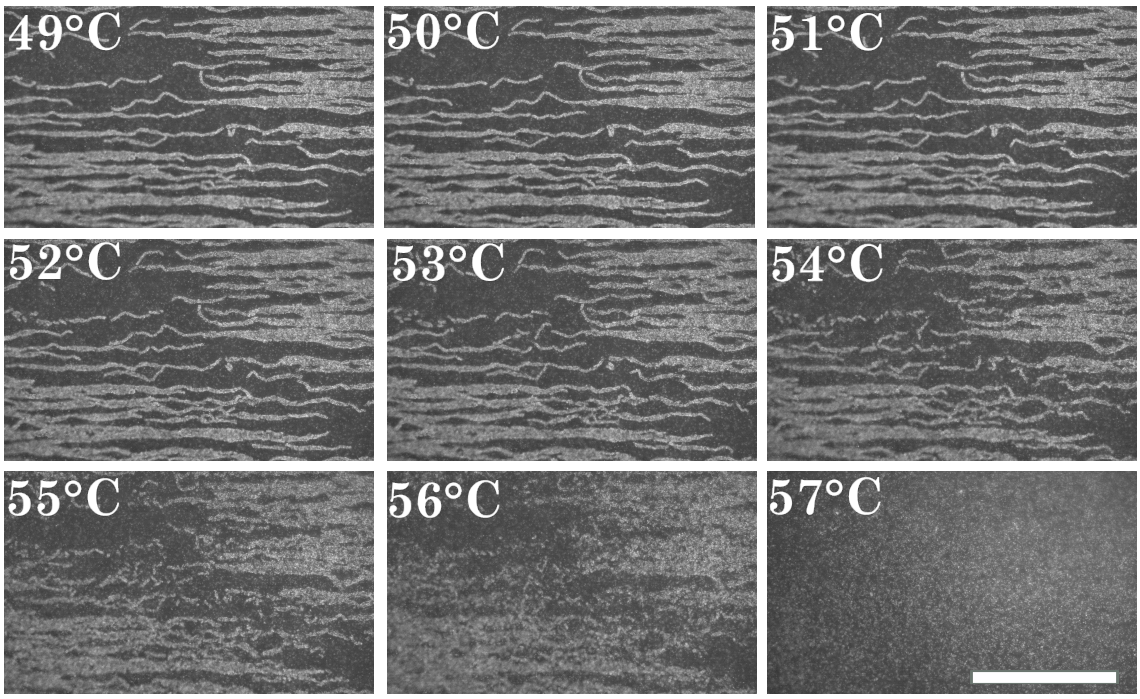

Fig. 6.4 Melting of long floppy chains in a two component system composed of 2.8 µm PS superparamagnetic colloids (M_1) coated with A_7 DNA and 0.5 µm green fluorescent PS colloids G_2 coated with A_7' DNA. As the system is heated above the melt temperature (T_m) for the $A_7 - A_7'$ DNA pair, the system can be fully redispersed into a homogeneous gaseous phase. Heating rate is 3 °C/min and scale bars are 100 µm

Further we hybridize 0.5 µm PS green fluorescent beads (G_1) to the 2.8 µm diameter polystyrene (PS) superparamagnetic (M_1) beads through surface grafted complementary DNA. Again the colloidal raspberries are formed if the system is cooled in the absence of magnetic field. However, if the magnetic field is switched on above T_m and the sample is cooled in the presence of a magnetic field (scheme(II)), we form large coaxial chains with the superparamagnetic (M_1) cores held together by small colloids through DNA hybridization. Fig 6.4 shows green fluorescent images of long coaxial chains several hundreds of µm in length, having G_2 wrapped around M_1 colloids. These chains curl up or become floppy when the magnetic field is removed, but they do not break and fall apart even after several hours of switching off the magnetic field. These coaxial scaffolds formed at low temperatures because of the DNA hybridization can be fully redispresed into a gaseous phase after heating it. Fig 6.4 shows green fluorescence snapshots of the system while it transitions from long, floppy chains at 49 °C to a fully dispersed homogeneous colloidal gas at 57 °C . We observe an increased melt temperature (T_m) for this system compared to the control experiment of a single component gel of 0.5 µm PS colloids hybridized via the same $A_7 - A_7'$ DNA pair. We believe this increase in T_m is because of the larger number of DNA bonds forming at the contact region due to a smaller curvature of the large sized superparamagnetic colloids.

Fig 6.5 shows another variation of the two component system wherein 0.5 µm green fluorescent PS colloids are hybridized to 1.5 µm PS superparamagnetic colloids (M_2) at lower temperatures. These components can be recycalably dispersed into a homogeneous gaseous phase at temperatures above T_m. Again formation of both 'raspberry' like (scheme(I)) and linear coaxial scaffolds (scheme (II)) are demonstrated.

6.3.3 Three component system

Self-assembly of long, straight, mesoscopic scaffolds is an important step towards the self-assembly of multi-hierarchical and more complicated colloidal superstructures. The

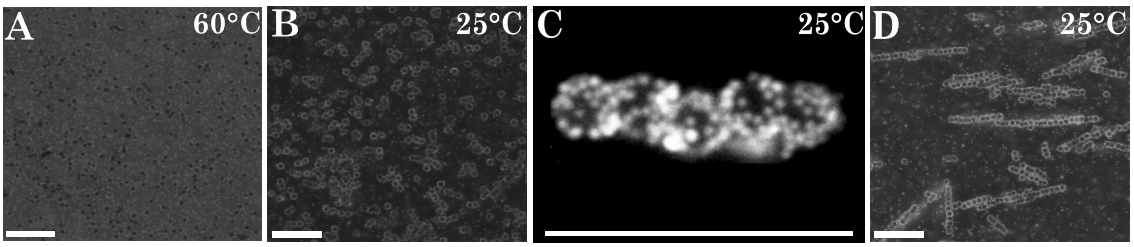

Fig. 6.5 A two component system composed of 1.5 µm PS superparamagnetic colloids (M_2) coated with A_7 DNA and 0.5 µm green fluorescent PS colloids (G_1) coated with A_7' DNA (A) Both M_2 and G_1 colloids exist in a homogeneous gaseous phase when heated to 60 °C (T>T_m for the $A_7 - A_7'$ DNA pair). Green fluorescence images showing locations of small G_1 colloids bound to the superparamagnetic M_2 colloids when (B) the 'raspberry' like superstructures are formed by cooling slowly (@ 0.1 °C/min) in the absence of magnetic field (C) zoomed in image of aligned colloidal raspberries on applying magnetic field after cooling to 25 °C (D) linear coaxial scafolds with a superparamagnetic core are formed by switching on the field at $T > T_m$ and then cooling slowly(@ 0.1 °C/min) in the presence of magnetic field. Scale bars are 10 µm

noncovalent nature of DNA interactions allows us to reversibly control the assembly of these thermoresponsive superstructures and the presence or absence of magnetic field dictates the final geometry of the assembled superstructure. Previous studies on using DNA as an 'intelligent glue' to bind magnetic colloids [95, 96, 98, 100] have demonstrated chains with short lengths (< 50 colloids). Linear coaxial scaffolds assembled in our system are much longer and more rigid compared to those reported earlier in the literature. Our two component strategy presents a unique way to assemble and switch between colloidal superstructures with topological complexity. Further we show that by using a third component and a suitably tailored sequential DNA interaction, these linear coaxial scaffolds can be additionally functionalized. As a proof of concept for functionalization, we present 'furry chains' assembled in a three component system.

Fig 6.6 shows a strategy for functionalizing linear coaxial scaffolds from a two component system into a 'furry chain' like geometry by adding a suitably tailored third component. At 60 °C all the components of the system exist in an isotropic gaseous phase. First the superparamagnetic (M) colloids are aligned into linear chains by applying a magnetic field and then the sequential DNA interactions are switched on by reducing the temperature of

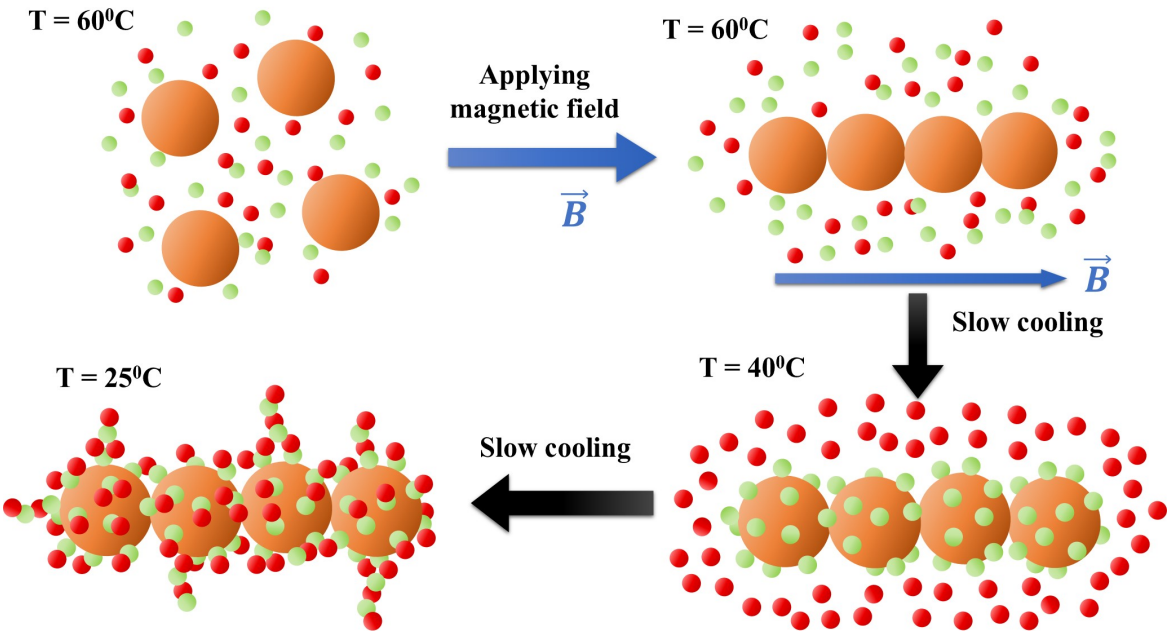

Fig. 6.6 Not to scale, schematic drawing demonstrating the strategy for functionalizing linear coaxial scaffolds from a two component system into 'furry chain' like geometry by adding a suitably tailored third component. All the components of the system exist in a homogeneous gaseous phase at 60 °C. When the magnetic field is switched on at 60 °C ($T > T_m$) and the system is cooled slowly in the presence of a magnetic filed, the linear coaxial scaffolds with a superparamagnetic core are formed. Further reducing the temperature activates the green(G)–red(R) interactions and the linear coaxial scaffolds (M–G) are functionalized and further stabilized by the R component. Note that for ease of clarity DNA strands are not shown in this schematic drawing. Also, the colours of components in this drawing do not represent the order of fluorescence on our actual colloidal components.

the system. As the system is slowly cooled, the first attractive interaction kicks in and the green component coat M beads forming linear coaxial scaffolds. Holding the system at 40 °C for a few hours allows for a good coverage of the superparamagnetic (M) colloids by the green (G) component. Further reducing the temperature of the system activates the second attractive interaction between the green and the red components, resulting in an additional functionalization of the linear scaffolds. For ease of clarity we have omitted the DNA linkers from this schematic drawing. Moreover, the colours of components in this drawing do not represent the order of fluorescence on our actual colloidal components. It is used as a guide.

Starting with a two component system having 1.0 µm PS superparamagnetic colloids (M_3) and 0.5 µm red fluorescent PS colloids(R_1) coated with coated with A_7 and A_7' DNA

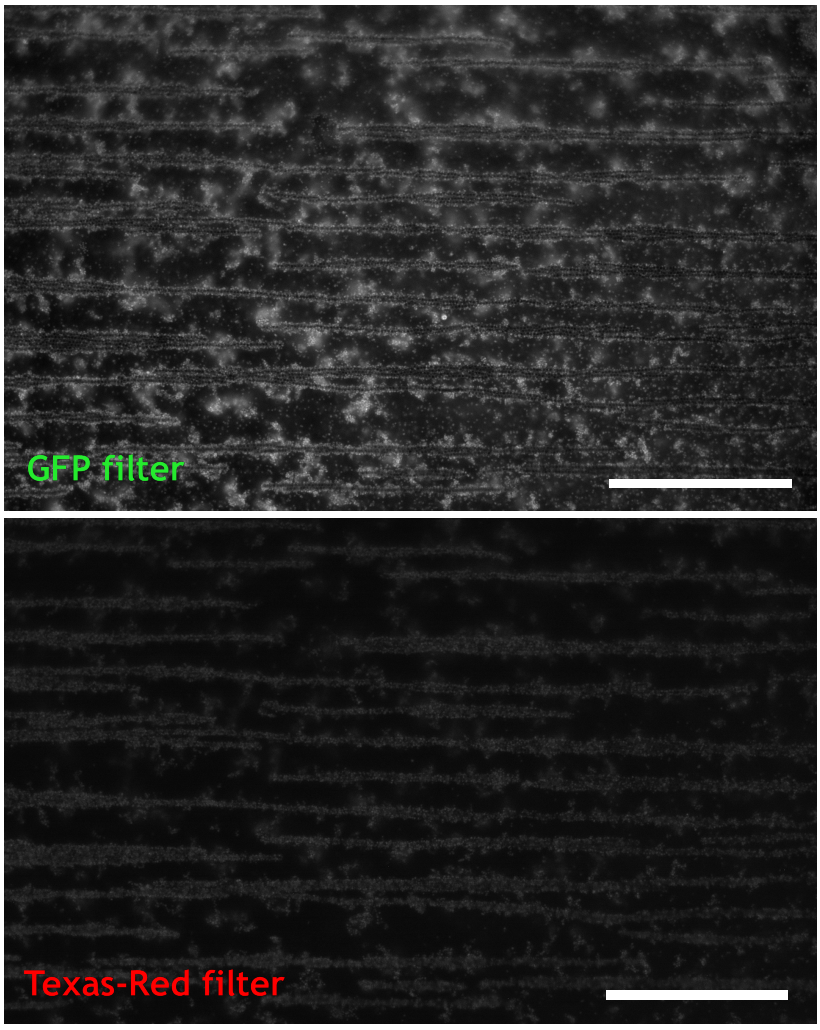

Fig. 6.7 Fluorescence images showing a three component system composed of 1.0 µm PS superparamagnetic colloids (M_3), 0.5 µm red fluorescent PS colloids(R_1) and 0.5 µm green fluorescent PS colloids(G_1) assembled into several hundreds of micron long coaxial 'furry chains'. The system imaged under Texas-Red and GFP illuminations clearly shows the positions of both kind of colloids coating the large superparamagnetic colloids. Scale bars are 100 µm

respectively, we add0.5 µm green fluorescent PS colloids (G_1) coated with A_6 DNA. As per the binding rules, binding is prohibited between colloids of the same kind. The only permitted binding is between, M_3 and R_1 and R_1 and G_1 colloids. While cooling from a high temperature homogeneous gaseous phase, the M_3 and R_1 binding switches on at a higher temperature (56 °C). Cooling the system slowly and holding around the T_m for about an hour ensures a good coverage of M_3 colloids by R_1 colloids. Further cooling the system below the

melt temperature for A_6 and A_6' DNA, the binding between R_1 and G_1 colloids is activated. Hence, we observe the G_1 colloids binding with R_1 colloids attached to the M_3 colloids. Fig 6.7 shows a fully assembled three component system imaged at room temperature under green and red fluorescences respectively. It can be seen that addition of the third species imparts extra rigidity to the linear coaxial chains and we observe very stable and extremely long (few hundreds of microns in length), linear chains without any floppiness. Since there are a number of R_1 colloids free in the bulk of the solution, we observe an additional G-R aggregation in the bulk and also additional G-R-G-R chains branching out from our 'furry chains' (Fig 6.6). This additional branching and aggregation can be mitigated by performing these experiments in a temperature controlled flow cell or microfluidic device where we flush in just enough R_1 colloids to coat the M_3-beads and not an excess of them.

6.4 Conclusion

We have demonstrated a thermally reversible assembly of colloidal components of various size ratios into 'raspberry' like and linear coaxial scaffolds for a two-component system in a magnetic field. Using superparamagnetic beads as one of the components enables us to employ a magnetic field to speed up the pathways to self-assembly of these superstructures while ensuring zero remanent magnetization upon removal of the magnetic field. Our strategy presents a unique way to assemble and switch between assembled colloidal superstructures by playing with the temperature and the applied magnetic filed. The addition of a suitably tailored third component imparts additional stability to these linear coaxial scaffolds. These structures could pave the way for designing novel multi- hierarchical superstructures by using new designing rules to create materials for the use in optoelectronics and drug delivery applications. Further, utilizing magnetic tweezers for bending and manipulating these chains and forcing the colloidal 'raspberries' into more complex topologies can open a plethora of opportunities for creating interesting macro-colloidal superstructures.

Chapter 7

Closing Remarks and Outlook

This thesis has outlined my work on the DNA driven assembly of colloids at liquid and solid interfaces. The central focus of the thesis has been on sculpting specific attractive interactions for colloidal self assembly by utilizing a combination of suitable DNA functionalization along with depletion forces and/or magnetic field. I have devised a novel approach for functionalizing oil droplets (ODs) with DNA that enabled a kinetically controlled and reversible adsorption of colloids onto them. This system was primarily utilized to study the phase behaviour and pattern formation of DNA coated colloids at the oil/water interface. Moreover, optical binding and the subsequent creation of optical crystals is another interesting dimension that has emerged out of my work in this system and is being currently pursued. Further in another project, we demonstrated that by utilizing sequential DNA interactions along with an externally applied magnetic field it is possible to create topologically complex colloidal superstructures such as 'raspberry like' and long coaxial scaffolds.

Chapter 3 discussed major experimental protocols utilized throughout the thesis along with presenting a new approach for introducing mobile DNA linkers on oil droplets. In comparison to previous cumbersome approaches involving expensive biotinylated lipids, our method provides a relatively higher grafting density of DNA anchors at the interface. Further,

by utilizing complementary DNA linkers, we were able to reversibly adsorb micron sized colloids to these DNA functionalized oil droplets.

In Chapter 4, we illustrated kinetically controlled and equilibrium nature of the adsorbed colloids by exploring their quasi two-dimensional (2d) phase behaviour. We demonstrated that it is possible to control the surface coverage of oil droplets by colloidal particles, by exploiting the fact that during slow adsorption, compositional arrest takes place well before the structural arrest occurs. Depending on the solvent conditions, our system transitioned from a fluid like phase to a compact crystalline packing of colloids at the interface forming colloidal 'islands'. This purely entropic transition was attributed to the attractive depletion interaction caused by the presence of excess surfactant micelles in the system. As the concentration of SDS in the system was increased beyond its critical micellar concentration (CMC), we observed that and attractive interaction was switched on between otherwise sterically stabilized DNA coated colloids. Further, colloids bound to the oil water interface were found to be significantly less diffusive compared their bulk counterparts due to the excess drag of PLL-PEG-DNA rafts. Simulation studies using a simple model system illustrated the nature of the compositional arrest and the structural ergodicity observed in our experiments.

Further in chapter 5, I presented some preliminary results on the phase behaviour of binary colloidal mixtures at the oil/water interface. Large (1.2 μm) and small (0.5 μm) polystyrene colloids were hybridized to the oil droplets in varying ratios, above and below the critical micellar concentration (CMC)of SDS respectively. Despite the colloids being mobile on the surface of ODs, we did not observe any phase segregation for various compositions of the mixtures. However, contrary to our expectations we observed significant colloidal aggregates even below the CMC of SDS. This aggregation is suspected to be due to the bridging by PLL-PEG-DNA rafts on the surface of ODs. These preliminary results present an

exciting opportunity for studying recyclable bi-dispersed systems. Incorporating competing sequential DNA interactions, it opens up prospects for designing novel delivery systems.

This novel approach for functionalizing oil droplets with DNA linkers and attaching colloids at the oil water interfaces, presents a versatile model system for studying colloids in a quasi-2d setting. An added advantage of the system is its ability to gently tune the colloidal interaction potential. One of the most promising and exciting extensions of this work has been the utilization of optical tweezers for trapping colloids at the liquid-liquid interface and the observation of optical binding (Fig 7.1). We have demonstrated that the system can be successfully used as a model system for colloids in quasi-2d settings and could be used to demonstrate optically induced crystallization at the fluid-fluid interface.

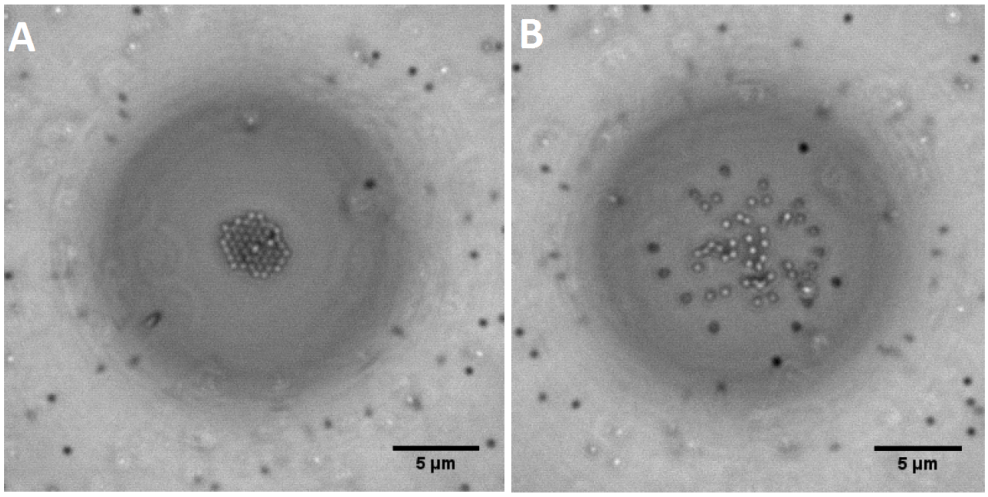

Fig. 7.1 Optical crystallization of 0.5 µm PS colloids on the OD surface. (A)Crystal forming after $\sim$ 5 min of continuous optical trapping.(B)Crystal "melting" after the trap is switched off.

Chapter 6 demonstrated an approach for creating novel superstructures of DNA coated colloids (DNAcc) directed via an externally applied magnetic field. A thermally reversible assembly of colloidal components of various size ratios into 'raspberry' like and linear coaxial scaffolds for a two-component system was demonstrated. Using superparamagnetic beads as one of the components enabled us to employ a magnetic field to speed up the pathways to self-assembly of these superstructures. The addition of a suitably tailored third component

was shown to imparts additional stability to these linear coaxial scaffolds. These structures could pave the way to designing novel multi- hierarchical superstructures by using new designing rules to create materials for use in optoelectronics and drug delivery applications. Further, utilizing magnetic tweezers for bending and manipulating these chains and forcing the colloidal 'raspberries' into more complex topologies can open a plethora of opportunities for creating interesting macro-colloidal superstructures. Among other applications, attempts for building a micron sized electrical fuse by utilizing a conducting layer in between our coaxial scaffolds are underway.

In conclusion, my research work has demonstrated the possibility of utilizing our experimental systems for designing novel materials under the influence of external force fields. The DNA-functionalized ODs represent an ideal system for studying and quantitatively characterizing novel phenomena such as lateral optical binding and the subsequent creation of optical crystals(Fig 7.1. Further attempts for modifying the scaffolds created using magnetic field assisted assembly to incorporate a conducting layer are in progress. Once achieved, these could be incorporated for applications in efficient energy harvesting or storage devices at macro-scale.

References

[1] G. M. Whitesides and B. Grzybowski, "Self-assembly at all scales.," *Science (New York, N.Y.)*, vol. 295, pp. 2418–21, mar 2002.

[2] E. Busseron, Y. Ruff, E. Moulin, and N. Giuseppone, "Supramolecular self-assemblies as functional nanomaterials.," *Nanoscale*, vol. 5, no. 16, pp. 7098–140, 2013.

[3] W. B. Rogers, W. M. Shih, and V. N. Manoharan, "Using DNA to program the self-assembly of colloidal nanoparticles and microparticles," *Nat. Rev. Mater.*, vol. 1, no. 3, p. 16008, 2016.

[4] A. E. Nel, L. Mädler, D. Velegol, T. Xia, E. M. V. Hoek, P. Somasundaran, F. Klaessig, V. Castranova, and M. Thompson, "Understanding biophysicochemical interactions at the nano–bio interface," *Nature Materials*, vol. 8, pp. 543–557, jul 2009.

[5] V. N. Manoharan, "Colloidal matter: Packing, geometry, and entropy," *Science (80-.).*, vol. 349, no. 6251, pp. 1253751–1253751, 2015.

[6] N. Geerts and E. Eiser, "DNA-functionalized colloids: Physical properties and applications," *Soft Matter*, vol. 6, no. 19, p. 4647, 2010.

[7] M. R. Jones, N. C. Seeman, and C. Mirkin, "Programmable materials and the nature of the DNA bond," *Science*, vol. 347, no. 6224, pp. 1260901–1260901, 2015.

[8] L. Di Michele and E. Eiser, "Developments in understanding and controlling self assembly of DNA-functionalized colloids.," *Physical chemistry chemical physics : PCCP*, vol. 15, pp. 3115–29, mar 2013.

[9] M. Hadorn, E. Boenzli, K. T. Sorensen, H. Fellermann, P. E. Hotz, and M. M. Hanczyc, "Specific and reversible DNA-directed self-assembly of oil-in-water emulsion droplets," *Proceedings of the National Academy of Sciences*, vol. 109, pp. 20320–20325, dec 2012.

[10] L. Feng, L. Pontani, R. Dreyfus, P. Chaikin, and J. Brujic, "Specificity, flexibility and valence of DNA bonds guide emulsion architecture," *Soft Matter*, vol. 9, no. 41, p. 9816, 2013.

[11] J N Israelachvili, *Intermolecular and Surface Forces*. Academic Press, third ed., 2010.

[12] D. Frenkel, "Lecture Notes, Graduate Course on Soft Materials, University of Cambridge 2010," 2010.

[13] H. Otsuka, Y. Nagasaki, and K. Kataoka, "PEGylated nanoparticles for biological and pharmaceutical applications," *Advanced Drug Delivery Reviews*, vol. 64, pp. 246–255, dec 2012.

[14] L S Hirst, *Fundamentals of Soft Matter Science*. CRC Press, Taylor and Francis Group, 1 ed., 2013.

[15] A. Einstein, "On the Motion of Small Particles Suspended in a Stationary Liquid, as Required by the Molecular Kinetic Theory of Heat," *Ann. Phys.*, vol. 322, pp. 549–560, 1905.

[16] Y. Min, M. Akbulut, and K. Kristiansen, "The role of interparticle and external forces in nanoparticle assembly," *Nature materials*, pp. 527–538, 2008.

[17] B. Derjaguin and L. Landau, "Theory of the stability of strongly charged lyophobic sols and of the adhesion of strongly charged particles in solutions of electrolytes," *Acta. Phys. Chem.,*, vol. 14, pp. 633–662, 1941.

[18] E. Verwey and J. Overbeek, *Theory of the stability of lyophobic colloids*. Elsevier, Amsterdam, 1948.

[19] S. Asakura and F. Oosawa, "Interaction between particles suspended in solutions of macromolecules," *J. Polym. Sci.*, vol. 33, pp. 183–192, dec 1958.

[20] S. Sacanna, W. T. M. Irvine, P. M. Chaikin, and D. J. Pine, "Lock and key colloids.," *Nature*, vol. 464, pp. 575–8, mar 2010.

[21] S. Alexander, "Adsorption of chain molecules with a polar head a scaling description," *Journal de physique*, no. 38, p. 983, 1977.

[22] P. D. Gennes, "Polymers at an interface; a simplified view," *Advances in Colloid and Interface Science*, vol. 27, pp. 189–209, 1987.

[23] C. M. Niemeyer, "Nanoparticles, Proteins, and Nucleic Acids: Biotechnology Meets Materials Science," *Angewandte Chemie International Edition*, vol. 40, pp. 4128–4158, nov 2001.

[24] A. C. Balazs, T. Emrick, and T. P. Russell, "Nanoparticle polymer composites: where two small worlds meet.," *Science (New York, N.Y.)*, vol. 314, pp. 1107–10, nov 2006.

[25] J. D. Watson and F. H. C. Crick, "Molecular Structure Of Nucleic Acids," *American Journal of Psychiatry*, vol. 160, pp. 623–624, apr 2003.

[26] Y.-J. Chen, B. Groves, R. A. Muscat, and G. Seelig, "DNA nanotechnology from the test tube to the cell," *Nat. Nanotechnol.*, vol. 10, pp. 748–760, sep 2015.

[27] M. H. Caruthers, "Gene synthesis machines: DNA chemistry and its uses," *Science*, vol. 230, no. 4723, pp. 281–285, 1985.

[28] R. K. Saiki, D. H. Gelfand, S. Stoffel, S. J. Scharf, R. Higuchi, G. T. Horn, K. B. Mullis, and H. A. Erlich, "Primer-directed enzymatic amplification of DNA with a thermostable DNA polymerase.," *Science (New York, N.Y.)*, vol. 239, pp. 487–491, jan 1988.

[29] K. B. Mullis, "The Polymerase Chain Reaction (Nobel Lecture) **," *Science*, vol. 92037, pp. 1209–1213, 1994.

[30] P. W. K. Rothemund, "Folding DNA to create nanoscale shapes and patterns.," *Nature*, vol. 440, pp. 297–302, mar 2006.

[31] H.-W. Fink and C. Schönenberger, "Electrical conduction through DNA molecules," *Nature*, vol. 398, pp. 407–410, apr 1999.

[32] A. P. Alivisatos, K. P. Johnsson, and X. Peng, "Organization of 'nanocrystal molecules' using DNA," *Nature*, vol. 382, 15 August 1996.

[33] C. A. Mirkin, R. L. Letsinger, R. C. Mucic, and J. J. Storhoff, "A DNA-based method for rationally assembling nanoparticles into macroscopic materials," *Nature*, vol. 382, no. 1996, pp. 607–609, 1996.

[34] L. D. Michele, *PhD Thesis : Multicomponent amorphous phases of DNA-functionalised colloids*. 2013.

[35] F. Sciortino, "DNA Hairs Provide Potential for Molecular Self-Assembly," *Physics*, vol. 5, p. 71, jun 2012.

[36] D. Nykypanchuk, M. M. Maye, D. Van der Lelie, and O. Gang, "DNA-guided crystallization of colloidal nanoparticles," *Nature*, vol. 451, pp. 549–552, jan 2008.

[37] B. J. Park, J. P. Pantina, E. M. Furst, M. Oettel, S. Reynaert, and J. Vermant, "Direct measurements of the effects of salt and surfactant on interaction forces between colloidal particles at water-oil interfaces," *Langmuir*, vol. 24, no. 5, pp. 1686–1694, 2008.

[38] R. J. Macfarlane, B. Lee, M. R. Jones, N. Harris, G. C. Schatz, and C. a. Mirkin, "Nanoparticle superlattice engineering with DNA.," *Science (New York, N.Y.)*, vol. 334, pp. 204–8, oct 2011.

[39] R. Dreyfus, M. Leunissen, R. Sha, A. Tkachenko, N. Seeman, D. Pine, and P. Chaikin, "Simple Quantitative Model for the Reversible Association of DNA Coated Colloids," *Physical Review Letters*, vol. 102, p. 048301, jan 2009.

[40] R. Dreyfus, M. E. Leunissen, R. Sha, A. Tkachenko, N. C. Seeman, D. J. Pine, and P. M. Chaikin, "Aggregation-disaggregation transition of DNA-coated colloids: Experiments and theory," *Physical Review E - Statistical, Nonlinear, and Soft Matter Physics*, vol. 81, pp. 1–10, apr 2010.

[41] F. Varrato, L. D. Michele, M. Belushkin, N. Dorsaz, S. H. Nathan, E. Eiser, and G. Foffi, "Arrested demixing opens route to bigels," *Proceedings of the National Academy of Sciences*, vol. 109, pp. 19155–19160, nov 2012.

[42] D. Joshi, D. Bargteil, A. Caciagli, J. Burelbach, Z. Xing, A. S. Nunes, D. E. P. Pinto, N. A. M. Araujo, J. Brujic, and E. Eiser, "Kinetic control of the coverage of oil droplets by DNA-functionalized colloids," *Science Advances*, vol. 2, pp. e1600881–e1600881, aug 2016.

[43] L. Parolini, B. M. Mognetti, J. Kotar, E. Eiser, Cicuta, and L. Michele, "Volume and porosity thermal regulation in lipid mesophases by coupling mobile ligands to soft membranes," *Nature Communications*, vol. 6, p. 5948, jan 2015.

[44] M. R. Jones, R. J. Macfarlane, B. Lee, J. Zhang, K. L. Young, A. J. Senesi, and C. a. Mirkin, "DNA-nanoparticle superlattices formed from anisotropic building blocks.," *Nature materials*, vol. 9, no. 11, pp. 913–917, 2010.

[45] S. Mann, "Self-assembly and transformation of hybrid nano-objects and nanostructures under equilibrium and non-equilibrium conditions.," *Nature materials*, vol. 8, no. 10, pp. 781–792, 2009.

[46] Y. Wang, Y. Wang, X. Zheng, É. Ducrot, J. S. Yodh, M. Weck, D. J. Pine, E. Ducrot, J. S. Yodh, M. Weck, and D. J. Pine, "Crystallization of DNA-coated colloids," *Nature Communications*, vol. 6, p. 7253, 2015.

[47] H. R. Vutukuri, A. F. Demirörs, B. Peng, P. D. J. Van Oostrum, A. Imhof, and A. Van Blaaderen, "Colloidal analogues of charged and uncharged polymer chains with tunable stiffness," *Angewandte Chemie - International Edition*, vol. 51, no. 45, pp. 11249–11253, 2012.

[48] P. Cigler, A. K. R. Lytton-Jean, D. G. Anderson, M. G. Finn, and S. Y. Park, "DNA-controlled assembly of a NaTl lattice structure from gold nanoparticles and protein nanoparticles.," *Nature materials*, vol. 9, no. 11, pp. 918–922, 2010.

[49] H. D. Hill, R. J. Macfarlane, A. J. Senesi, B. Lee, S. Y. Park, and C. a. Mirkin, "Controlling the lattice parameters of gold nanoparticle FCC crystals with duplex DNA linkers," *Nano Letters*, vol. 8, no. 8, pp. 2341–2344, 2008.

[50] M. E. Leunissen, R. Dreyfus, R. Sha, N. C. Seeman, and P. M. Chaikin, "Quantitative Study of the Association Thermodynamics and Kinetics of DNA-Coated Particles for Different Functionalization Schemes," *Journal of the American Chemical Society*, vol. 132, pp. 1903–1913, feb 2010.

[51] S. a. J. van der Meulen and M. E. Leunissen, "Solid colloids with surface-mobile DNA linkers," *Journal of the American Chemical Society*, vol. 135, no. 40, pp. 15129–15134, 2013.

[52] L. Ramos and P. Fabre, "Swelling of a Lyotropic Hexagonal Phase by Monitoring the Radius of the Cylinders," *Langmuir*, vol. 13, pp. 682–686, feb 1997.

[53] F. F. Rossetti, I. Reviakine, G. Csúcs, F. Assi, J. Vörös, and M. Textor, "Interaction of Poly(L-Lysine)-g-Poly(Ethylene Glycol) with Supported Phospholipid Bilayers," *Biophysical Journal*, vol. 87, pp. 1711–1721, sep 2004.

[54] S. Kawaguchi, G. Imai, J. Suzuki, A. Miyahara, T. Kitano, and K. Ito, "Aqueous solution properties of oligo- and poly(ethylene oxide) by static light scattering and intrinsic viscosity," *Polymer*, vol. 38, pp. 2885–2891, jun 1997.

[55] L. A. Ruiz-Taylor, T. L. Martin, F. G. Zaugg, K. Witte, P. Indermuhle, S. Nock, and P. Wagner, "Monolayers of derivatized poly(L-lysine)-grafted poly(ethylene glycol) on metal oxides as a class of biomolecular interfaces," *Proceedings of the National Academy of Sciences*, vol. 98, pp. 852–857, jan 2001.

[56] S. U. Pickering, "CXCVI Emulsions," *Journal of the Chemical Society, Transactions*, vol. 91, p. 2001, 1907.

[57] L. D. Michele, B. M. Mognetti, T. Yanagishima, P. Varilly, Z. Ruff, D. Frenkel, and E. Eiser, "Effect of Inert Tails on the Thermodynamics of DNA Hybridization," *Journal of the American Chemical Society*, vol. 136, pp. 6538–6541, may 2014.

[58] W. Ramsden, "Separation of Solids in the Surface-Layers of Solutions and 'Suspensions' (Observations on Surface-Membranes, Bubbles, Emulsions, and Mechanical Coagulation) - Preliminary Account," *Proceedings of the Royal Society of London*, vol. 72, no. 1903-1904, pp. 156–164, 1903.

[59] B. Binks and R. Murakami, "Phase inversion of particle-stabilized materials from foams to dry water," *Nature Materials*, vol. 5, pp. 865–869, nov 2006.

[60] E. P. Lewandowski, J. A. Bernate, A. Tseng, P. C. Searson, and K. J. Stebe, "Oriented assembly of anisotropic particles by capillary interactions," *Soft Matter*, vol. 5, p. 886, 2009.

[61] M. Cavallaro, L. Botto, E. P. Lewandowski, M. Wang, and K. J. Stebe, "From the Cover: Curvature-driven capillary migration and assembly of rod-like particles," *Proceedings of the National Academy of Sciences*, vol. 108, no. 52, pp. 20923–20928, 2011.

[62] B. Madivala, S. Vandebril, J. Fransaer, and J. Vermant, "Exploiting particle shape in solid stabilized emulsions," *Soft Matter*, vol. 5, no. 8, p. 1717, 2009.

[63] T. Saigal, H. Dong, K. Matyjaszewski, and R. D. Tilton, "Pickering emulsions stabilized by nanoparticles with thermally responsive grafted polymer brushes," *Langmuir*, vol. 26, no. 19, pp. 15200–15209, 2010.

[64] S. Melle, M. Lask, and G. G. Fuller, "Pickering emulsions with controllable stability," *Langmuir*, vol. 21, no. 6, pp. 2158–2162, 2005.

[65] A. D. Dinsmore, M. F. Hsu, M. G. Nikolaides, M. Marquez, A. R. Bausch, and D. A. Weitz, "Colloidosomes: selectively permeable capsules composed of colloidal particles.," *Science (New York, N.Y.)*, vol. 298, pp. 1006–9, nov 2002.

[66] Y. Wang, Y. Wang, D. R. Breed, V. N. Manoharan, L. Feng, A. D. Hollingsworth, M. Weck, and D. J. Pine, "Colloids with valence and specific directional bonding," *Nature*, vol. 490, no. 7422, pp. 51–55, 2012.

[67] E. M. Herzig, K. A. White, A. B. Schofield, W. C. K. Poon, and P. S. Clegg, "Bicontinuous emulsions stabilized solely by colloidal particles.," *Nature materials*, vol. 6, no. 12, pp. 966–971, 2007.

[68] C. a. Schneider, W. S. Rasband, and K. W. Eliceiri, "NIH Image to ImageJ: 25 years of image analysis," *Nature Methods*, vol. 9, no. 7, pp. 671–675, 2012.

[69] S. H. Nathan, *DNA directed self-assembly of colloidal systems*. PhD thesis, University of Cambridge, 2015.

[70] T. Yanagishima, D. Frenkel, J. Kotar, and E. Eiser, "Real-time monitoring of complex moduli from micro-rheology," *Journal of physics. Condensed matter : an Institute of Physics journal*, vol. 23, p. 194118, oct 2010.

[71] R. Cerbino and V. Trappe, "Differential Dynamic Microscopy: Probing Wave Vector Dependent Dynamics with a Microscope," *Physical Review Letters*, vol. 100, p. 188102, may 2008.

[72] E. Eiser, "Chapter 5 - Dynamic Light Scattering," in *Multi Length-Scale Characterisation* (D. O. Duncan W. Bruce and R. I. Walton, eds.), no. May, pp. 233–282, John Wiley & Sons, Ltd., 2014.

[73] L. D. Michele, T. Yanagishima, A. R. Brewer, J. Kotar, E. Eiser, and S. Fraden, "Interactions between colloids induced by a soft cross-linked polymer substrate," *Physical Review Letters*, vol. 107, no. 13, pp. 1–4, 2011.

[74] P. G. Saffman, M. Delbruck, and M. Delbrück, "Brownian motion in biological membranes," *Proc Natl Acad Sci USA*, vol. 72, pp. 3111–3113, aug 1975.

[75] T. M. Fischer, P. Dhar, and P. Heinig, "The viscous drag of spheres and filaments moving in membranes or monolayers," *Journal of Fluid Mechanics*, vol. 558, p. 451, jul 2006.

[76] G. G. Fuller and J. Vermant, "Complex Fluid-Fluid Interfaces: Rheology and Structure," *Annual Review of Chemical and Biomolecular Engineering*, vol. 3, pp. 519–543, jul 2012.

[77] M. Sickert and F. Rondelez, "Shear viscosity of langmuir monolayers in the low-density limit.," *Physical review letters*, vol. 90, p. 126104, mar 2003.

[78] F. Oosawa and S. Asakura, "Surface Tension of High-Polymer Solutions," *The Journal of Chemical Physics*, vol. 22, no. 7, p. 1255, 1954.

[79] A. P. Gast, C. K. Hall, and W. B. Russel, "Polymer-induced phase separations in nonaqueous colloidal suspensions," *Journal of Colloid and Interface Science*, vol. 96, pp. 251–267, nov 1983.

[80] M. H. J. Hagen and D. Frenkel, "Determination of phase diagrams for the hard-core attractive Yukawa system," *The Journal of Chemical Physics*, vol. 101, no. 5, p. 4093, 1994.

[81] P. N. Pusey, A. D. Pirie, and W. C. K. Poon, "Dynamics of colloid-polymer mixtures," *Physica A: Statistical Mechanics and its Applications*, vol. 201, pp. 322–331, dec 1993.

[82] T. D. Iracki, D. J. Beltran-Villegas, S. L. Eichmann, and M. A. Bevan, "Charged Micelle Depletion Attraction and Interfacial Colloidal Phase Behavior," *Langmuir*, vol. 26, pp. 18710–18717, dec 2010.

[83] G. Meng, J. Paulose, D. R. Nelson, and V. N. Manoharan, "Elastic Instability of a Crystal Growing on a Curved Surface," *Science*, vol. 343, pp. 634–637, feb 2014.

[84] D. Marenduzzo, K. Finan, and P. R. Cook, "The depletion attraction: an underappreciated force driving cellular organization," *The Journal of Cell Biology*, vol. 175, pp. 681–686, dec 2006.

[85] A. Tkachenko, "Morphological Diversity of DNA-Colloidal Self-Assembly," *Physical Review Letters*, vol. 89, p. 148303, sep 2002.

[86] Z. Zeravcic, V. N. Manoharan, and M. P. Brenner, "Size limits of self-assembled colloidal structures made using specific interactions," *Proceedings of the National Academy of Sciences*, vol. 111, no. 45, pp. 15918–15923, 2014.

[87] J. Byrom and S. L. Biswal, "Magnetic field directed assembly of two-dimensional fractal colloidal aggregates," *Soft Matter*, vol. 9, no. 38, p. 9167, 2013.

[88] A. Skjeltorp, "One-and two-dimensional crystallization of magnetic holes," *Physical review letters*, vol. 51, no. 25, pp. 2306–2309, 1983.

[89] R. M. Erb, H. S. Son, B. Samanta, V. M. Rotello, and B. B. Yellen, "Magnetic assembly of colloidal superstructures with multipole symmetry.," *Nature*, vol. 457, pp. 999–1002, feb 2009.

[90] Y. Yang, L. Gao, G. P. Lopez, and B. B. Yellen, "Tunable assembly of colloidal crystal alloys using magnetic nanoparticle fluids.," *ACS nano*, vol. 7, pp. 2705–16, mar 2013.

[91] D. Zerrouki, J. Baudry, D. Pine, P. Chaikin, and J. Bibette, "Chiral colloidal clusters.," *Nature*, vol. 455, pp. 380–2, sep 2008.

[92] S. K. Smoukov, S. Gangwal, M. Marquez, and O. D. Velev, "Reconfigurable responsive structures assembled from magnetic Janus particles," *Soft Matter*, vol. 5, no. 6, p. 1285, 2009.

[93] S. Sacanna, L. Rossi, and D. J. Pine, "Magnetic click colloidal assembly.," *Journal of the American Chemical Society*, vol. 134, pp. 6112–5, apr 2012.

[94] C. Goubault, F. Leal-Calderon, J.-L. Viovy, and J. Bibette, "Self-Assembled Magnetic Nanowires Made Irreversible by Polymer Bridging," *Langmuir*, vol. 21, no. 9, pp. 3725–3729, 2005.

[95] M. E. Leunissen, R. Dreyfus, R. Sha, T. Wang, N. C. Seeman, D. J. Pine, and P. M. Chaikin, "Towards self-replicating materials of DNA-functionalized colloids," *Soft Matter*, vol. 5, no. 12, p. 2422, 2009.

[96] D. Li, J. Rogers, and S. L. Biswal, "Probing the stability of magnetically assembled DNA-linked colloidal chains.," *Langmuir : the ACS journal of surfaces and colloids*, vol. 25, pp. 8944–50, aug 2009.

[97] D. Li, S. Banon, and S. L. Biswal, "Bending dynamics of DNA-linked colloidal particle chains," *Soft Matter*, vol. 6, no. 17, pp. 4197–4204, 2010.

[98] V. T. Mukundan, Q. M. Nhat Tran, Y. Miao, and A. T. Phan, "Connecting magnetic micro-particles with DNA G-quadruplexes," *Soft Matter*, vol. 9, no. 1, p. 216, 2013.

[99] Y. Lan, Y. Wu, A. Karas, and O. A. Scherman, "Photoresponsive hybrid raspberry-like colloids based on cucurbit[8]uril host-guest interactions," *Angewandte Chemie - International Edition*, vol. 53, no. 8, pp. 2166–2169, 2014.

[100] R. Dreyfus, J. Baudry, M. L. Roper, M. Fermigier, H. Stone, and J. Bibette, "Microscopic artificial swimmers.," *Nature*, vol. 437, no. 7060, pp. 862–865, 2005.